TURUN
YLIOPISTO
UNIVERSITY
OF TURKU

DYNAMIC REGULATION OF OXYGENIC PHOTOSYNTHESIS IN CYANOBACTERIA BY FLAVODIIRON PROTEINS

Anita Santana-Sánchez

TURUN YLIOPISTON JULKAISUJA – ANNALES UNIVERSITATIS TURKUENSIS
SARJA – SER. AI OSA – TOM. 655 | ASTRONOMICA – CHEMICA – PHYSICA – MATHEMATICA | TURKU 2021

TURUN
YLIOPISTO
UNIVERSITY
OF TURKU

DYNAMIC REGULATION OF OXYGENIC PHOTOSYNTHESIS IN CYANOBACTERIA BY FLAVODIIRON PROTEINS

Anita Santana-Sánchez

TURUN YLIOPISTON JULKAISUJA – ANNALES UNIVERSITATIS TURKUENSIS
SARJA – SER. AI OSA – TOM. 655 | ASTRONOMICA - CHEMICA - PHYSICA – MATHEMATICA | TURKU 2021

University of Turku

Faculty of Technology
Department of Life Technologies
Molecular Plant Biology
Doctoral programme in Molecular Life Sciences

Supervised by

Prof. Yagut Allahverdiyeva-Rinne
PhotoMicrobes group
Molecular Plant Biolog
Department of Life Technologies
University of Turku
Finland

Reviewed by

Prof. Amel Latifi
Aix Marseille Université
Laboratoire de Chimie Bactérienne
France

Prof. Josef Komenda
Centre Algatech
Laboratory of Photosynthesis
Institute of Microbiology
Czech Academy of Sciences
Czech Republic

Opponent

Prof. Tomas Morosinotto
University of Padova,
Dipartimento Biologia,
Italy

ISBN 978-951-29-8668-2 (PRINT)
ISBN 978-951-29-8669-9 (PDF)
ISSN 0082-7002 (Print)
ISSN 2343-3175 (Online)
Painosalama, Turku, Finland 2021

“Better to see something once,
than to hear about it a thousand times”
-Asian proverb

UNIVERSITY OF TURKU
Faculty of Technology
Department of Life Technologies
Molecular Plant Biology
ANITA SANTANA-SÁNCHEZ: Dynamic Regulation of Oxygenic Photosynthesis in Cyanobacteria by Flavodiiron Proteins
Doctoral Dissertation, 216 pp.
Doctoral Programme in Molecular Life Sciences
October 2021

ABSTRACT

The ability of oxygenic photosynthetic organisms to develop protective mechanisms for the regulation of the photosynthetic apparatus is crucial for their survival in continuously changing environmental conditions. The flavodiiron proteins (FDPs) represent a remarkable regulatory electron transport pathway evolved in all photosynthetic organisms, apart from angiosperms, red and brown algae. The FDPs act as photoprotective electron sinks in directing excess electrons from the photosynthetic electron chain to O_2, *via* the so-called Mehler-like reaction. In this thesis work, I focused on the regulatory mechanism, physiological relevance and functional regulation of FDPs in cyanobacteria.

In the unicellular cyanobacterium *Synechocystis* sp. PCC 6803 (hereafter *Synechocystis*), the Flv1/Flv3 heterodimer has long been regarded as solely responsible for the Mehler-like reaction downstream of PSI under both high (HC) and air level (low, LC) levels of CO_2. In this work, I revealed, for the first time, the contribution of the Flv2/Flv4 heterodimer to the Mehler-like reaction *in vivo*. Moreover, I directly compare the Mehler-like reaction kinetics under HC and LC conditions. My results demonstrate that, contrary to the apparent futile contribution of FDPs under HC, WT cells display a strong and steady-state Mehler-like reaction (biphasic kinetics) mediated by low amounts of the Flv1/Flv3 heterodimer. Whereas, under LC (at pH 6–8.2), the expression of FDPs is induced and WT cells show triphasic kinetics (*induction*, *quenching* and *steady-state*) of O_2 photoreduction driven by Flv1/Flv3 and Flv2/Flv4 functioning downstream of PSI. Furthermore, I was able to unravel the contribution of Flv1/Flv3 and Flv2/Flv4 to the O_2 photoreduction kinetics: Flv1/Flv3 was shown to be the main responsible for the strong but transient phase upon illumination, while Flv2/Flv4 mostly contributes to the slow steady-state phase under LC. Importantly, the mutants with defective NDH-1 complexes lacked the quenching phase of O_2 photoreduction after the initial induction, suggesting that the transient activity of Flv1/Flv3, under LC, is due to competition for electrons with the NDH-1 complex *via* reduced Fd. A more thorough examination demonstrated a partial functional redundancy between Flv1/Flv3 and NDH-$1_{1/2}$. Under constant illumination in LC, cells devoid of NDH-$1_{1/2}$ prioritize the oxidation of PSI by enhancing the accumulation and activity of all FDPs, over the efficient induction of CO_2 fixation. Under the same conditions, the absence of the transient activity of Flv1/Flv3 can be compensated for by the joint work of NDH-

$1_{1/2}$ and Flv2/Flv4 to maintain PSI oxidation. The absence of both Flv1/Flv3 and NDH-$1_{1/2}$ resulted in a diminished ability to oxidize PSI and, albeit at a high cost, this allowed the allocation of reductants towards CO_2 fixation. These results demonstrated a dynamic coordination between both pathways for the efficient oxidation of PSI and CO_2 fixation. In this work, I also demonstrated that the essential role of Flv1/Flv3 under fluctuating light (FL) conditions cannot be compensated for by neither Flv2/Flv4 nor NDH-1. Additionally, I demonstrated that Flv1/Flv1 and Flv3/Flv3 homodimers contribute to the acclimation of *Synechocystis* to FL, mediating an oxygen-independent reaction.

The filamentous N_2-fixing cyanobacterium *Anabaena sp.* PCC 7120 (hereafter *Anabaena*) contains, along with Flv2 and Flv4, two copies of genes encoding for Flv1 and Flv3 proteins: Flv1A and Flv3A are expressed in vegetative cells, whereas Flv1B and Flv3B are localized in mature heterocysts. My results indicate that Flv3A has an important role during light acclimation regardless of the of the nitrogen and CO_2 availability. Moreover, I demonstrated that unlike Flv3 in *Synechocystis*, Flv3A is capable of mediating, to some extent, O_2 photoreduction independently of Flv1A. My results suggest that Flv3A functions in coordination with Flv2 and Flv4, likely forming various oligomeric arrangement. Furthermore, I examined the physiological relevance of the vegetative cell-specific Flv1A and Flv3A on the diazotrophic metabolism of *Anabaena* and demonstrated that the deletion of the vegetative cell-specific Flv3A resulted in downregulation of the heterocyst specific-protein uptake hydrogenase (Hup) which led to enhanced H_2 photoproduction under both oxic and micro-oxic conditions. These results revealed a complex regulatory network between the Mehler-like reaction in the vegetative cells and the H_2 metabolism in the heterocysts of *Anabaena* that will need to be further elucidated in future studies.

TURUN YLIOPISTO
Teknillinen tiedekunta
Bioteknologian laitos
Molekulaarinen kasvibiologia
ANITA SANTANA-SÁNCHEZ: Dynamic regulation of oxygenic photosynthesis in cyanobacteria by flavodiiron proteins
Väitöskirja, 216 s.
Molekulaaristen biotieteiden tohtoriohjelma
Huhtikuu 2021

TIIVISTELMÄ

Happea tuottavaa fotosynteesiä hyödyntävien organismien kyky kehittää suoja-mekanismeja fotosynteettisen koneiston säätelemiseksi on ratkaisevan tärkeää, jotta eliöt selviytyisivät jatkuvasti muuttuvissa ympäristöolosuhteissa. Flavodiironi-proteiinit (FDP:t) toimivat elektroninsiirtoreitissä, joka on kehittynyt kaikissa fotosynteettisissä organismeissa, lukuun ottamatta koppisiemenisiä kasveja sekä puna- ja ruskoleviä. FDP:t suojaavat eliötä liialta valoenergialta toimimalla elektroninieluina, jotka ohjaavat ylimääräisiä elektroneja fotosynteettisestä elektroninsiirtoketjusta hapelle ns. Mehlerin kaltaisen reaktion välityksellä. Väitöskirjassani selvitin syanobakteerien FDP:en säätelymekanismeja, fysiologista merkitystä ja toiminnallista säätelyä.

Yksisoluisessa syanobakteerissa Synechocystis sp. PCC 6803:ssa (tästä eteenpäin Synechocystis) Flv1/Flv3-heterodimeerin on pitkään ajateltu olevan yksin vastuussa PSI:n vastaanottajapuolella tapahtuvasta Mehlerin kaltaisesta reaktiosta sekä korkeassa (HC) että normaalissa (LC) ilman hiilidioksidipitoisuudessa. Väitöskirjassani osoitin ensimmäistä kertaa, että Flv2/Flv4-heterodimeeri vaikuttaa Mehlerin kaltaiseen reaktioon in vivo. Lisäksi vertasin Mehlerin kaltaisen reaktion kinetiikkaa HC- ja LC-olosuhteissa. Tulokseni osoittavat, että HC-olosuhteissa, joissa FDP:n merkitys on ennen ajateltu olevan pieni, villityyppisissä (WT) soluissa oleva pieni määrä Flv1/Flv3-heterodimeeriä saa aikaan merkittävän ja vakaan Mehlerin kaltaisen reaktion (kaksivaiheinen kinetiikka). Sitä vastoin LC-olosuhteissa (pH 6–8,2) FDP:en ilmentyminen indusoituu, ja WT-solujen hapen valopelkistys noudattaa kolmivaiheista reaktiokinetiikkaa (induktio, vaimeneminen ja vakaa tila), jonka saavat aikaan PSI:n vastaanottajapuolella sijaitsevat Flv1/Flv3 ja Flv2/Flv4. Lisäksi pystyin selvittämään Flv1/Flv3:n ja Flv2/Flv4:n vaikutuksen hapen valopelkistyksen kinetiikkaan: Flv1/Flv3 on pääasiallisesti vastuussa sen voimakkaasta, mutta ohimenevästä vaiheesta valojakson aikana LC-olosuhteissa, kun taas Flv2/Flv4 vaikuttaa enimmäkseen hitaan ja vakaan vaiheen aikana. On tärkeää huomata, että mutanttikannat, joilta puuttuu toiminnallinen NDH-1-kompleksi, eivät osoittaneet hapen valopelkistyksen vaimenemista induktion jälkeen, mikä viittaa siihen, että Flv1/Flv3:n ohimenevä aktiivisuus LC-olosuhteissa johtuu kilpailusta NDH-1-kompleksin kanssa pelkistyneeltä ferredoksiinilta tulevista elektroneista. Perusteellisempi tutkimus osoitti osittaisen toiminnallisen päällekkäisyyden Flv1/Flv3:n ja NDH-11/2:n välillä. Jatkuvassa valaistuksessa LC-

olosuhteissa solut, joissa ei ole NDH-11/2:ta, asettavat etusijalle PSI:n hapettumisen tehostamalla kaikkien FDP:en kertymistä ja aktiivisuutta verrattuna tehokkaaseen hiilensidonnan indusointiin. Samoissa olosuhteissa Flv1/Flv3:n ohimenevä aktiivisuuden puuttuminen voidaan korvata NDH-11/2:n ja Flv2/Flv4:n yhteistyöllä PSI:n hapettumisen ylläpitämiseksi. Sekä Flv1/Flv3:n että NDH-11/2:n samanaikainen puuttuminen johti heikentyneeseen kykyyn hapettaa PSI ja, vaikkakin resursseja uhraten, tämä mahdollisti pelkistysvoimaa tarjoavien yhdisteiden kohdistamisen hiilensidontaan. Nämä tulokset osoittivat dynaamisen koordinoinnin molempien elektroninsiirtoreittien välillä PSI:n tehokkaan hapettumisen ja hiilensidonnan varmistamiseksi. Tulokseni myös osoittavat, että Flv2/Flv4 tai NDH-1 ei kykene korvaamaan Flv1/Flv3:a vaihtelevissa valo-olosuhteissa (FL) korostaen Flv1/Flv3:n olennaista merkitystä FL:n aikana. Lisäksi osoitin, että Flv1/Flv1- ja Flv3/Flv3- homodimeerit välittävät hapesta riippumattomia elektroninsiirtoreaktioita, jotka myötävaikuttavat Synechocystiksen sopeutumiseen FL-olosuhteisiin.

Filamenttisella, ilmakehän typpeä sitovalla syanobakteerilla Anabaena sp. PCC 7120 (tästä lähtien Anabaena) on Flv2:n ja Flv4:n lisäksi kaksi kopiota Flv1- ja Flv3 -proteiineja koodaavista geeneistä: kasvulliset solut ilmentävät Flv1A- ja Flv3A-proteiineja, kun taas Flv1B- ja Flv3B- proteiinit löytyvät kypsistä heterokysteistä. Tulokseni osoittavat, että Flv3A:lla on tärkeä rooli solujen sopeutuessa valoon riippumatta typen ja hiilidioksidin saatavuudesta. Olen myöskin osoittanut, että toisin kuin Synechocystiksen Flv3, Anabaenan Flv3A kykenee jossain määrin itsenäisesti välittämään hapen valopelkistystä Flv1A:lle. Tulokseni viittaavat siihen, että Flv3A toimii yhdessä Flv2:n ja Flv4:n kanssa muodostaen todennäköisesti erilaisia oligomeerisiä konformaatioita. Lisäksi tarkastelin vegetatiivisille soluille spesifisten Flv1A:n ja Flv3A:n fysiologista merkitystä Anabaenan typpiaineenvaihdunnassa ja osoitin, että vegetatiivisille soluille spesifisen Flv3A:n deleetio sai aikaan heterokystispesifisen uptake hydrogenase (Hup) -proteiinin ilmenemisen vähenemisen, mikä johti lisääntyneeseen vedyn tuotantoon valossa sekä ilmakehän normaalissa happipitoisuudessa että vähähappisissa olosuhteissa. Väitöskirjatyöni osoitti, että Anabaena-syanobakteerin kasvullisissa soluissa tapahtuvan Mehlerin kaltaisen reaktion ja heterokysteissä tapahtuvan vetyaineenvaihdunnan välillä toimii monimutkainen säätelyverkosto. Jatkotutkimuksissa selvitetään tämän säätelyverkoston rakennetta ja merkitystä syanobakteerin aineenvaihdunnalle.

Table of Contents

Abbreviations

2-OG	2-oxoglutarate
2-PG	2-phosphoglycolate
3-PGA	3-phosphoglycerate
ADP	Adenosine diphosphate
AET	Alternative electron transfer
AL	Actinic light
ATP	Adenosine triphosphate
ARTO	Alternative respiratory terminal oxidase
BG-11	Growth medium for cyanobacteria
BN-PAGE	Blue-native electrophoresis
CA	Carbonic anhydrase
CBB	Calvin-Benson-Bassham cycle
CCM	Carbon concentrating mechanisms
CET	Cyclic electron transport
CHES	N-Cyclohexyl-2-aminoethanesulfonic acid
Chl a	Chlorophyll a
C_i	Inorganic carbon
Cox	Cytochrome c oxidase
Cyd	Cytochrome bd quinol oxidase
Cyt *b_6f*	Cytochrome b_6f complex
Cyt *c_6*	Cytochrome c_6
D_2	Deuterium
DBMIB	2,5-dibromo-6-isopropyl-3-methyl-1,4-benzoquinone
DCMU	3-(3,4-dichlorophenyl)-1,1-dimethylurea
DIC	Dissolved inorganic carbon
DMPs	Differential model plots
ECS	Electrochromic shift
F_0	The mimimal fluorescence from dark-adapted samples
FC	Fold change
Fd	Ferredoxin
FdxH	Heterocyst-specific ferredoxin

FDP, Flv	Flavodiiron protein
FlR	NAD(P)H:flavin oxidoreductase-like domain
Fld	Flavodoxin
FL	Fluctuating light
F_m'	The maximum level of fluorescence under actinic light
F_m^D	The maximum level of fluorescence without actinic light
FMN	Flavin mononucleotide
$FNR_{(L/S)}$	Ferredoxin:NADP+ oxidoreductase (long/short form)
FR	Far-red
F_s	The steady state fluorescence
F_v	Variable fluorescence, (F_m-F_0)
F_v/F_m	The maximum quantum yield of PSII
GOE	Great Oxidation Event
H_2O_2	Hydrogen peroxide
HC	High CO_2 conditions (1-3% CO_2)
HCO_3^-	Bicarbonate
HEPES	4-(2-hydroxyethyl)-1-piperazineethanesulfonic acid
HL	High light conditions
Hox	Bidirectional hydrogenase
HQNO	2-heptyl-4-hydroxyquinoline n-oxide
Hup	Uptake hydrogenase
LC	Low CO_2 conditions (air level CO_2)
LET	Linear electron transport
MES	2-(N-morpholino) ethanesulfonic acid
MIMS	Membrane inlet mass spectrometry
ML	Moderate light
MV	Methyl violet
Na_2CO_3	Sodium carbonate
NADH	Nicotinamide adenine dinucleotide (reduced)
NADPH	Nicotinamide adenine dinucleotide phosphate (reduced)
Na_2CO_3	Sodium bicarbonate
NDH-1	NAD(P)H dehydrogenase-like complex 1
NH_3	Ammonia
NO	Nitric oxide
N_2O	Nitrous oxide
NPQ	Non-photochemical quenching
OD_{750}	Optical density at 750 nm
OEC	Oxygen-evolving complex
OPP	Oxidative pentose phosphate pathway
ORF	Open reading frame

P_m	The maximum level of oxidizable P700
PBR	Photobioreactor
PBS	Phycobilisomes
Pc	Plastocyanin
PC	Phycocyanin
PCC	Pasteur Culture Collection
PCR	Polymerase chain reaction
PGR5	Proton gradient regulation 5
PGRL1	PGR5-like photosynthetic phenotype 1
PETC	Photosynthetic electron transfer chain
Pheo	Pheophytin
PM	Plasma membrane
pmf	Proton motive force
PQ	Plastoquinone
PQH_2	Plastoquinol
PS	Photosystem
PTOX	Plastidic-type terminal oxidase
ROS	Reactive oxygen species
RTO	Respiratory terminal oxidase
RT-qPCR	Real-time quantitative reverse transcription PCR
RuBisCo	Ribulose bisphosphate carboxylase/oxygenase
RuBP	Ribulose-1,5-bisphosphate
SDH	Succinate dehydrogenase
SDS	Sodium dodecyl sulfate
SP	Saturating pulses
TCA	Tricarboxylic acid
TES	2-[[1,3-dihydroxy-2-(hydroxymethyl)propan-2-yl]amino]ethanesulfonic acid
TM	Thylakoid membrane
WT	Wild type
Y(I)	Quantum yield of Photosystem I
Y(II)	Quantum yield of Photosystem II
Y(NA)	Acceptor side limitation of Photosystem I
Y(ND)	Acceptor side limitation of Photosystem I
TCA	Tricarboxylic acid cycle (Krebs cycle, citric acid cycle)
YFP	Yellow fluorescent protein
ΔpH	Transmembrane proton gradient
$\Delta\psi$	Membrane electric potential

List of Original Publications

This dissertation is based on the following original publications, which are referred to in the text by their Roman numerals:

I Santana-Sánchez A., Solymosi D., Mustila H., Bersanini L., Aro E.M., and Allahverdiyeva Y. Flavodiiron proteins 1–to-4 function in versatile combinations in O_2 photoreduction in cyanobacteria. *eLife*, 2019; 8:e45766.

II Mustila H., Paananen P., Battchikova N., Santana-Sánchez A., Muth-Pawlak D., Hagemann M., Aro E.M., and Allahverdiyeva Y. The flavodiiron protein Flv3 functions as a homo-oligomer during stress acclimation and is distinct from the Flv1/Flv3 hetero-oligomer specific to the O_2 photoreduction pathway. *Plant Cell Physiol*, 2016; 57:1468-1483.

III Nikkanen L., Santana Sanchez A., Ermakova M., Rögner M., Cournac L., and Allahverdiyeva Y. Functional redundancy between flavodiiron proteins and NDH-1 in *Synechocystis* sp. PCC 6803. *The Plant Journal*, 2020; 103(4):1460-1476.

IV Santana-Sánchez A., Ermakova M., Kosourov S., Toth G., Nikkanen L., Walter J., He M., Aro E.M., and Allahverdiyeva Y. Elimination of the vegetative-cell specific Flv1A or Flv3A differently affects O_2 photoreduction and H_2 production in diazotrophic *Anabaena* filament. *Manuscript.*

1 Introduction

1.1 Cyanobacteria

Cyanobacteria, historically also referred to as blue-green algae, are Gram-negative bacteria unique in their capacity to convert sunlight into chemical energy *via* oxygenic photosynthesis.

1.1.1 Significance of cyanobacteria on our planet: Past, present, and future

Evolution **-** Oxygenic photosynthesis is undoubtedly one of the most important metabolic pathways to have evolved on Earth. The biological availability of O_2 drastically changed the redox state of the Earth's atmosphere and oceans, shaping the evolution of complex life forms (Fischer et al., 2016b; Sánchez-Baracaldo & Cardona, 2020). Traditionally, it has been assumed that water-splitting photosynthesis was invented by cyanobacteria 2.4 billion years ago (concomitant to the Great Oxidation Event, GOE) (Fischer et al., 2016a; Cardona et al., 2015). However, recent phylogenetic and structural evidence has challenged this perspective, suggesting that oxygen-evolving photosynthesis appeared at least a billion years earlier than was previously believed, at almost the beginning of life on Earth and possibly before the rise of cyanobacteria (Figure 1; Sánchez-Baracaldo & Cardona, 2020). Yet, the question as to how and when cyanobacteria inherited the capacity to perform oxygenic photosynthesis from its most recent common ancestor remains to be answered (see Oliver et al., 2021 and Soo et al., 2019).

What is clear in the timeline of photosynthesis, is the key role of GOE triggering the evolution of the majority of extant Cyanobacterial diversity (Fig. 1). The earliest forms of Cyanobacteria were most likely small unicellular thylakoid-less organisms, represented by the Gloeobacter genus (Rippka et al., 1974; Sánchez-Baracaldo, 2015). The subsequent emergence of multicellularity likely conferred a remarkable advantage for the colonisation of new environmental niches and increased the diversification rates of Cyanobacteria, closer to the GOE (Schirrmeister et al., 2015).

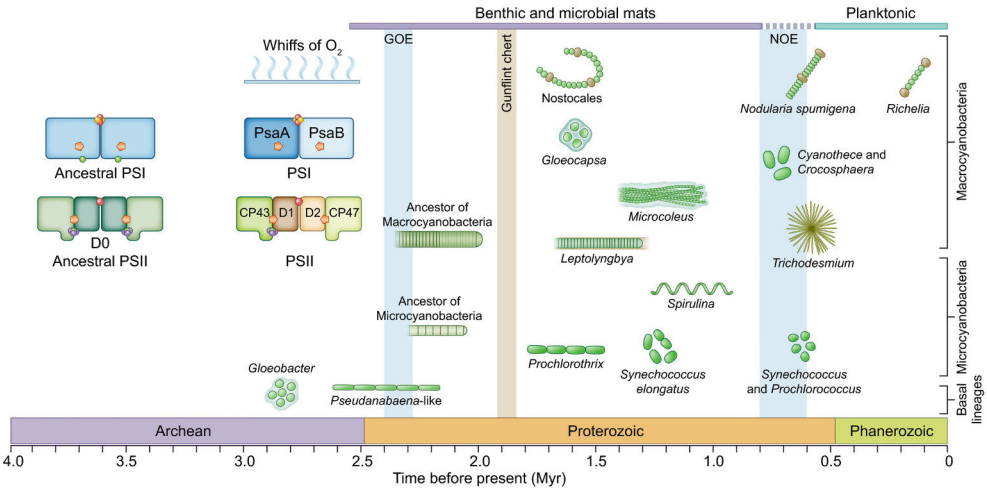

Figure 1. Timeline of the emergence of oxygenic photosynthesis and cyanobacterial lineages. Extracted from Sánchez-Baracaldo & Cardona, 2020.

Ecological impact - Today, cyanobacteria are one of the most widely distributed phyla on the planet. They can be, for example, components of benthos or plankton; and also occupy extreme environments such as hot deserts, Antarctic dry valleys, and tropical rain forests (reviewed in Stal, 2007). Due to their abundance, cyanobacteria play an important role at the base of marine food webs and in biogeochemical cycles (Ullah et al., 2018). About 25% of global primary photosynthetic productivity originates from cyanobacteria (Flombaum et al., 2013). Nearly one-fourth of total anthropogenic CO_2 emissions are taken up in the ocean (Friedlingstein et al., 2020), where planktonic cyanobacteria play a role in assimilating dissolved inorganic carbon during photosynthesis and benthic cyanobacterial mats likely work as "biological pumps" storing CO_2 in the deep ocean (Brocke et al., 2015). Additionally, N_2-fixing cyanobacteria are important in the global nitrogen cycle, whereby they provide biologically available nitrogen to their habitat and are the major N_2 fixers in the open ocean (reviewed in Zhang et al., 2020).

Potentials for the future blue bioeconomy - In the framework of a bioeconomy based on the use of renewable aquatic resources (the Blue Bioeconomy), cyanobacteria offer key advantages for light-powered biotechnological applications: (i) They are fast-growing photosynthetic bacteria; (ii) they have minimal nutritional requirements; (iii) they are capable of growing in closed PBRs and/or outdoor water surfaces such as the sea and ponds, without competing with arable land; and, importantly, (iv) they are readily genetically tractable microorganisms.

Valorization of cyanobacterial biomass for the production of nutritional products, bioactive compounds and biofuels has been extensively reported (Mazard et al. 2016; Sitther et al., 2020; Zahra et al., 2020), some applications are

commercially available (Singh et al., 2017; Chittora et al., 2020), but yet mostly requiring costly biorefinery processes (Chandra et al., 2019).

The development of a cyanobacterial chassis for the direct photoconversion of water and CO_2 into target chemicals represents a cost-efficient approach to bioproduction (Arora et al., 2020). For example, the capability of cyanobacteria to produce hydrogen (H_2), a clean energy carrier with high-energy yields, *via* the direct biophotolysis of water is currently at the center of research efforts in biohydrogen generation (Lindblad et al., 2019). Over recent decades, substantial progress in synthetic biology toolkits for cyanobacteria have allowed the rational design of engineered strains for the production of commodities (e.g., ethylene, bioplastics), biofuels (e.g., diesel-like compounds, butanol), and high-value products (e.g., pharmaceuticals, nutraceuticals, cosmetics) (reviewed in Khan et al., 2019). Despite several successful proof-of-concept studies, a number of technological challenges still need to be overcome before cyanobacteria become commercial cell factories. Scientific breakthroughs in metagenomics-based studies and CRISPR-based genome editing are expected to unlock the full potential of cyanobacteria for future light-powered biotechnology (Hitchcock et al., 2020).

1.1.2 Classification and model organisms

The extreme variety of morphological and ecological features found in cyanobacteria makes it challenging to determine taxonomic relations between species. The most traditional approach is based on their morphology, where cell complexity ranges from unicellular (Section I-II) to filament undifferentiated (Section III) to branching differentiated filaments (IV-V), the last being the most complex (Rippka et al., 1979). With the introduction of molecular sequencing, 20 years ago, the cyanobacterial species have been constantly updated (Shih et al., 2013; Komárek et al., 2014; Willis & Woodhouse, 2020). Additionally, α- and β-cyanobacteria have been grouped based on the type of carboxysome and their RuBisCo phylogeny (Rae et al., 2013).

***Synechocystis* sp. PCC 6803 - a model of all time:** Isolated in 1968, *Synechocystis* sp. PCC 6803 (hereafter *Synechocystis*) was the first phototroph having its genome fully sequenced (Kaneko et al., 1996), and ever since it has been the most widely studied model cyanobacterium. *Synechocystis* is a unicellular, non-N_2-fixing and non-toxic freshwater β-cyanobacterium belonging to the order Synechococcales. Its genome consists of a circular chromosome (3.6 Mb) and seven plasmids (Kaneko et al., 2003). Over the last decade, several molecular biology tools have been developed to engineer *Synechocystis* for photosynthetic research as well as biotechnological applications (reviewed in Mills et al., 2020).

***Anabaena* sp. PCC 7120 - a more complex model:** *Anabaena* sp. PCC 7120 (hereafter *Anabaena)* is a freshwater filamentous β-cyanobacterium belonging to the order Nostocales. *Anabaena* is a representative of the filamentous heterocyst-forming cyanobacterial group capable of N_2-fixation. Its genome (sequenced 20 years ago) contains a single chromosome of 6.41 Mb and six plasmids (Kaneko et al., 2001). The multicellular nature of *Anabaena* makes it a suitable model for studying cellular differentiation, cell-to-cell communication, and N_2 fixation.

1.1.3 The multicellular lifestyle of *Anabaena*

Anabaena filaments undergo cellular differentiation in order to deal with changes in environmental conditions. At least four types of specialized cells have been described in *Anabaena*: vegetative (photosynthetic) cells, heterocysts (N_2-fixing cells), akinetes (spore-like cells), and hormogonia (reproductive, small motile filaments) (Flores & Herrero, 2010). In this section, I will focus on the structural features of filaments containing the two cell types that most concern this thesis: vegetative cells and heterocysts. I will then discuss the physiology and bioenergetics of heterocysts in section 1.5.

The filament of vegetative cells: Under optimal growth conditions, filamentous cyanobacteria consist mainly of vegetative cells able to fix CO_2 by performing oxygenic photosynthesis. Each vegetative cell in the filament is surrounded by a cytoplasmic membrane and a peptidoglycan mesh, whereas the outer membrane is continuous along the filament, establishing a continuous periplasmic space (Mariscal et al., 2007). A functional continuous periplasm providing a communication conduit for the transfer of metabolites along the filament has been suggested (Flores et al., 2006), although direct evidence for this remains unresolved.

Structure of mature heterocysts: When combined nitrogen is limited in the medium, some specific vegetative cells in the filament (about 10% of cells in filament) will differentiate into a type of cell specialized in atmospheric N_2 fixation, the heterocyst. Heterocysts provide micro-oxic conditions required for the expression and function of the highly O_2-sensitive nitrogenase enzyme, which is responsible for N_2 fixation (Flores et al., 2015). The process of heterocyst differentiation involves massive changes orchestrated by complex gene expression patterns (reviewed in Herrero & Flores, 2019). Mature heterocysts display a thickened cell envelope consisting of two chemically different layers placed outside of the outer membrane: a glycolipid laminated layer (heterocyst glycolipid, Hgl) to limit the diffusion of gases (Xu et al., 2008), and a thicker layer of polysaccharides (heterocyst envelope polysaccharide, Hep), which seems to protect the glycolipid layer (Nicolaisen et al., 2009). A neck-like structure filled with a “cyanophycin plug”

is remarkable at the poles of the heterocysts (Fig. 2) and has a role limiting the entry of O_2 from the neighbouring vegetative cells into the heterocysts (Walsby, 2007).

Inside the heterocysts, the thylakoid membranes are rearranged into two contrasting membrane domains (Santamaría-Gómez et al., 2018): a highly contorted membrane system close to heterocysts poles, known as "honeycomb" (Lang & Fay, 1971); and less convoluted peripheral thylakoids in the cytoplasm (Sherman et al., 2000). While the "honeycomb" membranes are rich in terminal oxidases (Valladares et al., 2003) and cyclic phosphorylation (Kumazaki et al., 2013), the peripheral thylakoids harbour a similar protein composition to that observed in thylakoids of vegetative cells, although the amounts and relative stoichiometries of these proteins are changed (Cardona et al., 2009; Ow et al., 2009). Importantly, heterocysts lack the CO_2-fixing enzyme RuBisCO which is found in vegetative cells encapsulated in cytoplasmic microcompartments named carboxysomes. As a result, heterocysts rely on fixed carbon supply from the neighbouring vegetative cells, and in return heterocysts provide fixed nitrogen. The exchange of metabolites and signalling molecules occurs *via* cell-to-cell communication.

Intercellular communication and cell-cell joining structures: The molecular exchange between cells in the cyanobacterial filaments occurs by diffusion through proteinaceous structures connecting adjacent cells (Mullineaux et al., 2008; Wilk et al., 2011; Nieves-Morión et al., 2017). These proteinaceous structures, known as septal junctions (Mariscal, 2014; Flores et al., 2016), penetrate the septal peptidoglycan occurring between cells through holes called nanopores (Lehner et al., 2013), which are visible by electron microscopy (reviewed in Flores et al., 2019). The cytoplasmic membrane proteins SepJ (Flores et al., 2007) and FraC/FraD (Merino-Puerto et al., 2010) are proposed to be involved in the formation of two different types of septal junction complexes in *Anabaena* (Merino-Puerto et al., 2011). Recent studies have shown that the deletion of the genes encoding septal proteins has a significant impact beyond perturbed cell-cell communication, leading to global changes in the expression of genes involved in heterocyst differentiation, cell wall biogenesis, CO_2 fixation and photosynthesis (Camargo et al., 2021). It has further been demonstrated that, upon stress, septal junction complexes reversibly gate intercellular communication (Weiss et al., 2019). Recently, a correlation between the metabolic status of each individual cell in the filament and the activity of septal junctions has been proposed (Arévalo et al., 2021; Kieninger & Maldener, 2021).

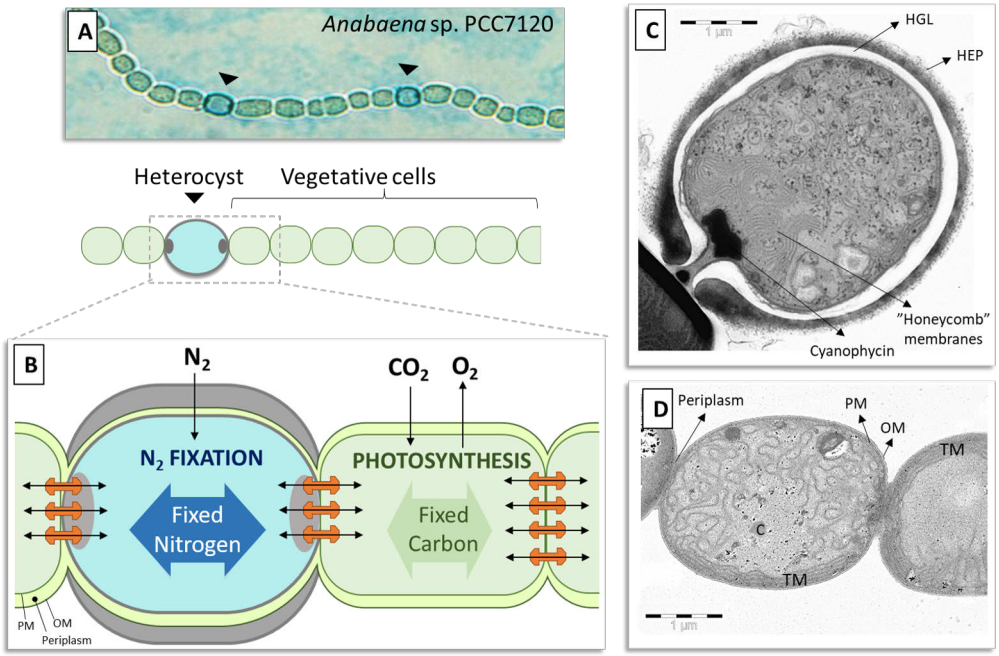

Figure 2. Filamentous N_2 fixing cyanobacteria. (**A**) Light micrograph of *Anabaena* filament of vegetative cells showing Alcian blue-stained heterocysts (pointed by black arrowheads). (**B**) Simplified representation of the multicellular nature of *Anabaena* showing cellular differentiation, distinct metabolisms, and intercellular communication between the two cell types. Electron micrographs showing (**C**) a terminal heterocyst and (**D**) vegetative cells from *Anabaena*. HGL, heterocyst glycolipid layer, HEP, heterocyst envelope polysaccharide, OM, outer plasma membrane. PM, inner plasma membrane, TM, thylakoid membranes. Micrographs by A. Santana-Sánchez.

1.2 Photosynthesis in cyanobacteria

All oxygenic phototrophs utilize sunlight energy to oxidize water to molecular oxygen and use the energy of electrons to synthesize carbohydrates that are essential for their metabolism. Oxygenic photosynthesis consists of two phases: in the first phase, several light reactions take place in the thylakoid membrane (TM). These reactions involve four integral protein complexes: photosystem II (PSII), photosystem I (PSI), cytochrome b_6f (Cyt b_6f) and ATP synthase (ATPase); in the second phase, NADPH and ATP produced during light reactions are used as reducing power and energy for CO_2 assimilation in the Calvin-Benson-Basham (CBB) cycle. Thus, oxygenic photosynthesis can be pictured as a metabolic supply–demand system (Hofmeyr & Cornish-Bowden, 2000) in which the balancing between the two phases (light reactions and CO_2 fixation) is essential for safe and optimal photosynthetic performance.

1.2.1 Energy supply: Light reactions

The use of light energy to extract electrons from water and transfer them to $NADP^+$, following a linear electron transport (LET), represents the major route to providing the reducing power (NADPH) and energy (ATP) needed for cell metabolism (Fig. 3). In cyanobacteria, photons of light are mostly absorbed by phycobilisomes (PBS), large antenna protein complexes containing linear tetrapyrrole pigments, phycobilins. The excitation energy is then transferred to the reaction centre chlorophylls of PSII and PSI (P680 and P700, respectively), where primary charge separation takes place and the radical pairs: $P680^{+\bullet}Pheo^{-\bullet}$ (at PSII) and $P700^{+\bullet}A_0^{-\bullet}$ (at PSI) are formed. These events are followed by rapid charge stabilization processes (reviewed in Stirbet et al., 2019*)*.

On the donor side of PSII, $P680^{+\bullet}$ (the strongest oxidant in nature!) obtains an electron from redox-active Tyrosine-Z and serves as a driving force for the oxidative splitting of H_2O by the oxygen-evolving complex (OEC) holding the Mn_4CaO_5 cluster in the active site (Ferreira et al. 2004; Umena et al. 2011). Four light absorption events are needed to oxidize two H_2O molecules to one molecule of O_2 with the release of four protons and four electrons to the lumen, as proposed in the water-oxidation cycle (Kok et al., 1970). Meanwhile, on the acceptor side of PSII, the electron available on $Pheo^{-\bullet}$ moves to Q_A (a PSII-tightly bound primary quinone, one-electron acceptor) and then to Q_B (a PSII-loosely bound secondary quinone, two-electron acceptor). After a second charge separation at P680, Q_B accepts two electrons and two protons from the cytosolic side of the TM forming plastoquinol, PQH_2, a mobile electron carrier. PQH_2 transfers two electrons to Cyt b_6f, one of which is returned to the PQ pool in a process known as Q-cycle (Cramer et al., 2011), and the second electron is transferred to plastocyanin (Pc) or cytochrome c_6 (Cyt c_6), either of which will transfer the electron to PSI. Both Pc and Cyt c_6 reduce PSI with similar kinetics (Durán et al., 2004). While Pc is the dominant electron carrier in *Synechocystis*, as in many other cyanobacteria (Lea-Smith et al., 2016), Cyt c_6 is expressed under copper-limiting conditions and has recently shown to be essential in the physiology of heterocysts in *Anabaena* (Torrado et al., 2019).

The electron transferred to PSI reduces the oxidized $P700^{+\bullet}$ (from the primary charge separation) and the electron available on $A_0^{-\bullet}$ moves through a series of intermediates to eventually reduce the mobile Fd, or flavodoxin (Fld) under iron limiting conditions (Pierella et al., 2014), on the cytosolic side of TM. In the LET pathway, Fd channels electrons towards ferredoxin $NADPH^+$-reductase (FNR) which reduces $NADP^+$ to NADPH. In cyanobacteria, two forms of FNR originated from a single gene have been described: the longer isoform FNR_L, bound to the PBS antenna, photoreduce NADP+ to NADPH, whereas the small isoform soluble FNR_s has been suggested to function in opposite direction (Thomas et al. 2006).

Proton budget: Overall, for every 2 molecules of H_2O split at PSII, 1 molecule of O_2 is released, 4 electrons enter to the photosynthetic electron transport chain (PETC), 2 molecules of NADPH are synthesized, and 12 protons are deposited into the lumen (4 protons derived from H_2O oxidation and 8 protons from the Q-cycle). The protons accumulated in the lumen generate a proton motive force (*pmf*), composed of a transmembrane proton gradient (ΔpH) and a membrane electric potential (Δψ), which is used to power the phosphorylation of ADP to ATP by ATPase (reviewed in Armbruster et al., 2017). The H^+:ATP stoichiometry of ATPase in cyanobacteria varies between species (Pogoryelov et al., 2007). In *Synechocystis* and *Anabaena,* as in other cyanobacteria, LET produces an ATP:NADPH ratio of 2.6:2, which does not satisfy the ATP:NADPH ratio of 3:2 required for the CBB cycle (Pogoryelov et al., 2007; Allen, 2003). In fact, the situation seems to be further complicated as there are many other cellular processes that consume ATP and the ATP:NADPH imbalance is worsened under stress conditions. Thus, cyanobacteria have had to develop adaptive responses based on the high flexibility of the photosynthetic machinery for their successful colonization on Earth.

1.2.2 Metabolic demand: CO_2 acquisition and fixation

Phototrophic organisms utilize the energy (ATP) and reducing equivalents (NADPH) generated during photosynthetic light reactions for almost all other cellular processes. The vast majority of metabolic networks begin with the fixation of CO_2 by Ribulose-1,5-bisphosphate carboxylase/oxygenase (RuBisCo) in the CBB cycle. RuBisCo, considered the most abundant enzyme in nature, performs a carboxylation reaction using CO_2 and ribulose 1,5-biphosphate (RuBP) to generate two molecules of 3-phosphoglycerate (3-PGA). The cycle uses 3 ATP and 2 NADPH molecules per molecule of fixed CO_2 (Allen, 2003). Nevertheless, cyanobacterial RuBisCo has a relatively low affinity for CO_2, and it requires a CO_2-rich environment to reach its optimal catalytic rate (Savir et al., 2010). Therefore, CO_2 fixation critically depends upon a complex Carbon Concentrating Mechanisms (CCM) evolved in cyanobacteria to increase the levels of inorganic carbon (C_i) around RuBisCO (Burnap et al., 2015). Cyanobacterial CCM consist of (1) highly efficient uptake systems for active transport of bicarbonate (HCO_3^-) and CO_2 into the cytoplasm, and (2) special microcompartments called carboxysomes to facilitate high rates of CO_2 fixation (Kerfeld & Melnicki, 2016; Turmo et al., 2017).

Five C_i transporters have been described in cyanobacteria, although not all are conserved between species (reviewed in Hagemann et al., 2021). Three plasma membrane-associated transporters are involved in the uptake of HCO_3^-: BicA (a low-affinity Na^+-dependent bicarbonate transporter), SbtA (a high-affinity Na^+/HCO_3^- symporter), and BCT1 (a high-affinity HCO_3^- transporter from the ATP-binding

cassette family) (Burnap et al., 2015). The CO_2 uptake system involves two thylakoid-bound complexes: NDH-1_3 (a high-affinity, low-flux, low C_i-inducible complex) and NDH-1_4 (a low affinity, high flux, constitutive complex). Both NDH-$1_{3/4}$ complexes possess unique subunits that have carbonic anhydrase (CA)-like activity, named "Cup" proteins, and use redox energy to trap CO_2 in the cytoplasm by hydration into HCO_3^- (Battchikova et al., 2011; Han et al., 2017; Miller et al., 2021). Working together, the uptake systems maintain elevated concentrations of HCO_3^- in the cytoplasm to supply the RuBisCo-containing carboxysomes. Carboxysomes are polyhedral bodies composed of a selective permeable protein shell that allows the diffusion of HCO_3^- but impedes CO_2 leakage into the cytoplasm (Mahinthichaichan et al., 2018). In addition to RuBisCo, carboxysomes contain the CA enzyme which facilitates the conversion of HCO_3^- into CO_2 near the active site of RuBisCo. Two types of carboxysomes (α and β) seem to have arisen by convergent evolution, with differences in composition and assembly, but essentially the same biological function in cyanobacteria from different niches (oceanic α-cyanobacteria and β-cyanobacteria found in freshwater/estuarine) (Kerfeld & Melnicki, 2016; Whitehead et al., 2014).

Besides the carboxylation reaction, RuBisCo also catalyzes the competing reaction of oxygenation between RuBP and O_2, in which only one molecule of 3-PGA is produced together with one molecule of the toxic 2-phosphoglycolate (2-PG). Detoxification of 2-PG is a costly process, in terms of CO_2 and ATP losses, called photorespiration (Bauwe et al., 2010). Although photorespiration is generally regarded as one of the most wasteful processes, several studies have shown regulatory feedback from photorespiration to both the Calvin–Benson cycle and photosynthesis (reviewed in Timm & Hagemann, 2020; Fernie & Bauwe, 2020). For instance, 2-PG works as a signal of C_i starvation (Zhang et al., 2018), and the photorespiration pathway can act as a valve for the dissipation of excess reducing equivalents under low C_i and high-light conditions (Hackenberg et al., 2009; Allahverdiyeva et al., 2011).

In cyanobacteria, the expression of the C_i uptake system is tightly regulated at transcript level (Herrero & Flores, 2019). The transcriptional factor NdhR acts as a repressor of the CCM-related genes. NdhR control is modulated upon binding 2-PG and 2-oxoglutarate (2-OG) effectors. In contrast, the CmpR and CyAbrB2 transcriptional regulators regulate several CCM-related genes positively (reviewed in Zhang et al., 2018). In *Anabaena*, an additional LysR-type transcriptional regulator, PacR, has been shown to activate the RuBisCo-encoding operon (Picossi et al., 2015).

1.3 Regulation of photosynthetic electron transport in cyanobacteria

The need to balance ATP/NADPH ratios: Cyanobacteria can be found in aquatic and terrestrial environments constantly exposed to changing environments. In this context, cyanobacteria are challenged to balance the photochemical production of ATP and NADPH to perfectly match the metabolic demand of the cells. Any imbalance in the production and/or consumption of ATP or NADPH could be fatal, as it can lead to over-reduction of the PETC and consequent accumulation of toxic reactive oxygen species (ROS), which in turn cause oxidative damage to photosystems leading to photoinhibition, and affecting proteins, DNA, and lipids (Allen, 2003; Latifi et al., 2009; Mullineaux, 2014a).

Therefore, cyanobacteria have evolved sophisticated regulatory mechanisms to maintain redox balance of the PQ pool and to avoid damage to the photosystems. Some of these photosynthetic mechanisms include: (1) the dissipation of excess excitation energy as heat by OCP-related nonphotochemical quenching (reviewed in Bao et al., 2017); (2) state transitions to regulate the distribution of excitation energy between PSII and PSI (see review by Calzadilla & Kirilovsky, 2020); and (3) the ΔpH-dependent control of Cyt b_6f which serves to protect PSI from damage (Checchetto et al., 2013; Malone et al., 2021).

The redistribution of electron flux through different auxiliary electron transfer (AET) pathways is another regulatory mechanism that allows fine tuning of the ATP:NADPH ratio and prevents over-reduction of the PETC (reviewed in Alboresi et al., 2019; Nikkanen et al., 2021). Cyanobacteria possess AET pathways that regulate the PETC by either recycling electrons around PSI or diverting electrons from the PETC.

1.3.1 Recycling electrons in the PETC: The role of NDH-1 complexes

Cyclic electron transport (CET) around PSI is considered as the main AET pathway contributing to ATP:NADPH balance (Allen, 2003; Shikanai, 2017). During CET, electrons are recycled from the acceptor side of PSI and shunted back to the PQ pool, generating *pmf* to synthesize extra ATP molecules, without net NADPH production (Kramer et al., 2004; Shikanai, 2007, Yamori & Shikanai, 2016). In cyanobacteria, the major CET pathway is mediated by the NAD(P)H dehydrogenase-like complex 1 (NDH-1) (Battchikova et al., 2011; Bernat et al., 2011; Miller et al., 2021). Cyanobacteria possess four functional versions of the NDH-1 complex that share homology with the respiratory Complex I found in bacteria and mitochondria (reviewed in Strand et al., 2019). Unlike Complex I, the NDH-1 complexes of cyanobacteria lack the NADH dehydrogenase domain and instead possess conserved

oxygenic photosynthesis-specific subunits which have been proposed to regulate the binding of NDH-1 complex with Fd, its electron donor (Laughlin et al., 2019; 2020; Schüller et al., 2019; 2020; Zhang et al., 2020; Pan et al., 2020). Of the four cyanobacterial NDH-1 complexes, the NDH-1_1 and NDH-1_2 (a.k.a. NDH-1L and NDH-1L' containing the NdhD1 and NdhD2 subunits, respectively) are primarily active in CET and respiration under standard growth conditions (Zhang et al., 2004; Battchikova et al., 2011; Peltier at el., 2016). The other two complexes, NDH-1_3 and NDH-1_4, (a.k.a. NDH-1MS and NDH-1MS' containing the NdhD3 and NdhD4 subunits, respectively) have shown a limited contribution to CET (Bernat et al., 2011) and are mostly involved in CO_2 acquisition (discussed in 1.2.2). Under environmental stress conditions, the formation of an NDH-1-PSI supercomplex has been shown to be essential in cyanobacteria to stabilize PSI, as it facilitates the transfer of electrons from reduced Fd (Gao et al., 2016). Moreover, a key role of NDH-$1_{3/4}$ complexes has recently been suggested under high-light stress to mediate both CO_2 uptake and CET, although further validation of the model is needed (Zhang et al., 2020).

A further CET pathway in cyanobacteria relies on the co-existence of photosynthetic and respiratory electron transport in the same TM (reviewed by Mullineaux 2014b; Fig. 3). This unique feature raises the possibility for an "unorthodox" electron transport route in which electrons cross over from respiratory donors to PSI (Liu et al., 2012; Bernat et al., 2011). The succinate dehydrogenase (SDH) and the NDH-$1_{1/2}$ complexes are regarded as principal respiratory electron donors in cyanobacteria (Cooley & Vermaas, 2001; Ogawa & Mi, 2007). The SDH complex was shown to play a role feeding electrons to the PQ pool in dark via succinate oxidation in the tricarboxylic acid (TCA) cycle (Cooley & Vermaas, 2001). The participation of NDH-$1_{1/2}$ complexes in respiratory electron transport has been suggested based on experiments showing decreased respiratory activity in *Synechocystis* mutants with disrupted NDH-$1_{1/2}$ complexes (Ohkawa et al., 2000b; Ogawa et al., 2013; Bernat et al., 2011; Zhao et al., 2015). Nevertheless, it is not clear how the NDH-$1_{1/2}$ complexes acquire and transfer electrons to the PQ pool in darkness. It is plausible that during respiration, NDH-$1_{1/2}$ complexes unconnected to PSI (Gao et al., 2016), receive electrons from NADPH *via* FNRs and Fd, as suggested from previous *in vitro* and co-elution studies (Strand et al., 2017). After electrons are loaded into the PQ pool, respiratory PQH_2 oxidation occurs by transferring electrons *via* Cyt b_6f to PSI (CET pathway) or to respiratory terminal oxidases (RTOs) (see *Terminal oxidases* in 1.3.2). Importantly, previous studies have shown both SDH and NDH-$1_{1/2}$ complexes to become more evenly distributed within TM when cells are exposed to moderate light, which increases the probability that respiratory electrons are transferred to PSI rather than to RTOs (Liu et al., 2012; Mullineaux, 2014b).

A "controversial" CET pathway mediated by the proton gradient regulation 5 (PGR5) and PGR5-like photosynthetic phenotype 1 (PGRL1) has been proposed (Munekage et al., 2002; DalCorso et al., 2008). Previous studies have shown a crucial role of the PGR5 and PGRL1 in survival of *Arabidopsis thaliana* under fluctuating light conditions (Suorsa et al., 2012; Yamori et al., 2016). A comparable importance of the PGR5/PGRL1 complex was reported in the green alga *Chlamydomonas reinhardtii* during anoxia, high light, or limited carbon fixation (Johnson et al., 2014). However, the detailed mechanism of the PGR5-mediated CET pathway is still a topic of debate. In cyanobacteria, functional counterparts of both plant PGR5 and PGRL1 (Ssr2016 and Sll1217, respectively) have been suggested in *Synechocystis* (Yeremenko et al., 2005; Dann & Leister, 2019) although their functional roles remain unclear (Allahverdiyeva et al., 2013; Sánchez-Riego et al. 2013).

The interdependence of LET and CET and the lack of reliable methods make it difficult to determine the relative contribution of CET around PSI *in vivo* (Fan et al., 2016). Recent attempts have shown contrasting results on the efficiency of CET in *Synechocystis* (Sétif et al., 2020; Theune et al., 2021), although the potential of the newly developed Dual-KLAS-NIR method for future investigations was demonstrated (Klughammer & Schreiber, 2016). The *pmf* generated during CET has been mostly attributed to the proton pumping activity of NDH-$1_{1/2}$ complexes and additional contribution of Cyt b_6f in the Q-cycle (Miller et al., 2021). It is plausible that the CET mediated by NDH-1 complexes would be prioritized under conditions when more *pmf* to fuel extra ATP production is needed, while other AET pathways (PGR5/PGRL1 and SDH) become relevant when cells urgently need to deal with excess reductant and less proton pumping is needed (Miller et al., 2021).

1.3.2 Diverting electrons from the PETC – Alternative electron sinks

Cyanobacteria have evolved diverse alternative electron sinks to remove excess electrons from the PETC in order to avoid the dangerous over-reduction of photosynthetic apparatus and contribute to the generation of *pmf* both during respiration and LET (Fig. 3). The major alternative electron sinks in cyanobacteria involve: (1) Terminal oxidases, (2) Bidirectional hydrogenases, and (3) Flavodiiron proteins (see 1.4)

Terminal oxidases: The use of O_2 as a powerful electron acceptor allows cyanobacteria to simultaneously divert excess of electrons from PETC and fine-tune the intracellular O_2 concentration. During respiration, RTOs catalyze the reduction of O_2 into H_2O using the electrons obtained from the breakdown of organic compounds. All RTOs are membrane-bound enzymes, and their expression varies between cyanobacterial species and growth conditions (reviewed in Schmetterer,

2016). Three RTOs have been described in *Synechocystis*: (1) the cytochrome bd quinol oxidase (Cyd); (2) the aa3-type cytochrome c oxidase (Cox); and, (3) the alternative respiratory terminal oxidases (ARTO type 1). Both Cox and Cyd have been localized in TM (Pils & Schmetterer, 2001). Cox has been suggested to function downstream of Cyt b_6f, receiving electrons from Pc/Cyt c_6 (Navarro et al., 2005; Paumann et al., 2004). While Cyd directly oxidizes PQH_2 (Berry et al., 2002; Ermakova et al., 2016), ARTO has instead been located in PM (Pisareva et al., 2011) where it removes electrons from the reduced PQ pool. Further to this, *Anabaena* employs 2 additional RTOs: (4) ARTO type 2; and (5) the plastidic-type terminal oxidase (PTOX) (Schmetterer, 2016). Interestingly, ARTO type 1 and type 2 (previously known as Cox2 and Cox3, respectively) in *Anabaena* are only expressed in the heterocysts and have been shown to be crucial in maintaining a low O_2 concentration, required for nitrogenase function, inside the heterocysts (Valladares et al., 2003; see 1.5). PTOX is found predominantly in marine cyanobacteria (Grossman et al., 2010) and has been involved in the direct oxidation of the PQ pool under iron-limiting conditions (McDonald et al., 2003; Bailey et al., 2008). All RTOs contribute to the proton gradient across the membrane by: (1) releasing protons from PQH_2 oxidation into the lumen; (2) consuming protons from the cytosol during the reduction of O_2; and, in the case of Cox, (3) by pumping protons from the cytosol into the lumen (Brändén et al., 2006).

As a result of the intertwined photosynthetic and respiratory electron transfer in the TM, the role of RTOs as alternative electron sinks seems not to be limited to darkness, but also extended to light. Growth experiments under different light regimes showed that the importance of Cyd and Cox depends on both the length of the dark and light periods and the level of photodamage produced during the light period (Ermakova et al., 2016; Lea-Smith et al., 2013). While Cox is the main RTO under dark respiration, it is able to compete for electrons with PSI during high light (Ermakova et al., 2016) and becomes essential under low light (Kufryk & Vermaas, 2006). However, Cyd contributes to O_2 reduction under light only when LET is interrupted at the Cyt b_6f site (Berry et al., 2002) or when PSI is drastically inhibited (Ermakova et al., 2016).

Bidirectional hydrogenase (Hox). Hox represents another alternative electron sink widespread in cyanobacteria, although its presence has not been reported in marine cyanobacteria isolated from the open ocean (Ludwig et al., 2006). Hox is a heteropentameric enzyme encoded by the *hoxEFUYH* operon consisting of a hydrogenase module (HoxYH) and a diaphorase moiety (HoxEFU) (reviewed in Bothe et al., 2010 and Mishra et al., 2018). Depending on the metabolic context, Hox can function by removing excess electrons to produce H_2 or reducing electron carriers *via* H_2 oxidation (Appel et al., 2000; Gutekunst et al., 2014). In the former case, Hox functions as a valve by diverting electrons from the acceptor side of PSI and generating

extra *pmf* as protons are consumed from the cytoplasm. Due to its O_2 sensitivity and soluble (or loosely bound) nature, Hox functions as a quick electron-transport switch, primarily important during the transition from anaerobiosis in the dark to aerobic conditions in the light (Cournac et al., 2002; 2004). A recent *in vitro* study has shown the function of HoxEFU subcomplex, independently of HoxYH, as an electron shuttle among NAD(P)H, Fld, and several Fds (Artz et al., 2020). These findings raise the possibility for a dynamic interaction between HoxEFU and different components of the PETC, although this study awaits confirmation in an *in vivo* system.

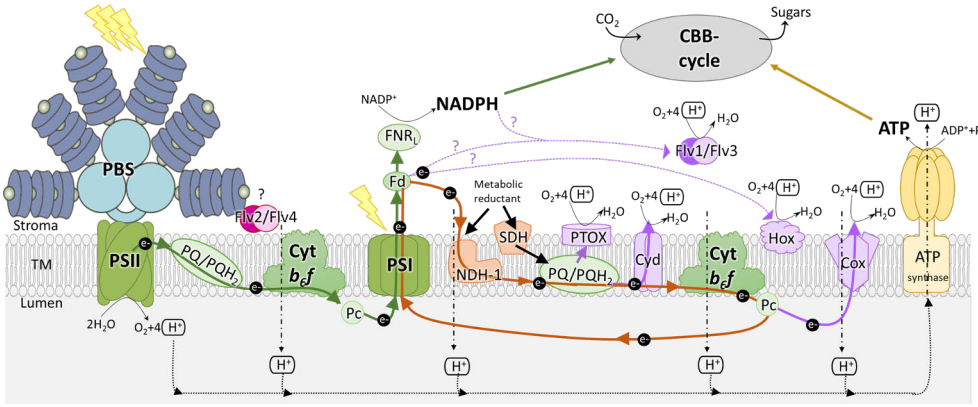

Figure 3. Schematic representation of the photosynthetic linear and alternative electron transport routes co-existing in the TM of *Synechocystis* (Knowledge excluding the research findings obtained in this thesis). LET is indicated by green arrows, and CET by orange arrows. Alternative electron sinks are indicated by purple arrows. Dotted purple arrows indicate possible/unverified electron transport pathways. Dotted black arrows indicate proton translocation across the TM.

1.4 Flavodiiron proteins in oxygenic phototrophs

The O_2 produced by ancestral cyanobacteria would have caused oxidative stress to most of the anoxic lifeforms on the early Earth, beginning with a self-poisoning. Therefore, the evolution of antioxidant strategies must have played an essential role in the transition to an oxygenated world (Fischer et al., 2016a). An advanced antioxidant system, widespread in all life Domains (Bacteria, Archaea and Eukarya), is mediated by the FDPs (Wasserfallen et al., 1998; Di Matteo et al., 2008; Vicente et al., 2008). The FDPs constitute a conserved family of enzymes that catalyze the reduction of O_2 to water and/or nitric oxide (NO) to nitrous oxide (N_2O), protecting cells from oxidative and nitrosative stress (Saraiva et al., 2004; Vicente et al., 2008, Folgosa et al., 2018). The diversity of the modular structure of FDPs has been associated with functions beyond their initially determined antioxidant role (Folgosa et al., 2018).

1.4.1 Modular structure

FDPs are modular proteins consisting minimally of two conserved core motifs: (1) the N-terminal metallo-β-lactamase-like domain, harbouring a non-heme diiron centre where O_2 and/or NO reduction take place; and (2) the C-terminal flavodoxin-like domain with a flavin mononucleotide (FMN) which serves as an electron carrier (Vicente et al. 2002; 2008, Saraiva et al., 2004). In addition to the common core domains, some members of the FDP family have extra C-terminal domains (such as rubredoxins, flavin reductases, iron-sulphur cluster, NADH:rubredoxin oxidoreductase-like and, Neelaredoxin-like domain) that have allowed them to be distinguished into nine classes (Classes A-I) (Romão et al., 2016b; Folgosa et al., 2018; Martins et al., 2019).

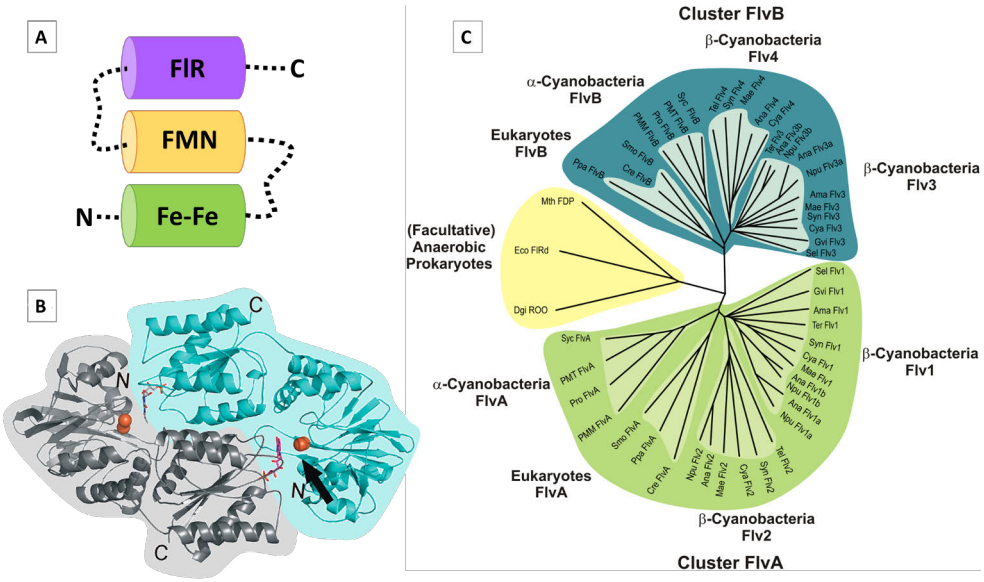

Figure 4. Structure and occurrence of class C FDPs. (**A**) Modular structure of a monomer (**B**) The 'head-to-tail' structure of *Synechocystis* Flv2/Flv4-heterodimer. (**C**) Phylogenetic analysis of FDPs in the obligate and facultative anaerobes and oxygenic photosynthetic organisms. See Zhang et al., 2009 for the detailed description of organisms included in the phylogenetic tree. Figures 4B and 4C are extracted from Zhang et al., 2012 and 2009, respectively.

All FDPs described in oxygenic phototrophs (with exception of *Picea sitchensis*) are endowed with an extra C-terminal NAD(P)H:flavin oxidoreductase-like (FlR) domain fused to the core modules, and constitute the class C FDPs (Fig. 4A). The presence of the FlR domain offers the possibility to directly receive electrons from NAD(P)H, without the need of external electron transfer partners (Vicente et al.,

2002). Importantly, almost half of the enzymes from class C FDPs display a large variability on the putative amino acid ligands binding the diiron site, suggesting a distinct coordination of the diiron centre, if any occurs (Goncalves et al., 2011). Based on this, class C FDPs can be assigned to two groups: Cluster FlvA consisting of FDPs with non-canonical ligands for the diiron site, and the Cluster FlvB housing FDPs with strictly conserved ligands (Zhang et al., 2009, Fig. 4C).

1.4.2 Occurrence and regulation of class C FDPs

The genomes of almost all oxygenic phototrophs studied so far contain at least two Class C FDP genes: one encoding a canonical FDP (Cluster FlvB) and the other one encoding a non-canonical FDP (Cluster FlvA) (Goncalves et al. 2011; Allahverdiyeva et al. 2015). Eukaryotic photosynthetic organisms possess only two FDP genes: *flvA* and *flvB*, homologous of cyanobacterial *flv1* and *flv3*, respectively, as shown in green algae, lower plants (mosses and lycophytes) and higher plants (gymnosperms) (Allahverdiyeva et al., 2015; Gerotto et al., 2016; Gonçalves et al., 2011; Ilik et al., 2017; Peltier et al., 2010; Shimakawa et al., 2017) (Fig. 4C). Strikingly, FDP genes were lost during evolution by diatoms, haptophytes and angiosperms (Allahverdiyeva et al., 2015; Alboresi et al., 2018). Cyanobacteria are likely the organisms with the higher number of FDP genes (*flv*) in a single genome (with up to six *flv* genes reported so far) (Allahverdiyeva et al., 2015). The genome of *Synechocystis* contains four *flv* genes: *flv1*(*sll1521*) and *flv2* (*sll0219*) belonging to cluster FlvA; and *flv3 (sll0550*) and *flv4* (*sll0217*) belonging to cluster FlvB (Helman et al. 2003; Zhang et al 2009). In *Anabaena*, as in all heterocystous filamentous β-cyanobacteria, two pairs of *flv1* and *flv3* genes have been described: *flv1A (all3891)* and *flv3A (all3895)* only expressed in vegetative cells; and *flv1b* (*all0177*) and *flv3b* (*all0178*), exclusively expressed in mature heterocysts (Ermakova et al., 2013; 2014). Besides these, *Anabaena* possesses the *flv2 (all4444),* and *flv4 (all4446)* genes which share high sequence similarity with those found in *Synechocystis*, thus having a total of 6 FDP genes (Ow et al. 2008; Ermakova et al. 2013; Allahverdiyeva et al. 2015). The *flv2* and *flv4* genes are organized in the *flv4-ORF-flv2* operon, which is found to be highly conserved in the genome of many β-cyanobacteria (Zhang et al., 2012; Allahverdiyeva et al., 2015). In contrast, the organization of *flv1* and *flv3* genes is more diverse. While *flv1* and *flv3* genes are spread out in the genome of *Synechocystis*, in *Anabaena* the two pairs of *flv1* and *flv3* genes are clustered as *flv3A-ORF$_3$-flv1A* and the operon *flv3B-flv1B* (Mitschke et al., 2011; Allahverdiyeva et al., 2015).

Global gene expression profiles of *Synechocystis* and gene expression and proteomic studies in *Anabaena* have shown that the expression of FDPs is strongly affected by diverse environmental factors (see Table 1 and Table 2). At the

transcriptional level, the expression of the *flv4-flv2* operon is differently regulated by the NdhR and the AbrB-like protein Sll0822 transcriptional factors, while the post-transcriptional regulation by the antisense RNA As1_flv4 prevents a premature accumulation of Flv2 and Flv4 during low carbon acclimation (Eisenhut et al., 2012). In *Anabaena*, the expression of *flv1A* and *flv4* were shown to be positively regulated by the global transcriptional regulator PacR, the closest homolog of *Synechocystis* NdhR (Picossi et al., 2015). While the expression of *flv3A* was found to be negatively regulated by the master regulator of iron homeostasis, FurA (González et al., 2014), the expression of *flv3B* may be activated by NtcA, a global regulator of heterocyst differentiation (Picossi et al. 2014).

Table 1. Summary of global expression profiles of the genes encoding FDPs in *Synechocystis* under different growth conditions. Induction of gene expression is depicted in green, while repression is shown in red. Fold change (Log_2) lower than -1 or higher than 1 is indicated by darker colors

Growth Condition		FDP genes				Reference
		flv1	*flv3*	*flv2*	*flv4*	
C_i limitation			↑	↑	↑	Wang et al., 2004; Eisenhut et al., 2007; Mitschke et al., 2011
High-Light				↑	↑	Hihara et al., 2001; Singh et al., 2008; Mitschke et al., 2011
O_2 limitation				↑	↑	Summerfield et al., 2011
Cadmium excess				↑	↑	Houot et al., 2007
UV-B light					↑	Huang et al. 2002
Oxidat. stress	H_2O_2 (3 mM)	↑	↑		↑	Houot et al., 2007
	MV+ HL	↓		↑	↑	Kobayashi et al., 2004
Heat	(38 °C)	↑	↑		↑	Rowland et al., 2010
	(43 °C)		↓		↓	Gunnelius et al., 2014
Zinc excess		↓		↑	↑	Houot et al., 2007
Iron limitation			↓	↓	↓	Hernández-Prieto et al., 2012; Houot et al., 2007
Dark-to-Light			↓	↓	↓	Lehmann et al., 2013; Mitschke et al., 2011
Cold			↓		↓	Prakash et al., 2010
Acidic stress				↓	↓	Ohta et al., 2005

Table 2. Summary of gene expression and proteomic studies in *Anabaena* using different techniques. Induction of gene expression is depicted in green, while repression is shown in red. Fold change (Log_2) lower than -1 or higher than 1 is indicated by darker colors.

Condition		Technology	FDP genes						Reference
			flv1A	*flv3A*	*flv1B*	*flv3B*	*flv2*	*flv4*	
C_i limitation		RT-qPCR	↑	↑			↑	↑	Ermakova et al., 2013; Picossi et al., 2015
High-Light		RT-qPCR	↑	↑					Ermakova et al., 2013
Diazotrophic		iTRAQ shortgun			↑	↑	↑		Ow et al., 2008
		RT-qPCR			↑	↑			Ermakova et al., 2013
		RNA seq			↑	↑			Flaherty et al., 2011
Heterocyst-enriched fraction		iTRAQ shortgun			↑	↑			Ow et al., 2008
		DNA microarray			↑	↑			Ehira et al., 2003
Ca^{+2}	Limited	RNA seq						↑	Walter et al., 2016
	Excess	RNA seq					↓	↓	Walter et al., 2016
H_2O_2 (100 µM)		DNA Microarray		↑					Yingping et al., 2014

1.4.3 Function of FDPs in cyanobacteria

The minimal functional unit of FDPs requires two monomers arranged in a head-to-tail orientation bringing the diiron centre from one monomer in close contact (ca. 6 Å) with the FMN from the other one, thus ensuring an efficient electron transfer between the two centres (Frazão, C. et al., 2000; Di Mateo et al., 2008) (Fig. 4B). Until now, all FDPs from anaerobic prokaryotes and eukaryotic protozoa have been isolated as soluble homodimers or homotetramers (dimer of dimers), and their crystallographic structures have confirmed these quaternary conformations (Romão et al., 2016a; 2016b; Vicente et al., 2012). In cyanobacteria and photosynthetic eukaryotes, the typical co-occurrence of canonical and non-canonical FDPs have suggested that the functional unit of FDPs consists of heterodimers (Helman et al., 2003; Zhang et al., 2012; Allahverdiyeva et al., 2011; Ermakova et al., 2013; Alboresi et al., 2019). It is likely, that the participation of a non-canonical FDP in electron transport would depend on the catalytic diiron centre from a canonical FDP arranged in a head-to-tail heterodimer (Zhang et al., 2009; 2012). Nevertheless, confirmation of the quaternary structure is still wanting as only partial

crystallographic structures are available for the class C FDPs (Borges et al., 2019). Additionally, the arrangements of homodimers of both canonical and non-canonical FDPs is also possible, although this would likely involve different enzymatic features.

In vitro characterization of *Synechocystis* FDP homodimers, recombinantly produced in *E. coli*, suggested the ability of Flv1, Flv3 (Vicente et al., 2002; Brown et al., 2019) and Flv4 (Shimakawa et al., 2015) homodimers to catalyse NAD(P)H-mediated O_2 reduction to water, without the formation of ROS. These *in vitro* analyses suggested NADH and NADPH as electron donors of FDPs, albeit at divergent catalytic efficiencies. Thereby, the precise identity of the electron donor of FDPs remains unclear. Moreover, potential interactions between FDPs and Fd isoforms, demonstrated by two-hybrid tests in both *Synechocystis* (Cassier-Chauvat & Chauvat, 2014) and *Chlamydomonas reinnhardtii* (Peden et al., 2013), has suggested the involvement of Fd as a potential electron donor to FDPs. A recent *in vivo* study using a state-of the-art DUAL-KLAS-NIR spectrophotometer for the measurement of redox changes of Fd, P700 and Pc (Klughammer & Schreiber, 2016; Schreiber, 2017; Setif et al., 2019) has attempted to identify the electron donor to FDPs and suggested that Fd, or possibly F_AF_B iron–sulfur clusters of PSI, and not NADPH, is the redox partner of Flv1/3 (Sétif et al., 2020).

The first *in-vivo* demonstration of the role of FDPs in the photoreduction of O_2 was performed by Helman et al. (2003). In this study, Helman et al. showed the lack of the light-induced O_2 consumption in *Synechocystis* Δ*flv1* and Δ*flv3* mutants and proposed that Flv1 and Flv3 mediate the reduction of O_2 to water using electrons produced on the acceptor side of PSI, without the concomitant formation of ROS (Helman et al., 2003). This pathway is referred to as the "Mehler-like" reaction (Allahverdiyeva et al., 2013), which contrasts with the non-enzymatic H_2O_2 producing "true" Mehler reaction described in eukaryotic phototrophs (Mehler et al., 1951; Asada 1999). Indeed, there is no clear evidence of the "true" Mehler reaction in cyanobacteria as they have shown high sensitivity to H_2O_2, even at low concentrations (Drábková et al., 2007; Matthijs et al., 2012), likely due to the deficit of an effective H_2O_2 scavenging system.

1.4.3.1 Role of Flv1(A) and Flv3(A) proteins

The Mehler-like reaction mediated by the Flv1/Flv3 heterodimer was shown to work as an electron sink downstream of PSI, albeit to varying degrees and depending on the availability of C_i and light regime. While in cells grown under high levels of CO_2 up to 40% of electrons originating from water-splitting PSII can be directed to O_2 (Helman et al., 2003; 2005), O_2 photoreduction activity was ~20% under ambient CO_2 and high-light exposure (Allahverdiyeva et al., 2011). Moreover, under severe

limitation of C_i, where carboxylation of RuBisCO is suppressed, the Flv1/3-mediated Mehler-like reaction was shown to work in cooperation with photorespiration, and together were able to direct up to 60% of electrons from the PETC to photoreduction of O_2 (Allahverdiyeva et al., 2011). The importance of this cooperative relationship is demonstrated in the double mutant lacking GcvT (a glycine decarboxylase complex subunit involved in one photorespiratory 2-PG metabolism) and Flv3, which could not be fully segregated, and was unable to survive high-light acclimation (Hackenberg et al., 2009).

Regardless of light intensity, under constant light conditions, the deletion of Flv1 and/or Flv3 does not affect the growth or wellbeing of cells, suggesting the compensating activity of other protective mechanisms (Helman et al., 2003; Zhang et al., 2009; Allahverdiyeva et al., 2011). Indeed, most of the Flv1/Flv3 contribution seems to be limited to the first seconds during dark-to-light transition or sudden increase in light intensity, as observed in the transient and strong PSI acceptor side limitation in *Synechocystis* Δ*flv1*, Δ*flv3* and Δ*flv1/flv3* mutants (Helman et al., 2003; Allahverdiyeva et al., 2013). This potent and transient activity of the Flv1/Flv3 heterodimer has a crucial biological significance for the survival of cyanobacteria under the fluctuating light (FL) conditions characteristic of aquatic environments (Allahevrdiyeva et al., 2013). The growth and photosynthesis of the *Synechocystis* Δ*flv1*, Δ*flv3 and* Δ*flv1*/*flv3* mutants exposed to a severe FL regime were drastically impaired (Allahverdiyeva et al., 2013). A similar growth phenotype was observed in *Anabaena* mutants lacking the vegetative-specific Flv1A and Flv3A proteins, suggesting a conserved role for the Flv1 and Flv3 proteins in cyanobacteria (Allahverdiyeva et al., 2013). The drastic inhibition of PSI observed in the Δ*flv1*/*flv3* mutant grown under severe FL stimulates O_2 photoreduction by Cyd, although on a limited scale, indicating an interplay between Flv1/Flv3 and RTOs (Ermakova et al., 2016). Nevertheless, Cyd activity during illumination is unable to rescue the fatal phenotype of Δ*flv1/3* under this suboptimal condition.

1.4.3.2 Role of Flv2 and Flv4 proteins

In *Synechocystis*, Flv2 and Flv4 are encoded by the *flv4-sll0218-flv2* operon, together with the small membrane protein Sll0218 (Zhang et al., 2012; Bersanini et al., 2017). Zhang et al., (2012) performed biochemical and biophysical experiments providing compelling evidence for the occurrence of the Fv2/Flv4 heterodimer with strong affinity for the membrane fraction in the presence of divalent cations. The important role of Flv2/4 in photoprotection of PSII was initially evidenced by the reduced accumulation of PSII centres and increased susceptibility to high-light of the Δ*flv4* mutant (lacking the expression of the *flv4-2* operon-encoded proteins). This severely contrasted the phenotype of the mutant overexpressing the *flv4–flv2* operon (*flv4-*

2/OE) which showed improved PSII photochemistry and enhanced resistance to high light intensity under ambient levels of CO_2 (Zhang et al., 2009; 2012; Bersanini et al., 2014). In-depth studies of the electron transfer by the Flv2/Flv4 heterodimer indicated the release of excess electrons from the Q_B pocket on the acceptor side of PSII, as a response of the increased redox potential of Q_B, maintaining a more oxidized PQ pool under high-light and C_i limiting conditions (Zhang et al., 2012; Bersanini et al., 2014; Chukhutsina et al., 2015). Nevertheless, the identity of the electron acceptor of Flv2/Flv4 is still unclear. Further studies demonstrated the cooperative work between Sll0218 and Flv2/Flv4 to ensure efficient PSII photoprotection: while the Sll0218 protein stabilizes the assembly and/or repair of PSII and optimizes energy transfer from PBSs to stabilized PSII dimers, the Flv2/Flv4 heterodimer was suggested to work as an electron sink at the acceptor side of those PSII complexes, receiving energy from PBSs (Chukhutsina et al. 2015; Bersanini et al. 2017). Importantly, the expression of the *flv4-2* operon was shown to be dependent on the presence of PBSs and correct energy transfer from PBSs to the reaction centres. Moreover, the *flv4-2* operon-encoded proteins and carotenoids were shown to work in a complementary manner to provide protection against damage mediated by singlet oxygen (Bersanini et al., 2014).

1.4.3.3 Heterocyst specific FDPs

The heterocyst-specific Flv3B, likely forming homodimers, was shown to mediate light-induced O_2 uptake (Mehler-like reaction), providing the micro-oxic environment required inside heterocysts for proper function of the N_2-fixing machinery during illumination (Ermakova et al., 2014). Nevertheless, the overexpression of the Flv3B protein itself has not been enough to enhance nitrogen fixation rates in the heterocysts (Roumezi et al., 2020). The role of Flv1B remains to be elucidated, as it has not been found to contribute to O_2 photoreduction activity, and the phenotype of the mutant lacking the Flv1B protein is comparable to WT (Ermakova et al., 2014). Importantly, the lack of the protective function of Flv3B was, at least, partially compensated by the upregulation of other terminal oxidases such as *coxA3*, part of an operon encoding a heterocyst-specific terminal oxidase; *lox*, which encodes lactate oxidase that is thought to reduce O_2; and genes encoding rubrerythrin and Mn catalase, both reducing H_2O_2. Furthermore, the deletion of the heterocyst-specific *flv3B* was concomitant with the downregulation of the vegetative cell-specific *flv3A* and higher transcript levels of *flv4*, which might suggest a co-dependent expression of FDPs in *Anabaena* under diazotrophic growth (Ermakova et al., 2014).

1.5 Heterocyst metabolism and bioenergetics

The heterocyst has evolved to become a specialized cell for the fixation of N_2, in order to supply the filament with organic nitrogen compounds. The reduction of N_2 (a very stable gas) into NH_3, along with the evolution of molecular hydrogen (H_2), is an energetically expensive process. This process is catalyzed by the O_2-sensitive nitrogenase complex, as shown in the following equation (Bothe et al., 2010):

$$N_2 + 16\ ATP + 8\ H^+ + 8e^- \rightarrow 2\ NH_3 + H_2 + 16\ ADP + 16\ P_i \quad \text{(equation 1)}$$

To satisfy the high demand of ATP and reductants for the N_2 fixation reaction, heterocysts employ a variety of electron transport pathways (reviewed in Magnuson, 2019). The rate of N_2 fixation is shown to be several times higher in light than in darkness, since the major supply of ATP in the heterocyst is mediated by light reactions taking place in the TM. The lack of functional PSII and the increased accumulation of PSI, NDH-1 complex and Cyt *b*$_6$*f* protein subunits in heterocysts, compared to vegetative cells (Ow et al., 2008; 2009; Cardona et al., 2009), suggest a major role of the light-driven CET around PSI in the generation of reductants to nitrogenase (Almon & Böhme, 1982). As described in 1.3.1, CET provides extra ATP molecules, contributing to the ATP:NADPH balance, and for a long time CET was recognized as the only source of energy in the heterocysts (Munekage et al., 2004). Nevertheless, the occurrence of an "unorthodox" LET in the TM, providing both reductants and ATP, is still a very feasible alternative (Magnuson & Cardona, 2016). In the absence of water oxidation at PSII, electrons are donated from the NADPH generated by the OPP pathway and transferred to the NDH-1 complex *via* FNR and Fd. The NDH-1 complex would shunt the electrons to the TM and transfer them all the way to PSI passing through Cyt *b*$_6$*f* and generating a proton gradient across the membrane. A recent work has shown the fundamental role of *cyt* c_6, unlike Pc, in the transfer of electrons from Cyt *b*$_6$*f* to PSI in heterocysts (Torrado et al., 2019). The light-driven electron transfer from the acceptor side of PSI to nitrogenase is mediated by the heterocyst-specific ferredoxin, FdxH, which has been proposed as the main electron donor to nitrogenase (Bothe et al., 2010) (Fig. 5).

N_2 fixation and H_2 metabolism are closely related processes in the heterocyst, since H_2 is produced as an unavoidable by-product of the N_2 fixation reaction (see equation 1). H_2 happens to be one of the most promising clean energy carriers and thus, the photobiological production of H_2 by cyanobacteria has attracted great interest due to its potential biotechnological applications (recently reviewed in Kosourov et al., 2021). Nonetheless, the H_2 produced by nitrogenase is rapidly oxidized by membrane bound Uptake hydrogenase (Hup), thus the net H_2 production in the heterocyst is rather limited (Schütz et al., 2004; Tsygankov et al., 2007). The recycling of H_2 by Hup is proposed to contribute: (1) to the consumption of O_2 close

to nitrogenase *via* the respiratory oxyhydrogen (Knallgas) reaction, (2) providing an additional source of electrons and protons for the activity of nitrogenase, and (3) preventing a deleterious accumulation of H_2 which affects nitrogenase activity (Dixon, 1972). A common strategy for increasing H_2 production yield in filamentous heterocystous cyanobacteria is to inactivate Hup. Mutants with either disrupted structural *hupLS* genes (Yoshino et al. 2007; Happe et al., 2000; Masukawa et al., 2002; Lindberg et al., 2002) or disruption of a gene encoding the maturation protein *hupW* (Lindberg et al. 2012; Nyberg et al., 2015) have been constructed, and all have demonstrated increased H_2 production. The inactivation of Hup in cyanobacteria not only increases H_2 production but also results in reprogramming of the overall cell metabolism (Ekman et al., 2011; Kosourov et al., 2014; Kourpa et al., 2019).

A remarkable feature of heterocysts is the enhanced respiratory activity required in order to ensure a micro-oxic environment for N_2 fixation. In *Anabaena*, this is accomplished by the heterocyst-specific ARTO type 1 and 2 (see *Terminal oxidases* in 1.3.2) located in the honeycomb membranes (Valladares et al., 2003, Magnuson & Cardona, 2016). ARTO type 1 has been shown to play a major role in the protection of nitrogenase by reducing O_2 into H_2O using electrons from the PQ pool (Valladares et al., 2007), however, the deletion of both heterocyst-specific RTOs was required to disable diazotrophic growth (Valladares et al., 2003). Interestingly, ARTO type 2 and PSI were shown to compete for electrons from Cyt b_6f. Since they share the same electron donor, Cyt c_6, this suggests a regulatory mechanism of electron transfer through PSI (Torrado et al., 2019). The level of O_2 in the heterocyst cytoplasm is further decreased by the activity of heterocyst-specific Flv3B mediating the Mehler-like reaction (see 1.4.3.3, Ermakova et al.,2014).

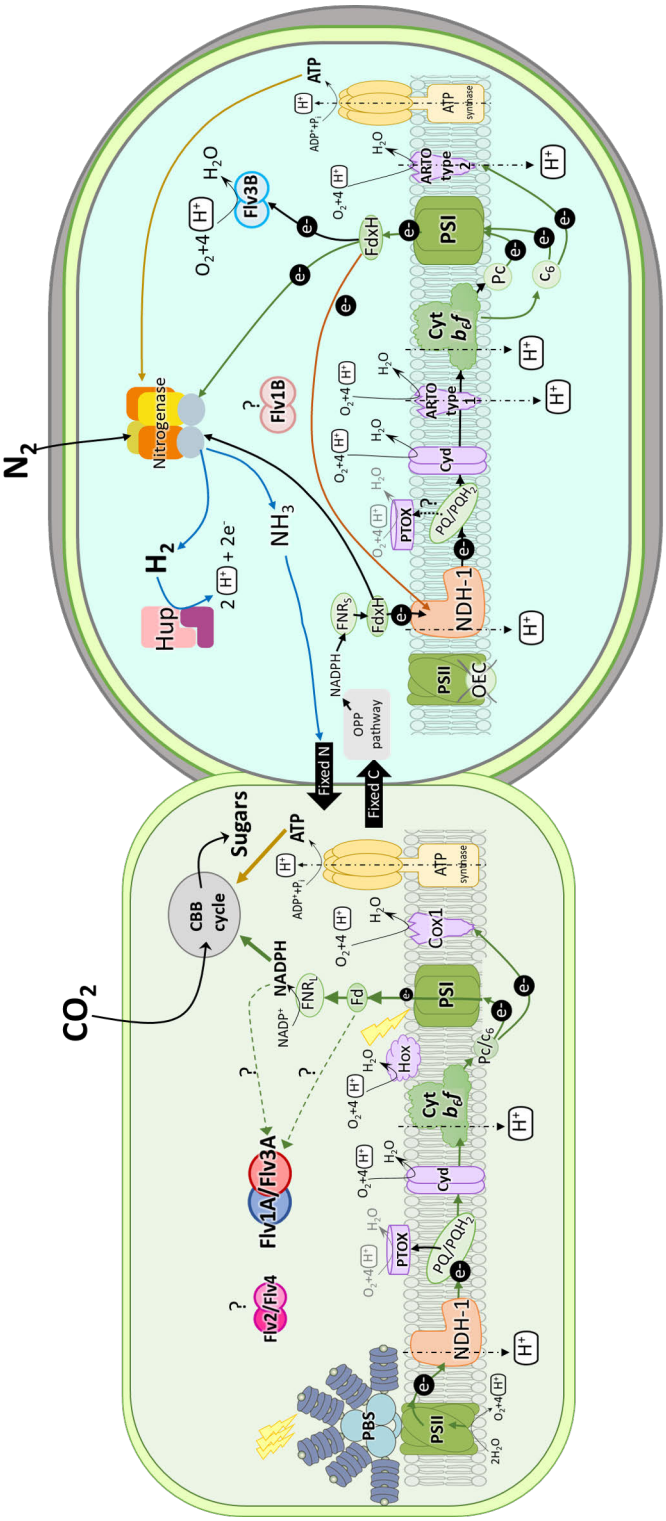

Figure 5. Schematic representation of the bioenergetic processes occurring in the vegetative cell and heterocyst of diazotropic filaments of *Anabaena*. LET is indicated by green arrows, and CET by orange arrows. Alternative electron sinks are depicted in purple. Question marks indicate possible/unverified electron transport pathways. Dotted black arrows indicate proton translocation across the TM. The sizes of the proteins are not in scale. The membrane-bound Hup protein is depicted in the cytosol close to the nitrogenase for clarity of the scheme. Based on Magnuson, 2019 & Pernil and Schleiff, 2019.

2 Aims of the study

From the transition to an oxygenated environment in the past to current ecological impacts, cyanobacteria have played a major role in shaping the history of life on Earth. Their remarkable success is likely due to the evolution of photoprotective pathways, like FDPs, which allowed cyanobacteria to colonize highly variable environments avoiding damage to the photosynthetic apparatus. Furthermore, cyanobacteria might also impact our future as next-generation biotechnological hosts for the sustainable bioproduction of target chemicals. The study of cyanobacterial FDPs has attracted increasing interest from researchers due to the potential to modulate their powerful electron sink capacity and redirect photosynthetic reducing equivalents towards desired target metabolites. Modulating this redirection requires a comprehensive understanding of the mechanisms and complex endogenous networks regulating the activity of FDPs under variable environments. Therefore, in the present thesis, I aimed to characterize the functional regulation of FDPs in the photo-protection of unicellular non-N_2-fixing and filamentous N_2-fixing cyanobacteria. To this end, I employed MIMS technology coupled with the use of $^{18}O_2$ isotope which, to this day, represents the finest strategy to examine the Mehler-like reaction in a real-time fashion on intact organisms. An extensive analysis of the function and regulation of FDPs was performed using a number of FDP deletion and overexpression mutants, exposed to conditions of variable CO_2 and light availability.

More specifically the aims of my thesis were:

1. To elucidate the *in vivo* contribution of the Flv1/Flv3 and Flv2/Flv4 hetero-oligomers in the Mehler-like reaction under different levels of dissolved C_i.
2. To study the photo-protective role of the hetero- and homo-oligomers of Flv1 and Flv3 during the acclimation of *Synechocystis* cells to fluctuating light conditions.
3. To study the interplay between FDPs and NDH-1 complexes.
4. To understand the physiological relevance of vegetative cell-specific FDPs in the diazotrophic metabolism of *Anabaena*.

3 Methodology

3.1 Cyanobacterial strains and growth conditions

Table 3. Cyanobacterial strains used in this work. A detailed description of the mutants can be found in the provided references. All strains are constructed based on a glucose-tolerant WT strain.

Strain	Deleted genes	Reintroduced genes	Paper	Reference
***Synechocystis* strains**				
WT sp. PCC 6803	-		I, II, III	Williams, 1988
Δ*flv1*	*sll1521*::Cm^R		II, III	Helman et al., 2003
Δ*flv2*	*sll0219*::Sp^R		I	Zhang et al., 2012
Δ*flv3*	*sll0550*::Sp^R		II, III	Helman et al., 2003
Δ*flv4*	*sll0217-0218-0219*::Km^R		I	Zhang et al., 2012
Δ*flv1/3*	*sll1521*::Cm^R *sll0550*::Sp^R		I, II	Allahverdiyeva et al., 2011
Δ*flv3/4*	*sll0550*::Sp^R *sll0217-19*::Km^R		I	Helman et al., 2003
Δ*sll0218*	*sll0218-0219*::Hg^R, *psbA2*::Sp^R	*flag-sll0217*::Km^R, *sll0219*::Sp^R	I	Bersanini et al., 2017
WT::*flv4-2* (*flv4-2*/OE)	*psbA2*::Sp^R	*sll0217-0218-0219*::Sp^R	I	Bersanini et al., 2014
Δ*flv1/oeflv3*	*sll1521*::Cm^R	*sll0550*::Sp^R	II	Paper II
Δ*flv3/oeflv1*	*sll0550*::Sp^R	*sll1521*::Km^R	II	Paper II
Δ*flv1::flv1*	*sll1521*::Cm^R	*sll1521*::Sp^R	II	Allahverdiyeva et al., 2013
Δ*ndhD1/D2* (Δ*d1d2*)	*slr0331*::Km^R *slr1291*::Cm^R		III	Ohkawa et al., 2000a
Δ*ndhD3/D4* (Δ*d3d4*)	*slr1733*::Km^R *slr0027*::Cm^R		III	Ohkawa et al., 2000a

Strain	Deleted genes	Reintroduced genes	Paper	Reference
***Synechocystis* strains**				
Δ*flv1/ndhD1D2* (Δ*flv1d1d2*)	*sll1521*::Gm^R *slr0331*::Km^R *slr1291*::Cm^R		III	Nakamura et al., 1999
Δ*flv3/ndhD1D2* (Δ*flv3d1d2*)	*sll0550*::Sp^R *slr0331*::Km^R *slr1291*::Cm^R		III	Nakamura et al., 1999
Δ*flv1/ndhD3D4* (Δ*flv1d3d4*)	*sll1521*::Gm^R *slr1733*::Km^R *slr0027*::Cm^R		III	Nakamura et al., 1999
Δ*flv3/ndhD3D4* (Δ*flv3d3d4*)	*sll0550*::Sp^R *slr1733*::Km^R *slr0027*::Cm^R		III	Nakamura et al., 1999
M55 (Δ*ndhB*)	*sll0223::*Km^R		I	Ogawa, 1991
***Anabaena* strains**				
WT sp. PCC 7120	-		IV	
Δ*flv1A*	*all3891*::Nm^R		IV	Allahverdiyeva et al., 2013
Δ*flv3A*	*all3895*::Nm^R		IV	Allahverdiyeva et al., 2013
Δ*flv1A/flv3A*	*all0687*::Sp^R		IV	Paper IV

All cyanobacterial strains used in this work are listed in Table 3, whereas a summary of the conducted experimental setups is presented in Table 4. Stock cultures of *Synechocystis* and *Anabaena* strains were routinely grown in BG-11 medium (pH 7.5) supplemented with the appropriate antibiotics and under air enriched with 1-3% CO_2. Pre-experimental cultures were harvested at logarithmic growth phase and used to inoculate the experimental cultures at the starting OD_{750}: 0.1, 0.2, 0.4 or 0.5 for a period of time (days) according to the experimental setup (Table 4). Pre- and experimental cultivations were not supplemented with antibiotics, except in Paper III. *Synechocystis* strains were cultivated in 30 mL batches of BG-11 medium (Rippka et al., 1979) inside Erlenmeyer flasks (100 mL) gently shaken (100 r.p.m.) at 30°C. *Anabaena* strains were grown at 30°C in 200 mL of Z8x medium (Z8 medium without combined nitrogen sources, Kotai, 1972) bubbled with air or 1% CO_2 in air ($LC^{(1)}$ and $HC^{(2)}$ in Table 4, respectively).

BG-11 medium was buffered with 20 mM 2-(N-morpholino) ethanesulfonic acid (MES, pH 6.0), 20 mM HEPES-NaOH (pH 7.5), 10 mM TES-KOH (pH 8.2) or 10 mM N-Cyclohexyl-2-aminoethanesulfonic acid (CHES, pH 9.0), according to the pH of the experimental setup. Cells were illuminated with continuous white fluorescent light (L 30W/865, Osram) at an intensity of 50 (Moderate light, ML) or 220 μmol photons m^{-2} s^{-1} (High light, HL).

Table 4. Summary of the experimental setups conducted in this work.

Experimental setup	Pre-culture			Experimental culture					Paper	Analysis
	$[CO_2]$	Light	pH	$[CO_2]$	Light	pH	Starting OD_{750}	Days		
HC → HC	**HC**	ML	8.2	**HC**	ML	8.2	0.2	3	I	Gas exchange, protein
			7.5			7.5	0.1	4	III	Growth curve
HC → LC	**HC**	ML	7.5	**LC**	ML	7.5	0.1-0.2	4	I, III	Growth curve, biophysics, protein and transcript
			8.2			8.2	0.2	4	I	
			8.2			6.0	0.2	4	I	
			9.0			9.0	0.2	4	I	
			8.2			8.2	0.5	3	I	Gas exchange, protein
			7.5			7.5	0.4	2	II	DNA microarray
			7.5	**C_i limitation without Na_2CO_3**		7.5	0.2	4	I	Gas exchange, protein, transcript
ML → FL	LC	**ML**	7.5 8.2	LC	**FL 20/500** **FL 50/500**	7.5 8.2	0.1–0.4	4-7	II	Growth curve, gas exchange, protein and transcript
HC, ML → LC, FL	**HC**	**ML**	7.5	**LC**	**FL 20/500**	7.5	0.4	2	II	DNA microarray
			7.5			7.5	0.1	8	I	Growth curve
			8.2			8.2	0.1	8	I	
			8.2		**FL 20/500**	6.0	0.1	8	I	
			9.0		**FL 50/500**	9.0	0.1	8	I	
LC, ML → LC, HL	**LC**	**ML**	7.5	**LC**	**HL**	7.5	0.2	4	III	
HC, ML →LC, HL	**HC**	**ML**	7.5	**LC**	**HL**	7.5	0.2	4	III	Growth curve, biophysics and protein
LC → LC	**$LC^{(1)}$**	**ML**	~7.0	**$LC^{(1)}$**	**ML**	~7.0	0.1	4	IV	Growth curve, biophysics, protein and transcript
HC → HC	**$HC^{(2)}$**	**ML**	~7.0	**$HC^{(2)}$**	**ML**	~7.0	0.1	4	IV	Biophysics and transcript

HC and $HC^{(2)}$: High carbon at 3% shaking and 1% CO_2 bubbling, respectively. LC and $LC^{(1)}$: Low carbon, air shaking and bubbling , respectively. ML: Moderate light, 50 µmol photons m^{-2} s^{-1}(also called Growth Light (GL) in Paper II). HL: Hight light, 220 µmol photons m^{-2} s^{-1}. FL: Fluctuating light regime.

AlgaeTron AG 130-ECO (PSI) growth chambers equipped with LED white light were used for fluctuating light (FL) experiments. Two different FL regimes were applied: severe FL 20/500 (20 µmol photons m^{-2} s^{-1} for 5 min and 500 µmol photons m^{-2} s^{-1} for 30 s) and mild FL 50/500 (50 µmol photons m^{-2} s^{-1} for 5 min and 500 µmol photons m^{-2} s^{-1} for 30 s). Different experimental conditions also included various levels of CO_2 supply: 3% in air (High carbon, HC); atmospheric 0.04% in air (Low carbon, LC), or C_i limitation (LC and Na_2CO_3 omitted from BG-11 medium). For activity measurements, cells were harvested at the logarithmic growth phase and resuspended in fresh growth medium at the desired Chl concentration. Samples were acclimated for 1 hr to the same experimental growth conditions. Chl *a* was extracted using 90% methanol and an extinction coefficient of 78.74 L g^{-1} cm^{-1} was applied to determine and adjust the Chl *a* concentration (Meeks & Castenholz, 1971).

3.2 Biophysical analysis

3.2.1 Gas exchange measurements

In vivo measurements of O_2, CO_2 (m/z=44), and H_2 (m/z=2) fluxes were performed using membrane inlet mass spectrometry (MIMS) coupled with isotopic $^{18}O_2$ (isotope purity >98%; CK Gas Products) enrichment. This method distinguishes between gross oxygen produced by PSII and oxygen uptake under illumination based on increase of $^{16}O_2$ (m/z=32) and decrease of $^{18}O_2$ (m/z=36) respectively, in the reaction medium (Beckmann et al. 2009, Shevela et al., 2018).

Harvested cells were resuspended with fresh growth medium, adjusted to Chl *a* 10 µg mL^{-1} and acclimated for 1 hr to the same experimental growth conditions. Only for LC samples, the concentration of dissolved total inorganic carbon was saturated with 1.5 mM $NaHCO_3$ before the measurement. Cells were dark-adapted for 15 min, after which gas exchange was monitored over a 5-min illumination period of 500, 1000, or 1500 µmol photons m^{-2} sec^{-1} of white actinic light, according to the experimental treatment.

3.2.2 Spectrometry

Simultaneous measurement of Chlorophyll a fluorescence and P700: Dual-PAM-100 (Walz, Effeltrich, Germany), was used to monitor Chl *a* fluorescence and P700 oxido-reduction in intact cells. Measurements were performed at 30°C, and samples with Chl *a* adjusted to 10-15 µg mL^{-1} were initially incubated in darkness for 10 min with stirring. Specific setting details of the experimental measurements are provided in the respective Papers. The maximal photochemical efficiency of PSII (F_v/F_m) was measured from dark-adapted cells in the presence of 10 µM DCMU, as $(F_m-F_0)/F_m$.

In Paper III, cells were subjected to a fluctuating light regime alternating between 1-min periods of 25 and 530 µmol photons m^{-2} sec^{-1} of red (620 nm) actinic light (AL). Saturating pulses (SP1-SP9) of 5000 µmol photons m^{-2} sec^{-1} (500 msec) were administered at 15 sec intervals in order to probe photosynthetic parameters. In Paper IV, filaments were illuminated with red AL of 50 µmol photons m^{-2} sec^{-1} and saturating pulses of 5000 µmol photons m^{-2} sec^{-1} (300 msec) were applied every 1 minute. The transient rise in fluorescence was measured after switching off AL (F_0 rise normalised to F_s). The maximum level of oxidizable P700 (P_m) was calculated by the application of a saturating pulse after pre-illumination of the cells using far-red light (720 nm) for 10 s. Photosynthetic parameters were calculated as follows: $Y(NA) = (P_m - P_m')/P_m$; $Y(ND) = P/P_m$; $Y(I) = 1 - Y(ND) - Y(NA)$ (Klughammer and Schreiber, 2008); $Y(II) = (F_m' - F_s)/F_m'$ (Genty et al., 1989).

The fluorescence emission spectra at 77K were measured from intact cells using a QE Pro spectrophotometer (Ocean Optics, Dunedin, FL, USA). Harvested cells were adjusted to Chl *a* concentration of 7.5 µg ml^{-1} with fresh BG-11 media. Cells were frozen in liquid N_2 and excited at 440 nm. Raw spectra were normalized to the PSII-fluorescence peak at 685 nm.

Analysis of P700, PC, and Fd redox changes: A DUAL-KLAS-NIR spectrophotometer (Walz) was used to measure absorbance difference changes at 780–820, 820–870, 840–965 and 870–965 nm, from which PC, P700 and Fd redox changes were deconvoluted based on differential model plots (DMPs) for PC, P700 and Fd (Klughammer & Schreiber, 2016; Schreiber, 2017; Setif et al., 2019). The DMPs were measured using scripts provided with the instrument software. The DMPs from *Synechocystis* Δ*flv3 d1d2* (in Paper III) and *Anabaena* Δ*flv1A*/*flv3A* (in Paper IV), where P700 oxidation was severely delayed, were used as model spectra.

Analysis of NADPH redox kinetics: NADPH fluorescence changes between 420 and 580 nm, induced by excitation at 365 nm, were measured simultaneously with Chl a fluorescence with the Dual-PAM 100 and its 9-AA/NADPH accessory module (Walz) (Schreiber & Klughammer, 2009; Kauny & Setif, 2014). Samples were adjusted to Chl *a* concentration of 5 µg mL^{-1}. Cells were dark-adapted for 20 min and subjected to the same fluctuating light regime as for Chl induction measurements, but without saturating pulses.

Analysis of the electrochromic shift (ECS): The ECS was measured as the absorbance difference between 500 and 480 nm (Viola et al., 2019). Experimental samples were adjusted to Chl *a* 7.5 µg mL^{-1}, and illuminated with green AL of 500 µmol photons m^{-2} sec^{-1} for 1 or 60 sec interspersed with 500 msec dark intervals at 2, 7.5, 18, 30 and 45 sec. *Pmf* was calculated as the extent of ECS decrease at the dark intervals. Thylakoid conductivity (gH^+) was calculated as the inverse of the time constant of a first-order fit to ECS relaxation kinetics during a dark interval, and proton flux (vH^+) as *pmf* × gH+ (Cruz et al., 2005).

3.3 Transcript analysis

3.3.1 Isolation of total RNA

Total RNA was isolated using the hot-phenol method according to Tyystjärvi et al. (2001). In the case of *Synechocystis*, cells were incubated with phenol solution for 10 min at 60°C, whereas *Anabaena* cells were treated for 5 min at 95°C. Genomic DNA was removed using the TURBO DNA-freeTM kit (InvitrogenTM) according to the manufacturer's manual. RNA concentration and purity were measured with a NanoDrop spectrophotometer (Thermo Scientific). RNA integrity was verified by agarose gel electrophoresis.

3.3.2 Real-time quantitative PCR (RT-qPCR)

First strand cDNA was synthesized from purified RNA using SuperScript® III First-Strand Synthesis System (Invitrogen^{TM}) according to the manufacturer's protocol. The generated cDNA was then used as a template for RT-qPCR. Negative controls contained ultrapure water and samples lacking reverse transcriptase or template. Reference genes with a constitutive transcription were used: for *Synechocystis rimM* and *cysK* in Paper I and additionally *rnpB* in Paper II, and *rpoA* for *Anabaena* in Paper IV. RT-qPCR was performed with the IQ5 detection system (Bio-Rad) using iQ SYBR Green Supermix (BioRad) as described in Mustila et al. (2014). Relative changes in gene expression were examined using the Pfaffl method (Pfaffl, 2001). Primers were designed with Primer3 Plus software to generate a similar amplicon length (about 200 bp), and the list of primers used are specified in the respective Paper.

3.3.3 Transcriptional profiling

In Paper III, DNA Microarray analysis was performed at the Finnish DNA Microarray and Sequencing Centre (Turku, Finland). Microarrays were analyzed by pairwise comparisons between groups using the LinearModels for Microarray Data (Limma) package from Bioconductor software. A gene was considered up-regulated if $\log_2$ of the fold change was ≥ 1 and down-regulated if fold change was ≤ -1. Genes with statistically significant ($p<0.05$) values were considered differentially expressed. Gene annotation was performed with definitions listed in CyanoBase (http://genome.annotation.jp/cyanobase/Synechocystis).

In Paper IV, the cDNA synthesis, library construction and Illumina HiSeq2500 sequencing were performed at BGITech (https://www.bgi.com/). The obtained raw reads were subjected to a general quality control analysis which guided pre-

processing steps to remove low-quality artefacts and bases. Read quality was checked with the FastQC tool. This step was followed by aligning the reads to the reference genome using the TopHat tool available at CSC's High-Performance Computing site (https://research.csc.fi/csc-s-servers). The Cufflinks tool available at the same site was used to estimate transcript abundances. Sequencing was made for three independent biological replicates for each strain. Differentially expressed genes were determined for Δ*flv1A* and Δ*flv3A* mutants compared to the WT, with $q<0.01$ and a cut-off $\log_2$ value of 0.9.

3.4 Protein analysis

Total protein extracts and the soluble fractions of *Synechocystis* cells and *Anabaena* filaments were isolated as described by Zhang et al. (2009). Protein concentration was determined using the Lowry protein assay (BioRad). Total protein extracts were solubilized in Laemmli sample buffer containing 5% β-mercaptoethanol and 6 M urea and separated using 10-12% (w/v) SDS-PAGE containing 6 M urea. In paper II, the analysis of soluble protein complexes in their native structures was performed using 5–15% gradient blue-native electrophoresis (BN-PAGE) as described by Zhang et al. (2012). Further two-dimensional (2D) separation of protein complexes was conducted by denaturing the proteins from the strips of the BN-PAGE gel in the Laemmli SDS sample buffer for 30 min at 20°C. After solubilization, the strips were placed onto a 1-mm-thick 12% SDS-PAGE gel containing 6 M urea to separate the protein subunits of the complexes.

After electrophoresis, the proteins were electro-transferred from gels to a polyvinylidene fluoride membrane (Immobilon-P; Millipore) and immuno-detected with protein-specific primary antibodies. Horseradish peroxidase (HRP) conjugated secondary antibody (anti-rabbit IgG from donkey) was used for recognizing the primary antibodies and Amersham ECL Western Blotting Detection Reagent (GE Healthcare) was used for visualization of the antibodies.

3.5 Nitrogenase activity

Activity of the nitrogenase enzyme was determined by an acetylene reduction assay, as described in Kosourov et al., 2014.

3.6 Determination of H_2 production and Deuterium uptake

H_2 concentration was monitored under anaerobic conditions using a Clark-type Pt-Ag/AgCl electrode chamber (DW1/AD, Hansatech) connected to a home-made

polarographic box. Experimental cultures were harvested, resuspended in fresh Z8x medium and adjusted to a Chl a concentration of about 3-4 µg mL^{-1}. The resulting suspensions (30 mL) were transferred into 75 mL glass vials, sealed and sparged with either nitrogen (N_2) or argon (Ar) for 30 min in the dark, in order to achieve anaerobic conditions. Then, cultures were incubated under the corresponding atmosphere for another 2 h in darkness at 25°C. Finally, 4 mL of the dark-adapted suspension was transferred into the electrode chamber. H_2 concentration was monitored during 6 min of illumination with actinic light of 800 µmol photons m^{-2} s^{-1}.

Deuterium (D_2, m/z=4) uptake measurements were performed on samples pre-treated in an Ar atmosphere inside gas-tight vials for 15 min.After Ar pre-treatment, 1.2 mL of pure D_2 (2 % in headspace) was injected into each vial. D_2 concentrations were measured at 2 h and 24 h after addition using 250 µL gas sampled from the headspace of the vials, which was injected into the MIMS chamber (1.0 mL). The calibration of D_2 concentration was performed by injecting known concentrations of D_2.

3.7 Microscopy

Heterocysts were detected by staining heterocyst-specific exopolysaccharides with 0.5% Alcian Blue stain in 50% ethanol. Bright-field microscopic images were taken with a digital camera (Leica DFC420C) attached to a Wetzlar light microscope (Leitz). For each *Anabaena* strain, 1000–2000 cells were counted from micrographs using x400 magnification. The heterocyst frequency was determined by counting the number of vegetative cells per each heterocyst.

4 Overview of the results

4.1 The kinetics of the Mehler-like reaction are strongly dependent on ambient cues

4.1.1 The Flv2/Flv4 heterodimer mediates O_2 photoreduction *in vivo*

Mutants lacking functional Flv2 and/or Flv4 and grown under LC exhibited a substantial decrease in O_2 photoreduction (Fig. 2 in Paper I); whereas, the mutant overexpressing the *flv4-2* operon, but maintaining WT levels of Flv3 protein, showed an elevated rate of O_2 photoreduction compared to the WT (Fig. 1A and 1C in Paper I). These results indicate the *in vivo* contribution of Flv2/Flv4 to the Mehler-like reaction under LC conditions. The participation of Sll0218 in O_2 photoreduction was further excluded (Fig. 2-Fig. Suppl. 1).

Importantly, the contribution of Flv2/Flv4 to O_2 photoreduction was not evidenced in the Δ*flv1* and/or Δ*flv3* mutants when cells were pre-cultivated in HC and shifted to LC for 3 days at the high starting OD_{750} of 0.4–0.5 (Fig. 6A in Paper I and Fig. 7 in Paper II), as previously reported in Allahverdiyeva et al., 2011, 2013; and Ermakova et al., 2016. This was accompanied with low Flv2 and Flv4 protein accumulation (Fig. 6B in Paper I). Nevertheless, improving the light penetration of the cultures by lowering the starting OD_{750} to 0.2, and the LC acclimation by extending the cultivation to 4 days, resulted in higher accumulation of Flv2 and Flv4 and subsequent steady-state O_2 photoreduction. Which, although residual, was detected in the Δ*flv1/flv3* mutant. A similar effect was observed in WT cells shifted to LC at $OD_{750}\approx0.2$ for 4 days, which exhibited a higher accumulation of Flv2, Flv3 and Flv4 and the concomitant increase in O_2 photoreduction rates compared to cells shifted to LC at the higher $OD_{750}\approx0.5$ for 3 days (Fig. 6 in Paper I). These results highlight the impact of light penetration and low C_i acclimation on the functional expression of Flv2, Flv3 and Flv4, especially upon a shift of cells from pre-culture conditions to different experimental conditions.

4.1.2 The activity of FDPs is modulated by the availability of dissolved C_i (DIC) in the growth medium

The accumulation of FDPs has been demonstrated to be highly responsive to changes in the concentration of DIC available in the medium (Zhang et al., 2009, 2012; Wang et al., 2004; Battchikova et al., 2011; Hackenberg et al., 2009). In order to verify a direct correlation between the level of FDP and their activity, I examined the activity of FDPs present in cells grown at different concentrations of DIC: ambient level of CO_2 (0.04% CO_2, LC), C_i limitation (LC and Na_2CO_3 omitted from the growth medium), and a high level of CO_2 (3% CO_2, HC), *via* direct comparison of the efficiency and kinetics of O_2 photoreduction.

Under LC (at pH 6–8.2), WT cells showed high accumulation of Flv2, Flv3 and Flv4 proteins (Fig. 1C, 3A, and 6B in Paper I) which drive triphasic kinetics of O_2 photoreduction consisting of: (I) a fast *induction* phase, reaching a maximum rate; followed by (II) a *quenching* phase lasting about one minute; and eventually (III) a *quasi-stable state* (Fig. 1A in Paper I). Interestingly, WT cells grown under C_i limitation (at pH 7.5 without Na_2CO_3) demonstrated increased rates of O_2 photoreduction (Fig. 2, the middle panel in Paper I), however, this was not correlated with any significant change neither in transcript nor protein levels of the Flv2, Flv3 and Flv4 (Figure 3B and 3C in Paper I). Surprisingly, despite the low amount of Flv3 and nearly undetectable levels of Flv2 and Flv4 in WT cells grown under HC conditions, these cells exhibited an induction phase of O_2 photoreduction comparable to LC-grown cells (phase I), which was maintained relatively stable during illumination (phase III) (Fig. 1B in Paper I). It is noteworthy that the Flv2/Flv4 heterodimer was capable of contributing to steady-state O_2 photoreduction under HC when artificially overexpressed in the *flv4-2/*OE strain (Fig. 1B in Paper I).

The availability of DIC to cells not only depends on the total concentration of DIC, but also on the pH-dependent composition of DIC (dissolved CO_2, HCO_3^-, and CO_3^{2-}) (Mangan et al., 2016). I, therefore, examined whether the pH of the medium is an additional factor in modulating the functional expression of FDPs under LC conditions. At alkaline conditions (pH 9), where the formation of CO_3^{2-} is expected, the expression of Flv2 and Flv4 were strongly repressed at transcript and protein level. WT cells, resembling the Δ*flv4* mutant, demonstrated a strong and transient O_2 photoreduction upon illumination likely originating from the sole activity of Flv1/3 heterodimer. On the other side of the spectrum, acidic conditions (pH 6) that favors dissolved CO_2 in the medium, enhanced the O_2 photoreduction rates without involving a significant change in the accumulation of FDPs. The sole activity of Flv2/Flv4 heterodimer in the Δ*flv1/flv3* mutant showed a relatively large steady-state photoreduction of O_2 (Fig. 2, 3A, and 3B in Paper I).

The lack of light-induced O_2 reduction in the deletion mutants devoid of all FDPs, i.e., Δ*flv3/flv4,* HC-grown Δ*flv1/flv3* and alkaline-grown Δ*flv1/flv3*, discarded

the contribution of other terminal oxidases under the conditions tested (Fig. 2, Fig. 1-Fig. Suppl. 1). Importantly, there was no significant difference in the gross O_2 evolution rates observed between the wild-type and the FDP mutants (Fig. 1-source data 2 in Paper I).

4.1.3 Flv1/Flv3 and Flv2/Flv4 have a different electron-sink capacity

To examine the electron-sink capacity of Flv1/Flv3 and Flv2/Flv4 heterodimers at the onset of light, I assessed the maximum rate of light-induced O_2 uptake in WT, Δ*flv4* and Δ*flv1/flv3* mutants in response to increasing high light illumination.

WT cells and the Δ*flv4* mutant, which accumulates WT levels of Flv3 protein, displayed an efficient increase of the maximum rate of light-induced O_2 uptake as a response to increasing the light intensities. In contrast, the Δ*flv1/flv3* mutant, accumulating WT level of Flv2 and Flv4, was less responsive to increasing light intensities. These results demonstrate the high capacity of Flv1/Flv3-mediated O_2 photoreduction to act as a fast and stronger electron sink at dark-to-light transition, in comparison with Flv2/Flv4 (Fig. 5 in Paper I). Interestingly, the presence of all FDPs in WT cells provided greater O_2 photoreduction rates, in response to the increasing light intensities, than the sum of the individual O_2 photoreduction rates exhibited by Δ*flv1/flv3* and Δ*flv4*, suggesting a strong enhancement of O_2 photoreduction by various oligomer activities.

4.2 Role of FDPs under fluctuating light conditions

In cyanobacteria, both Flv1(A) and Flv3(A) have shown to be essential for the survival of *Synechocystis* cells and *Anabaena* filaments under FL intensities, providing protection for PSI (Allahverdiyeva et al., 2013). In this section, I examined the photoprotective role of different FDPs under FL conditions and the global transcriptional response of cyanobacterial cells.

4.2.1 Unlike Flv1/Flv3, the Flv2/Flv4 heterodimer is not essential for the cell survival under severe FL conditions

To examine the role of Flv1/Flv3 and Flv2/Flv4 heterodimers in the acclimation of *Synechocystis* cells to FL, cultures of different FDP deletion mutants were grown in media at different pHs (6.0, 7.5, 8.2, 9.0) and exposed to mild (FL 50/500) and severe (FL 20/500) FL regimes for a prolonged period of time (7-8 d).

In line with previous work, the deletion of Flv1 and/or Flv3 resulted lethal when mutants were exposed to severe FL 20/500, regardless of the pH of the growth medium (Fig. 4, Suppl. Fig. 4-1 in Paper I and Fig. 5A in Paper II). In contrast, under mild FL 50/500, the lack of Flv1/Flv3 heterodimer is likely compensated by another mechanism that allows cells to grow similar to WT at pH ≤7.5, or slower than WT at pH ≥8.5 (Fig. 4 in Paper I and Fig. 5C, 5D in Paper II). Importantly, the inactivation of the *flv4-2* operon did not affect the cell growth under FL (both severe and mild FL) regimes, regardless of the growth medium pH (Fig. 4 and Suppl. Fig. 4-1 in Paper I).

4.2.2 Exposure to FL upon C_i step-down prevents proper LC acclimation in WT and nitrogen assimilation in Δ*flv1* and Δ*flv1/flv3* mutants

To gain a comprehensive understanding of how cells respond to FL conditions during LC acclimation, a global DNA microarray analysis of *Synechocystis* WT and Δ*flv1* and Δ*flv1*/Δ*flv3* mutants, grown both under severe FL 20/500 and constant growth light (GL, 50 μmol photons m^{-2} s^{-1}), was performed.

WT cells exposed to FL 20/500 for 48 h induced the differential expression of 108 genes in comparison with the WT grown under constant GL conditions. Several components of CCM were among the highly down-regulated genes. Alongside this, the transcript abundance of *flv4-2* operon and *flv3* were significantly down-regulated (Table 1 in Paper II). On the other hand, among the up-regulated genes were those involved in nitrogen uptake and assimilation pathways, including nitrate/nitrite transporters (*nrtC-D*) and nitrate reductase (*narB*), albeit the expression of nitric oxide reductase (*norB*) was diminished. Hence, the exposure to a severe FL 20/500 regime upon CO_2 step-down impairs LC acclimation in *Synechocystis* WT and instead, cells induce nitrogen assimilation pathways as a trade-off for survival.

Unlike WT cells, the Δ*flv1* and Δ*flv1*/Δ*flv3* mutants exposed to severe FL 20/500 were unable to induce the expression of several genes involved in nitrogen assimilation pathways. These results suggest that the simultaneous lack of the Flv1/Flv3 heterodimer and diminished nitrogen assimilation results in lethal photodamage to PSI when exposed to severe FL 20/500 for long-term period. Interestingly, the expression of *fed1* was essentially affected by the inactivation of Flv3 regardless of the light regime (Fig 1 in Paper II).

4.2.3 Flv1/Flv1 and Flv3/Flv3 homodimers contribute to the acclimation of cells to fluctuating light conditions

In order to assess the function of FDP homodimers *in vivo*, *Synechocystis* mutants solely overexpressing Flv1 or Flv3 were constructed. In the obtained strain Δ*flv3/oeflv1* devoid of Flv3, only a 0.68-fold expression of the Flv1 protein was reached. This was despite significantly higher levels of *flv1* transcript, evidencing that the expression of Flv1 is dependent on the expression of Flv3 (Fig. 3 in Paper II). Meanwhile, in Δ*flv1/oeflv3* devoid of Flv1, the expression of Flv3 was 16-fold higher compared to the WT, and the formation of Flv3 homodimers was confirmed with immunodetection upon separation with BN-PAGE. Additionally, the possible organization of a Flv3 homotetramer *in vivo* cannot be dismissed, given that gel filtration elution profiles of purified Flv3 heterologously expressed in *E. coli* was shown to form tetramers (Fig. 3 and 4 in Paper II). Finally, the presence of oligomers formed by Flv2 and Flv3 was not demonstrated under the studied conditions (Fig. Suppl. S2A in Paper II).

Next, I examined whether Flv1 and Flv3 homodimers provide photoprotection of PSI under FL conditions. Both overexpression strains (Δ*flv3/oeflv1* and Δ*flv1/oeflv3*) showed improved growth under the severe FL 20/500 regime, in comparison to the Δ*flv1* and/or Δ*flv3* mutants (Fig. 5A in Paper II). This is likely due to the enhanced CO_2 uptake and net O_2 evolution observed in the overexpression mutants compared to Δ*flv1*/Δ*flv3* after 4 d of growth under FL 20/500 (Fig. 6 in Paper II). Moreover, the presence of homodimers of Flv1 or Flv3 increased the maximum oxidizable amount of P700 (P_m) and the accumulation of PsaB (PSI core subunit) in comparison to Δ*flv1*/Δ*flv3*. Nevertheless, gas exchange analysis demonstrated that homodimers of Flv1 or Flv3 do not function in O_2 photoreduction in the Δ*flv3/oeflv1* and Δ*flv3/oeflv1*, respectively, and are likely involved in another electron transport route (Fig. 7 in Paper II).

4.3 Interaction between FDPs and other components of the photosynthetic apparatus

4.3.1 All FDPs function downstream of PSI

To determine whether the Flv2/Flv4 heterodimer mediates an electron transport route at PSII or the PQ pool level, I assessed O_2 photoreduction in the *flv4-2*/OE mutant in the presence of specific inhibitors of electron transport. When LET was blocked at Cyt b_6f level using DBMIB inhibitor (Draber & Hart, 1970; Yan et al., 2006), both WT and *flv4-2*/OE mutant cells demonstrated a strong light-induced O_2 uptake. Nevertheless, the simultaneous addition of DBMIB and HQNO, the latter

being an inhibitor of Cyd (Pils et al., 1997) and Cyt b_6f (Fernández-Velasco et al., 2001), abolished the light-induced O_2 uptake in WT and *flv4-2*/OE mutant (Fig.3—Fig. supp. 1 in Paper I), demonstrating that Cyd was solely responsible for the observed O_2 photoreduction occurring at the PQ-pool level. These results are congruent with the lack of light-induced O_2 uptake in the Δ*cyd* mutant in presence of DBMIB (Fig.3—Fig. supp. 1 in Paper I, Ermakova et al., 2016). Altogether, these results demonstrate that Flv2/Flv4 does not mediate the removal of electrons at PSII nor at the PQ pool, but rather downstream of PSI, similarly to Flv1/Flv3.

Next, I aimed to determine the electron donor of FDPs. The analysis of NADPH fluorescence changes during a dark-to-high light (530 µmol photons m^{-2} sec^{-1}) transition did not show a significant difference in NADPH redox kinetics of WT and Δ*flv3* mutant cells: both strains reached the maximal reduction of $NADP^+$ within approximately 0.25 sec (Fig. 4F in Paper III) and this was maintained throughout a 40 sec illumination period (Fig. 4E in Paper III). These results argue against NADPH being a primary electron donor to the Flv1/3 heterodimer, at least over short time scales. However, the contribution of NADPH during longer time scales or in steady-state conditions cannot be dismissed.

Ferrodoxine has been proposed to interact with Flv3, based on two-hybrid tests (Cassier-Chauvat and Chauvat, 2014), and with both Flv1 and Flv3, using Fd-affinity chromatography (Hanke et al., 2011), suggesting that Fd is the direct electron donor of Flv1/Flv3. To test this hypothesis *in vivo*, I examined the redox changes of Fd by means of DUAL-KLAS-NIR spectrophotometer (Klughammer and Schreiber, 2016; Schreiber, 2017; Setif et al., 2019) upon exposure of dark-adapted cells to HL (503 µmol photons m^{-2} sec^{-1}). In contrast to the quick reoxidation of Fd after 0.5 sec in light observed in WT cells (Fig. 5A in Paper III), Fd remained strongly reduced in the Δ*flv3* mutant for several seconds in light and became gradually reoxidized over the 30 sec of illumination period (Fig. 5B in Paper III). These results strongly support the hypothesis that Fd, rather than NADPH, is the primary electron donor of the Flv1/Flv3 heterodimer *in vivo*.

4.3.2 Dynamic coordination between FDPs and the NDH-1 complex

Recent functional and structural studies have demonstrated that Fd directly mediates electron transfer from PSI to the NDH-1 complex (Laughlin et al., 2020; Schüller et al., 2019; C. Zhang et al., 2020). I, therefore, asked whether a shared electron donor between FDPs and NDH-1 may allow crosstalk between both electron transfer pathways.

Under LC conditions, the Δ*ndhB* mutant, also called M55 (Ogawa, 1991), deficient in all forms of the NDH-1 complex (Zhang et al., 2004) demonstrated the

complete absence of quenching (phase II) of O_2 photoreduction (Fig. 1B in Paper I). Moreover, the steady-state O_2 photoreduction observed in M55 was not due to increased electron flow from PSII, as the gross O_2 evolution rate was considerably diminished compared to the WT cells (Fig.1-source data 2 in Paper I). These results resemble the kinetics of the Mehler-like reaction of HC-grown WT cells in which the expression of the NDH-1 complex is strongly downregulated (Fig. 1D and 3D in Paper I). This suggests competition for electrons between FDPs and the NDH-1 complex, so that the decay of O_2 photoreduction rates in phase II corresponds to the redirection of electrons towards NDH-1, resulting in a decrease in O_2 photoreduction.

4.3.2.1 Flv1/Flv3 and NDH-$1_{1,2}$ are essential for survival upon CO_2 step-down coupled with increased irradiance

Growth assessment under conditions of differing CO_2 availability and light intensity demonstrated that the simultaneous inactivation of Flv1/3 and NdhD1 and NdhD2 (NDH-$1_{1,2}$) was lethal upon a shift from HC and moderate light (ML, 50 µmol photons m^{-2} sec^{-1}) to LC and HL (220 µmol photons m^{-2} sec^{-1}) both in liquid (after 4 days) and in solid (after 7 days) media (Fig 1D and 1E in Paper III). Then, 24 h after the shift to LC/HL, both Δ*flv1 d1d2* and Δ*flv3 d1d2* mutants showed strong downregulation of PSI (PsaB, Fig. 6C in Paper III), congruent with a dramatic decrease of the relative PSI fluorescence cross-section revealed by 77K fluorescence spectra (Fig. 6E in Paper III).

In contrast, triple mutants lacking either Flv1 or Flv3 and NDH-$1_{3,4}$ only exhibited slightly reduced growth compared to the WT (Fig. S1B, S1D in Paper III). Importantly, the sole lack of either NDH-$1_{1,2}$ or Flv1/Flv3 did not significantly affect the growth upon the same experimental shift. It is noteworthy that the absence of all NDH-1 complexes and Flv1/Flv3 likely disrupt essential cell metabolism and reduce cell viability as no single colony of M55/Δ*flv1* was viable and M55/Δ*flv3* was unable to fully segregate (Fig. S1E in Paper III).

4.3.2.2 Flv1/Flv3 and NDH-$1_{1,2}$ contribute to efficient oxidation of PSI during a sudden increase in light intensity

To understand in more detail the functional cooperation between Flv1/Flv3 and NDH-$1_{1,2}$, I focused analysis on Δ*flv3 d1d2,* Δ*flv3,* and Δ*d1d2* mutants grown under standard growth conditions, LC/ML, where mutant strains exhibited similar growth to the WT in liquid cultures (Fig. 1B in Paper III) and reduced viability on solid media (Fig. 1E in Paper III).

MIMS analysis with the Δ*d1d2* mutant demonstrated a strong and sustained O_2 photoreduction during HL (500 µmol photons m^{-2} sec^{-1}) illumination, despite halved gross O_2 evolution (Fig. 2C in Paper III). This was likely due to the increased accumulation of FDPs already observed 24 h after the shift to LC (Fig. 6A in Paper III). In contrast, in the Δ*flv3 d1d2* mutant, the expression of Flv2 and Flv4 was strongly downregulated, and the cells exhibited only a transient light-induced O_2 uptake during the first minute of illumination (Fig. 2D in Paper III), possibly mediated by the thylakoid terminal oxidases (Ermakova et al., 2016), or by photorespiration (Allahverdiyeva et al., 2011).

The functional measurements of PSI and PSII efficiencies were monitored during repeated light fluctuations between low (25 µmol photons m^{-2} sec^{-1}, LL) to high irradiance (530 µmol photons m^{-2} sec^{-1}, HL). Here, NDH-$1_{1,2}$ was shown to have a role in maintaining photosynthetic redox poise under light-limited conditions. Whereby, the Δ*d1d2* mutant exhibited slightly elevated acceptor-side limitation during the LL phases, whereas PSI oxidation during the HL phases was similar to the WT. In line with previous studies (Helman et al., 2003; Allahverdiyeva et al., 2013), the inactivation of Flv1/Flv3 demonstrated transient PSI acceptor side limitation during the transition from LL to HL, resulting in delayed PSI oxidation. Nevertheless, the Δ*flv3* mutant was able to improve PSI oxidation during the following HL phases, suggesting the activity of a compensating mechanism, such as NDH-1, that would allow the acclimation of Δ*flv3* to fluctuating light conditions. Indeed, the simultaneous inactivation of Flv1/Flv3 and NDH-$1_{1,2}$ caused more severe acceptor side limitation of PSI during LL to HL transitions. Unlike the Δ*flv3* mutant, the Δ*flv3 d1d2* mutant did not show improvement in the PSI acceptor side limitation during subsequent HL phases (Fig. 3A in Paper III). These results indicate that NDH-$1_{1/2}$ and Flv1/Flv3 can compensate for each other's absence to some extent, and both contribute to efficient oxidation of PSI during increases in light intensity.

In vivo measurement of the light-induced redox changes of P700, Pc and Fd in WT and mutant strains was performed with the DUAL-KLAS-NIR spectrophotometer. Upon dark-to-light transition, NDH-$1_{1,2}$ was shown to be involved in initial PSI oxidation, during the first 50 ms of illumination, accepting electrons from Fd (Fig. 5C in Paper III). In contrast, Flv1/Flv3 was demonstrated to be the main electron sink after approximately 0.5 sec in light, likewise accepting electrons from reduced Fd which slowly reoxidize over the 30 sec illumination period (Fig. 5B in Paper III). The simultaneous inactivation of Flv1/Flv3 and NDH-$1_{1,2}$ resulted in a more rapid reduction of Fd than in any other strains, followed by a slow reoxidation over 30 sec of illumination (Fig. 5D in Paper III). Altogether, these NIR-spectroscopic measurements revealed that Flv1/3 and NDH-$1_{1,2}$ control the redox poise between PSI, Pc and Fd during distinct time frames at dark-to-light

transition and support the hypothesis of Fd functioning as the electron donor to Flv1/3 and NDH-$1_{1,2}$.

4.3.2.3 Flv1/Flv3 and NDH-$1_{1,2}$ contribute to the build-up of *pmf* during dark-to-light transitions

In cyanobacteria, both NDH-$1_{1/2}$ and FDPs contribute to the generation of ΔpH, a *pmf* component, via H^+ pumping activity and H^+ consumption in the cytosol, respectively. Therefore, I examined the differential regulation and build-up of *pmf* driven by NDH-$1_{1/2}$ and Flv1/Flv3, monitoring the light-induced electrochromic shift (ECS) signal via dual-wavelength (500–480 nm) transmittance changes *in vivo* (Viola et al., 2019).

During dark-to-light transition, *pmf* generation was decreased by 75% in the absence of Flv1/3. This decrease was further enhanced when Flv1/Flv3 and NDH-$1_{1,2}$ were simultaneously inactivated. The resultant diminished ΔpH generation in Δ*flv3* and Δ*flv3 d1d2* was compensated by the downregulation of ATPase conductivity (gH^+), resulting in WT levels of *pmf* after at least 30 sec of illumination. In contrast, the inactivation of NDH-$1_{1/2}$ was mostly compensated for by elevated FDP levels in terms of proton flux (vH^+), albeit *pmf* remained slightly lower than in the WT due to elevated ATPase conductivity (Fig 5E, 5F, 5G in Paper III). These results indicate that both Flv1/3 and NDH-$1_{1,2}$ contribute to proton flux, however, Flv1/Flv3 is the main contributor of *pmf* during dark-to-light transitions.

4.3.2.4 Lack of FDPs and NDH-$1_{1/2}$ impacts the assimilation of CO_2

Synechocystis strains devoid of Flv2/Flv4 (i.e., Δ*flv2*, Δ*flv4*, Δ*sll0218*/Δ*flv2* and, WT-grown at pH 9, Fig.3D in Paper I), as well as the mutants lacking Flv1/Flv3 and/or NDH-$1_{1/2}$ (Fig. 8 in Paper II, Fig. 6A and 6C in Paper III), were unable to induce the accumulation of CCM proteins upon CO_2 step-down. Moreover, the number of carboxysomes per cell was found to be significantly lower in Δ*flv3,* compared to the WT (Paper II). Interestingly, the severe delay of CO_2 fixation observed in the Δ*d1d2* mutant was largely recovered in Δ*flv3 d1d2,* which exhibited only a transient delay of CO_2 fixation (Fig. 2 in Paper III). These results might imply a regulatory mechanism interlinking the Mehler-like reaction, NDH-$1_{1/2}$-driven CET and CCM in cyanobacteria, although further studies are required to elucidate such a coordination.

4.4 Role of vegetative cell-specific Flv1A and Flv3A in the diazotrophic metabolism of filamentous heterocystous *Anabaena*

Despite the extensive characterization of the genetics and physiology of heterocyst differentiation, little is yet known about the bioenergetics between the two contrasting metabolisms of N_2 fixation and oxygenic photosynthesis occurring in heterocysts and vegetative cells, respectively. In this work, I investigated the physiological significance of vegetative cell-specific FDPs in the diazotrophic metabolism of *Anabaena* by employing Δ*flv1A* and Δ*flv3A* mutants.

4.4.1 Growth and photosynthetic electron transport in *Anabaena* filaments deficient in Flv1A and Flv3A

Flv1A and Flv3A proteins were found to be crucial for the survival of diazotrophic and non-diazotrophic filaments of *Anabaena* under severe FL 20/500 at both LC and HC (1% CO_2) conditions (Suppl. Fig. 1A in Paper IV and Allahverdiyeva et al. 2013). Conversely, under standard diazotrophic growth conditions (constant light of 50 μmol photons m^{-2} sec^{-1}, LC), *Anabaena* Δ*flv1A* and Δ*flv3A* did not show any significant differences in growth phenotype or heterocyst differentiation, compared to the WT filaments (Table 1, Suppl. Fig. 1B in Paper IV). Nevertheless, the increased light sensitivity of Δ*flv3A*, in comparison to the WT and Δ*flv1A*, was observed via spot assays on solid media, regardless of nitrogen and C_i availability (Suppl. Fig. 1C in Paper IV).

Analysis of photosynthetic electron transport properties was assessed by Chl *a* fluorescence and *in vivo* gas exchange analysis in cultures grown under LC and HC diazotrophic conditions. In *Anabaena* filaments acclimated to LC, the inactivation of Flv1A and Flv3A led to a more reduced PQ pool in the dark (Fig. 1A and Table 1 in Paper IV), likely due to increased respiratory NDH-1 activity in darkness (Suppl. Fig. 3A). During the dark-to-light transition, the Δ*flv1A* and Δ*flv3A* mutants exhibited delayed induction of O_2 photoreduction, which was congruent with the rapid over-reduction of the PQ-pool, transient decrease in PSII yield, and impairment of the PSI oxidation (Fig. 1A, 1C, 2, and 3A in Paper IV). Notably, this phenotype is aggravated in the Δ*flv3A* mutant, compared to Δ*flv1A*. Furthermore, the initial peak in CO_2 uptake rates associated with the activation of CCM (Liran et al., 2018) and the steady-state of CO_2 fixation of both deletion mutants were significantly diminished compared to the WT (Suppl. Fig. 7B in Paper IV).

In contrast to the observed near depletion of O_2 photoreduction in the *Synechocystis* Δ*flv1* mutant (Suppl. Fig. 6 in Paper IV), the sole inactivation of Flv1A resulted in a decrease of only about 45% of steady-state O_2 photoreduction in diazotrophic *Anabaena* under LC conditions (Fig. 3A in Paper IV). It is also worth

noting, that unlike the co-regulation of Flv1 and Flv3 accumulation in *Synechocystis* (Fig. 3A in Paper II), the Δ*flv1A* mutant displayed WT-like *flv3A* transcript and protein levels, while the Δ*flv3A* mutant showed an elevated *flv1A* transcript level compared to the WT (Suppl. Figure 9A, B). These results suggest that under diazotrophic LC conditions, both Flv1A and Flv3A contribute to the Mehler-like reaction to differing extents, likely forming a variety of functional homo/hetero-oligomers.

The strong depletion of O_2 photoreduction in the double mutant Δ*flv1A*/*flv3A* supports a possible contribution of Flv1A homodimers in Δ*flv3A* and conversely, Flv3A homodimers in Δ*flv1A* mutant (Fig. 3A in Paper IV). Additionally, transcriptional analysis demonstrated that the lack of Flv1A and Flv3A significantly induced the expression of *flv2* and *flv4* (Suppl. Fig. 4A in Paper IV), suggesting the contribution of Flv2 and Flv4 to O_2 photoreduction in diazotrophic Δ*flv1A* and Δ*flv3A* filaments grown under LC conditions. This hypothesis found stronger support in the HC-acclimated experiments, as the strong repression of *flv2* and *flv4* genes in both Δ*flv1A* and Δ*flv3A* mutants resulted in depleted O_2 photoreduction (Fig. 3B in Paper IV) and strong over-reduction of the electron transport chain during the dark-to-light transition (Fig. 1B in Paper IV). These results suggest a major role of Flv3A, and not Flv1A, in mediating O_2 photoreduction together with Flv2 and Flv4 under LC diazotrophic conditions, although the exact mechanism is still unclear.

4.4.2 A lack of Flv1A or Flv3A results in transcriptional adjustments to maintain redox poise and metabolic balance

Global transcriptome analysis of diazotrophic filaments acclimated to LC revealed 35 differentially expressed genes common to both Δ*flv1A* and Δ*flv3A*. Of them, 24 were strongly upregulated genes involved in nitrogen and C_i assimilation (Fig. 5 and Table 2 in Paper IV). Interestingly, 60 genes were identified as differentially expressed only in Δ*flv3A* but not in the Δ*flv1A* mutant. Among these, several genes encoding proteins involved in photoprotection and stress-response were found to be significantly upregulated, such as the ortholog of PTOX. It is noteworthy that FurA-regulated genes of iron assimilation were both up- and down-regulated in the Δ*flv3A* mutant. On the other hand, a lower number (34) of differentially expressed genes were unique for Δ*flv1A* (Fig. 5 in Paper IV).

4.4.3 Downregulation of Hup in the Δ*flv3A* mutant caused increased H_2 photoproduction

Previous studies using different diazotrophic *Anabaena* species have demonstrated that the disruption of PSII activity in vegetative cells has implications for N_2 and H_2 metabolism inside the heterocysts (Khetkorn et al. 2012; Chen et al., 2014). To examine whether the lack of Flv1A or Flv3A in vegetative cells has an impact on heterocyst metabolism, I analyzed the nitrogenase activity and H_2 fluxes of *Anabaena* WT, Δ*flv1A* and Δ*flv3A* mutants.

Both Δ*flv1A* and Δ*flv3A* mutants showed decreased nitrogenase activity compared to the WT, although only Δ*flv3A* exhibited significantly lower values. Real-time H_2 exchange measurements demonstrated an elevated production of H_2 gas in the Δ*flv3A* mutant, unlike the WT and Δ*flv1A*. This production was rapidly induced upon exposure to light and was concomitant to the evolution of O_2 in the neighbouring vegetative cells (Figure 4 in Paper IV). It is known that in the absence of N_2 substrate, the nitrogenase enzyme reduces all H^+ to H_2 (Burgess and Lowe, 1996, Hoffman et al. 2014). In this work, the removal of N_2 substrate, by replacing it with an Argon atmosphere, led to a 10 times higher H_2 photoproduction rate in Δ*flv3A*, demonstrating that H_2 photoproduction in this mutant is mediated by nitrogenase (Suppl. Fig. 8A in Paper IV). Moreover, the contribution of Hox-mediated H_2 photoproduction in the Δ*flv3A* mutant was discarded based on the significant downregulation of *hoxH* and *hoxW* (Suppl. Fig. 8B and Table 2 in Paper IV).

Protein and transcript analysis demonstrated that the increased H_2 photoproduction yield observed in the Δ*flv3A* mutant was due to the significant downregulation of Hup at the transcript level (Fig 4 C, D in Paper IV). The inactivation of HupL protein suppressed the H_2 recycling pathway (Fig 4B in Paper IV) and consequently H_2 photoproduced by nitrogenase is released from Δ*flv3A* heterocysts (Fig 3, Fig 4A). Here, I provide evidence for a regulatory crosstalk between vegetative cell and heterocyst specific metabolisms. Although, the molecular mechanism underlying this regulatory network needs further elucidation.

5 Discussion

In nature, constant environmental conditions seem to be the exception rather than the rule. Indeed, environmental fluctuations of various types (e.g., irradiance, nutrient, temperature) and timescales (seconds to seasons) have shown to have a crucial impact on evolutionary fitness (Melbinger & Vergassola, 2015; Nguyen et al., 2020). Cyanobacteria are one of the most successful colonizers on Earth, with a long history of adaptation to changes in the Earth's environment. In the aquatic environment, cyanobacteria are constantly exposed to sudden changes in the light intensity mainly caused by movements of water and clouds, and to even faster changes in irradiance due to the lens effect of waves (Iluz et al., 2012; Schubert et al., 2001). This scenario usually initiates an energetic imbalance in the production and/or consumption of ATP and NADPH, which creates over-reduction in the PETC and consequent oxidative damage of the photosynthetic apparatus by increased accumulation of ROS.

The AET pathway, mediated by FDPs, represents a remarkable mechanism evolved in all photosynthetic organisms (apart from angiosperms, red and brown algae), to alleviate electron pressure on the photosynthetic apparatus under varying environmental conditions. Nevertheless, under controlled conditions, FDPs may wastefully divert electrons and reducing power from the PETC, which could instead be funnelled towards the bioproduction of valuable solar-driven fuels and chemicals. To this end, a comprehensive understanding of the distribution of photosynthetic electrons and metabolic fluxes is essential in order to engineer a photosynthetic microbial chassis for the efficient production of targeted chemicals. In the present thesis, I focused on the mechanisms, physiological relevance, and regulation of the AET pathway mediated by FDPs in cyanobacteria.

5.1 Fd is the electron donor of Flv1/Flv3

In *Synechocystis*, the Flv1/Flv3 heterodimer has long been regarded as solely responsible for the Mehler-like reaction downstream of PSI under both HC (Helman et al., 2003) and LC conditions (Allahverdiyeva et al., 2011; 2013; Ilík et al., 2017). This conclusion was based on a lack of light-induced O_2 reduction in Δ*flv1* and/or Δ*flv3* mutant strains, as measured *in vivo* (Helman et al., 2003; Allahverdiyeva et al.,

2011; 2013; Ermakova et al., 2016). Thus, discarding the possibility of the Flv2/Flv4 heterodimer contributing to the Mehler-like reaction. In Paper I, I was able to induce a higher accumulation of Flv2, Flv3 and Flv4 by improving the light penetration of the cultures and extending LC acclimation. This allowed me to demonstrate, for the first time, the contribution of the Flv2/Flv4 heterodimer to O_2 photoreduction in the *Synechocystis* Δ*flv1/flv3* mutant. This was particularly clear at pH 6. Likewise, residual O_2 photoreduction was also observed in diazotrophic *Anabaena* Δ*flv1A/flv3A*, which upregulates the expression of *flv2* and *flv4*, suggesting that *Anabaena* Flv2 and Flv4 are analogous in function with the corresponding genes in *Synechocystis* (Paper IV).

The long-term overlooked contribution of Flv2 and Flv4 to the Mehler-like reaction can be explained by the strong downregulation, and therefore inhibited activity, of the *flv4-2* operon-encoded proteins under the HC conditions used in Helman et al., 2003. Meanwhile, the activity of the Flv2/Flv4 heterodimer accumulated in the Δ*flv1* and/or Δ*flv3* mutants grown in previous LC experiments (Allahverdiyeva et al., 2011; 2013; Ermakova et al., 2016; Paper II) was most likely below the minimum detectable by means of the MIMS setup employed. Compelling evidence for the *in vivo* contribution of the Flv2/Flv4 heterodimer to the Mehler-like reaction was further demonstrated with real-time gas-exchange measurements and immunodetection analysis using both deletion and overexpression mutants of the *flv4-flv2* operon (Paper I).

Furthermore, the application of specific inhibitors of electron transport allowed me to demonstrate that both Flv2/Flv4 and Flv1/Flv3 function as electron sinks downstream of PSI (Paper I), in contrast to previous studies that proposed Flv2/Flv4 to function removing electrons from PSII or the PQ pool (Zhang et al., 2009; Zhang et al., 2012; Bersanini et al., 2014; Chukhutsina et al., 2015).

In Paper III, i*n vivo* measurements of redox changes in Fd and NADPH using state-of-the-art DUAL-KLAS-NIR spectrophotometery and NADPH fluorescence, respectively, demonstrated that the deletion of Flv1/3 caused impaired oxidation of the Fd pool during dark-light transitions, whereas no effect was observed in NADPH redox kinetics. These results provide strong support to the hypothesis that Fd, and not NADPH, is the electron donor to Flv1/Flv3 heterodimer, in line with the independent work published by Sétif group (Sétif et al., 2020). Moreover, my conclusion is in agreement with Fd-chromatographic assay suggesting interaction between Flv1 and Flv3 and Fd (Hanke et al., 2011) and two-hybrid tests both in *Synechocystis* Flv3 (Cassier-Chauvat & Chauvat, 2014) and *Chlamydomonas reinnhardtii* FLVB (Peden et al., 2013). The lack of evidence for the interaction of Fd with Flv2/Flv4 in a previous protein-protein interaction assay, is possibly due to experimental conditions whereby Flv2 and Flv4 expression is repressed (e.g., 2% CO_2 in Hanke et al., 2011) and therefore requires careful examination. On the other

hand, excluding the involvement of NADPH as a redox partner of Flv1/Flv3 might seem paradoxical as cyanobacterial FDPs (class C) are endowed with all the domains needed for the proteins to be catalytically active with NAD(P)H as a substrate (Wasserfallen et al., 1998; Vicente et al., 2002). Indeed, *in vitro* studies have tested the NAD(P)H-dependent O_2 reduction activity of Flv1, Flv3 and Flv4 homodimers, reporting contrasting results. While initial work by Vicente et al., (2002) and Shimakawa et al. (2015) described low reaction rates and minimal affinities of Flv3 and Flv4 homodimers to NADPH, as compared to NADH, Brown et al. (2019) recently reported high catalytic efficiencies and affinities of Flv1 and Flv3 homodimers to both NADH and NADPH. Thereby, the use of NADPH, a reducing equivalent produced during LET, as an electron donor of Flv1/Flv3 or Flv2/Flv4 *in vivo* is still controversial. However, the possibility of NADPH acting as an electron donor to homodimeric forms of FDPs cannot be excluded.

5.2 FDPs function in versatile oligomeric combinations for an efficient response to dynamic environmental conditions

5.2.1 The Flv1/Flv3 and Flv2/Flv4 heterodimers function in a coordinated manner under LC conditions

The functional expression of FDPs has been shown to be tightly regulated by the concentration and the pH-dependent composition of DIC in the growth medium (Wang et al., 2004; Eisenhut et al., 2007; Zhang et al., 2009; Mitschke et al., 2011; Paper I). Under LC conditions (at pH 6-8.2), the expression of Flv2, Flv3, and Flv4 is induced, and the Mehler-like reaction exhibits triphasic kinetics of O_2 photoreduction, originating from the coordinated activity of Flv1/Flv3 and Flv2/Flv4 heterodimers (Paper I). Interestingly, strong alkaline conditions (pH 9) prevented the expression of Flv2 and Flv4, and the downregulation of CCM proteins such as NdhD3 and SbtA. Although the mechanism underlying this transcriptional repression is still unclear, it is possible that the carbonate ions (CO_3^{2-}) formed in the growth medium at pH 9 act as the signalling factor (Paper I).

The use of distinct FDP deletion mutants grown at different pH values allowed me to successfully separate the distinct contributions of Flv1/Flv3 and Flv2/Flv4 to the kinetics of the Mehler-like reaction in LC. While Flv1/Flv3 mediates a strong but transient O_2 photoreduction during dark-light transition, Flv2/Flv4 facilitates a slow steady-state O_2 photoreduction (Paper I).

The distinctive efficiency of Flv1/Flv3 and Flv2/Flv4 as electron sinks could be partially attributed to their intracellular location: the soluble nature of Flv1 and Flv3 would enable a rapid association with soluble Fd and direct electrons towards

O_2 photoreduction, whereas it is conceivable that the Mg^{2+}-induced docking of Flv2/Flv4 to the TM when lights are turned on (Zhang et al., 2012), would result in a delayed and limited O_2 photoreduction activity. In line with this, it is possible that the enhanced induction of O_2 photoreduction observed in the overexpressing mutant *flv4-2*/OE (Fig 1 in Paper I) was due to the efficient activity of soluble Flv2/Flv4 that exceeded the available docking space in the TM. Lastly, it is also possible that Flv2/Flv4 receives electrons from FNR or another specific Fd isoform that would regulate its O_2 reduction efficiency.

5.2.2 Low level of Flv1(A)/Flv3(A) is sufficient to catalyse strong steady-state O_2 photoreduction under HC

Under HC conditions (1-3% CO_2), when excess CO_2 could offer a strong sink for electrons, the expression of Flv2 and Flv4 is strongly downregulated and only a small amount of Flv3(A) protein is detectable at protein level (Paper I; Paper IV; Zhang et al. 2009; Bersanini et al., 2014). Contrary to the apparent futile contribution of FDPs under HC, my results demonstrated a strong and steady-state O_2 photoreduction driven by the small amount of Flv1(A)/Flv3(A) accumulated in the HC-grown WT *Synechocystis* and *Anabaena* WT (Paper I and IV). Although, *Synechocystis* Flv2/Flv4 was shown to be capable of performing O_2 photoreduction if artificially overexpressed under HC (Paper I), its expression is naturally repressed *via* antisense RNA *as1-flv4* (Eisenhut et al., 2012). Contrastingly, under LC conditions at pH 9, where Flv2 and Flv4 was repressed, a moderate amount of Flv1/Flv3 mediates a strong but transient O_2 photoreduction. It is likely that under these conditions, Flv1/Flv3 works in coordination with other AET expressed under LC, like the NDH-1 complex, in order to maintain redox poise between the PETC and cytosolic carbon assimilation. Indeed, the LC-grown mutants defective in NDH-1 complex (M55 and Δ*d1/d2*) lacked the quenching phase of O_2 photoreduction after the initial induction and exhibited a strong and steady-state O_2 photoreduction (Paper I and Paper III) similar to the HC-grown WT. Therefore, I hypothesize that the transient activity of Flv1/Flv3 under LC is due to competition for electrons with the NDH-1 complex *via* reduced Fd.

5.2.3 Efficient photoprotection of cells exposed to long-term FL is achieved by limiting the Mehler-like reaction and inducing photosynthetic nitrate assimilation

In contrast to Flv2/Flv4, the Flv1/Flv3 heterodimer demonstrated a higher capacity to function as a rapid and efficient electron sink in response to increasing light intensity (Paper I). This data expounds the essential role of Flv1/Flv3, and not

Flv2/Flv4, on the prompt photoreduction of O_2, as a rapid response to excessive reduction of PSI, enabling the survival of cells exposed to FL conditions (Allahverdiyeva et al., 2013; Paper I and II). The photoprotective role of Flv1 and Flv3 under FL conditions described in this work has been shown to be conserved in their homologs Flv1A and Flv3A in *Anabaena* (Paper IV, Allahverdiyeva et al., 2013), as well as FlvA and FlvB in other photosynthetic eukaryotes (Gerotto et al., 2016; Chaux et al., 2017; Jokel et al., 2018). Furthermore, the role of Flv1(A) and Flv3(A) proteins was shown to be indispensable, regardless of CO_2 availability, in *Synechocystis* (Mustila et al., 2021) and *Anabaena* (Paper IV) exposed to FL 20/500.

Nevertheless, and contrary to expectations, the induction of Flv1 and Flv3 expression is not a direct metabolic response of *Synechocystis* WT cells exposed to FL conditions. Indeed, immunodetection and global transcriptomic analysis revealed a significantly downregulation of all FDPs in *Synechocystis* WT cells exposed for 48 hr to FL conditions, compared to those grown under constant light (Paper II). This response was concomitant with the downregulation of CCM genes, both in cultures well-adapted to LC (Fig. 2 in Paper II) and during the LC acclimation process (Table 1 in Paper II). Instead, FL-grown WT cells showed an up-regulation of nitrogen assimilation pathways, including the nitrate reductase gene, *narB.* In cyanobacteria, nitrate reductase uses reduced Fd as an electron donor (Flores & Herrero, 2005) and has been shown to act as an electron sink downstream of PSI during nitrogen starvation (Klotz et al., 2015). It is conceivable that the induction of Fd-dependent nitrate reductase could serve as an important electron valve under FL conditions, as recently suggested (Mustila et al., 2021). I hypothesize that the stimulation of the Flv1/Flv3- mediated Mehler-like reaction under long-term FL conditions would likely result in an energetically disadvantageous situation, as considerable amounts of photosynthetic electrons and reductants would be diverted from the LET. Accordingly, the inability of Δ*flv1* and Δ*flv1*/Δ*flv3* mutants to induce the expression of several genes involved in nitrogen assimilation pathways would likely result in increased acceptor side limitation of PSI and lethality of the FL conditions (Paper II). Importantly, the global transcriptional analysis presented in Paper II were supported by a strong correlation with global proteomic analysis from the exact same experimental conditions (Mustila et al., 2021).

5.2.4 The role of various oligomeric arrangements: FDPs beyond O_2 photoreduction

The oligomeric structure of FDPs requires two monomers arranged in a head-to-tail orientation to form a minimal functional unit (Vicente et al., 2008). In line with this, biochemical analysis demonstrated that, at least, Flv2 (Zhang et al., 2012), Flv1 and Flv3 (Paper II, Allahverdiyeva et al., 2011) proteins are mostly present in dimeric

arrangements (homo- or heterodimer) in *Synechocystis* WT cells. In addition to the Flv1/Flv3 and Flv2/Flv4 heterodimers functioning in the photoreduction of O_2, it is conceivable that cyanobacterial FDPs form homodimers or tetramers *in vivo*, similarly to all FDPs from anaerobic prokaryotes and eukaryotic protozoa described so far (Romão et al., 2016a; 2016b; Vicente et al., 2012). The functional characterization of Flv1/Flv1 or Flv3/Flv3 homodimers is challenged by the crosswise downregulation of the Flv1 and Flv3 proteins in single deletion mutants (Paper II and Allahverdiyeva et al., 2011). Therefore, *Synechocystis* mutants solely overexpressing Flv1 or Flv3 were constructed and characterized in Paper II. The biochemical analysis of soluble protein complexes in their native structures confirmed the presence of homodimeric arrangements of Flv1/Flv1 and Flv3/Flv3 *in vivo*, albeit overexpression of the Flv1/Flv1 homodimer was less efficient (Paper II; Allahverdiyeva et al., 2011). Both Flv1/Flv1 and Flv3/Flv3 homodimers demonstrated photoprotection of PSI under FL conditions, resulting in a significantly improved, but not fully recovered, growth phenotype (Paper II). In contrast to previous *in vitro* studies (Vicente et al., 2002; Brown et al., 2019), my results of gas-exchange analysis demonstrated that Flv1/Flv1 or Flv3/Flv3 homodimers do not catalyse O_2 photoreduction *in vivo*, but likely mediate another electron transport pathway other than the Mehler-like reaction pathway (Paper II).

Similarly, in order to overcome the strong co-regulation of Flv2 and Flv4 proteins (encoded by the same operon), the formation of Flv2/Flv2 homodimers *in vivo* has been previously demonstrated in a *Synechocystis* overexpression mutant containing only Flv2 (Zhang et al., 2012). Although molecular modelling data suggested inefficient transfer of electrons by Flv2/Flv2 homodimers (Zhang et al. 2012), further studies are needed to understand the physiological function of FDP homodimers *in vivo*. So far, the extent of functional contribution by homodimeric arrangements in WT cells remains unclear. Furthermore, the fact that all four FDPs are required for efficient O_2 photoreduction exhibited in WT cells (Paper I), suggests a possible inter-regulation of Flv1/Flv3 and Flv2/Flv4 heterodimers, or even the occurrence of alternative oligomeric arrangements involving all four FDPs. In effect, the possibility of tetrameric arrangements of FDPs *in vivo* cannot be excluded, as the formation of Flv3 homotetramers was demonstrated *in vitro* (Paper I) and it is possible that the tetrameric forms are lost during the protein isolation procedure.

Contrary to *Synechocystis*, the expression of vegetative cell-specific Flv1A and Flv3A in *Anabaena* did not show interdependency (Paper IV). Therefore, the occurrence of Flv1A and Flv3A homodimers in single deletion mutants is conceivable. Interestingly, the expression of *flv2* and *flv4* was found to be strongly upregulated in the absence of Flv1A or Flv3A (Paper IV), which hints at possible oligomeric arrangements between Flv2/Flv4 and Flv1A or Flv3A (see 5.4). An additional distinctiveness reported in diazotrophic *Anabaena*, is the capacity of the

heterocyst-specific Flv3B to mediate O_2 photoreduction likely forming homodimers. This function was demonstrated to be of great importance to maintain the micro-oxic conditions required for nitrogenase activity inside the heterocysts (Ermakova et al., 2014). The functional role of the second heterocyst-specific Flv1B remains unclear and it is likely involved in an alternative pathway (other than O_2 photoreduction), in a similar manner to *Synechocystis* homodimers.

5.3 Synergy between FDPs and the NDH-1 complex: Balancing PSI oxidation and CO_2 fixation

Functional and structural evidence presented so far have demonstrated that both NDH-1 and FDPs function downstream of PSI, receiving electrons from reduced Fd (Paper I; Paper III; Laughlin et al., 2019; 2020; Schüller et al., 2019; 2020) and suggesting competing electron pathways.

As shown in Paper I and Paper III, the deficiency of the competing NDH-1 pathway, specifically the NDH-$1_{1/2}$ complexes, resulted in a strong steady-state O_2 photoreduction mediated by FDPs. Based on these results, I propose that: In LC, upon illumination, Flv1/Flv3 mediates the fast induction of O_2 photoreduction, reaching its maximum rate during the first ~30s in light (phase I). After this, electrons are redirected *via* Fd towards NDH-$1_{1/2}$ resulting in a rapid quenching of O_2 photoreduction (phase II). At this point, the low but steady-state activity of Flv2/Flv4 takes over O_2 photoreduction in order to maintain LET in an oxidized state (phase III) (Fig. 6). This suggestion is also in agreement with the more oxidized state of the PQ pool in cells overexpressing Flv2/Flv4, indirectly safeguarding PSII activity (Zhang et al., 2012; Bersanini et al., 2014; Chukhutsina et al., 2015).

Further examination of the cooperative work between Flv1/Flv3 and NDH-$1_{1/2}$ revealed that:

(1) During the dark-to-high light transition, NDH-$1_{1/2}$ was suggested to be involved in the oxidation of P700 and Fd immediately upon the onset of illumination (~50-200 ms). The short timescale of action of NDH-$1_{1/2}$ might be achieved by the formation of an NDH-1-PSI supercomplex in cyanobacteria (Gao et al., 2016) which has been described in conditions of environmental stresses such as LC or HL (Zhao et al., 2018). However, further studies are required to support this hypothesis.

(2) The inactivation strain of NDH-$1_{1/2}$ showed no significant change in the capacity to oxidize PSI during HL periods. This competence can be attributed to the strong accumulation and activity of the FDPs (Fig. 7). These results demonstrate that FDPs can functionally compensate the absence of CET mediated by NDH-$1_{1/2}$ during sudden increases in light intensity. Instead, NDH-$1_{1/2}$ activity was shown to be more

relevant under LL periods, in agreement with previous studies on angiosperms (Yamori et al., 2011, 2015) and bryophytes (Ueda et al., 2012).

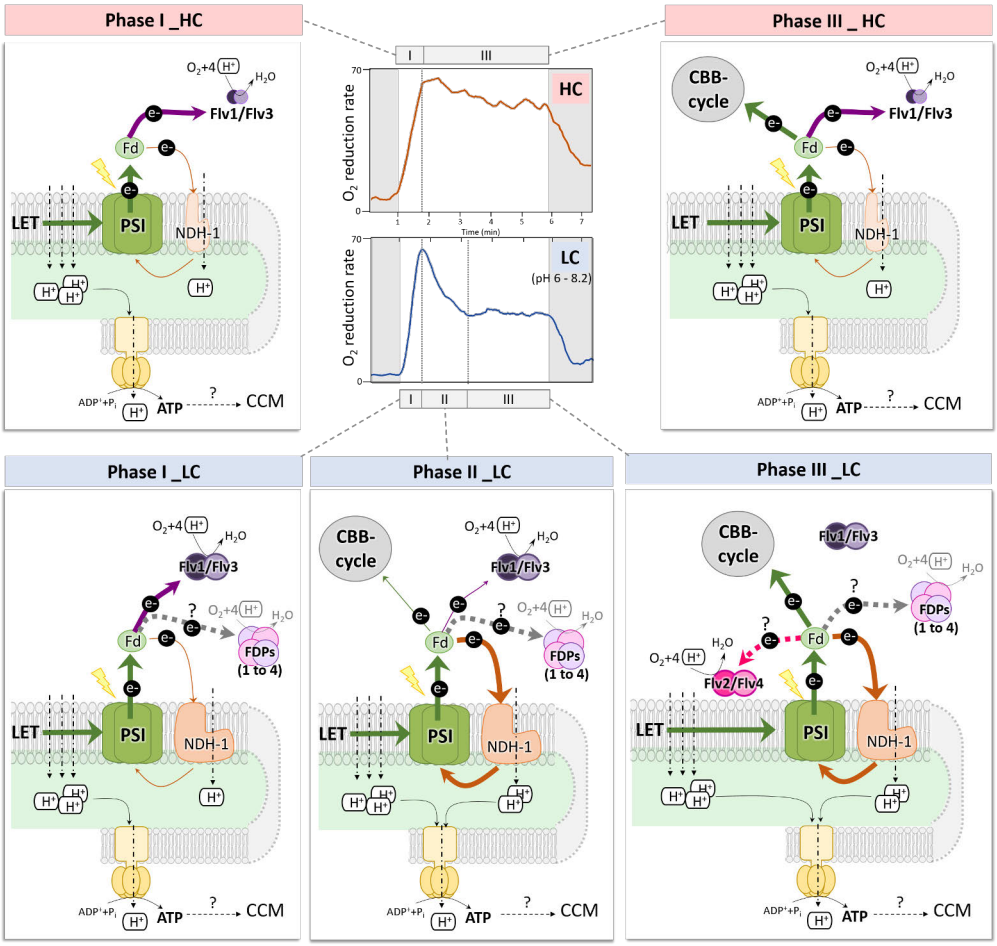

Figure 6. Schematic model of the kinetics of the Mehler-like reaction in *Synechocystis* WT cells acclimated to high (HC) and low C_i (LC) conditions. The higher abundance of total NDH-1 complexes and Flv1/Flv3 in LC, compared to HC conditions, is represented by the larger size of the protein complexes. Thicker arrows reflect increased electron flux through the corresponding pathway. Dotted arrows indicate possible/unverified electron transport pathways. Dotted black arrows indicate proton translocation across the TM. See the text for details.

(3) The inactivation of Flv1/Flv3 resulted in transient inability to oxidize PSI during sudden increases in light intensity (Paper III; Helman et al., 2003; Allahverdiyeva et al., 2013; Ilik et al., 2017) (Fig. 7). Contrasting Δ*flv3 d1d2*, the Δ*flv3* mutant showed a gradual improvement in PSI oxidation during subsequent cycles of LL-HL, suggesting a compensatory activity of NDH-$1_{1/2}$ during short-term acclimation to FL.

A similar contribution of NDH-1 has been previously reported in angiosperm, where FDPs have been lost during evolution (Yamori et al., 2016; Nikkanen et al., 2018; Shimakawa & Miyake, 2018a) and recently in the nonvascular plant *Physcomitrella patens* (Storti et al., 2020a, 2020b). Nevertheless, the contribution of NDH-$1_{1/2}$ to PSI oxidation does not prevent the lethal phenotype of the inactivation strains of Flv1 and/or Flv3 under FL (Paper I, Paper II, Allahverdiyeva et al., 2013), suggesting that NDH-$1_{1/2}$ cannot fully substitute the Flv1/Flv3 contribution, especially under FL conditions. The inactivation of both Flv1/Flv3 and NDH-$1_{1/2}$ resulted in an inability to oxidize PSI under HL, resulting in lethal photodamage to PSI, indicating a lack of other mechanism that could compensate their PSI oxidation activity.

One obvious question that arises from these results is: how does the NDH-1-mediated cycling of electrons from the acceptor side of PSI, back to the donor side, enhance the oxidation of PSI? Two possible mechanisms are: (1) As the major driver of CET coupled with proton pumping activity (Miller et al., 2021), NDH-$1_{1/2}$ could slow down the electron supply to PSI by inducing acidification of the lumen *via* the process known as photosynthetic control (Shimakawa & Miyake, 2018b; Malone et al., 2021). Moreover, (2) the respiratory activity of NDH-$1_{1/2}$ could contribute to PSI oxidation by alleviating electron pressure *via* RTO-mediated O_2 reduction, albeit RTOs have shown poor electron sink capacity (Ermakova et al., 2016).

In turn, both NDH-1 and FDPs compete for reducing power with CO_2 fixation. Therefore, a coordinated activity and efficient allocation of reductants among these pathways must be tightly regulated to maintain a balance between PSI photoprotection and metabolic demands. Some examples of this energetically efficient regulation are described as follows:

(1) As previously described in this thesis, the rapid and powerful nature of the electron sink mediated by Flv1/Flv3 is required during the first seconds after an increase in light intensity, in order to avoid over-reduction of PSI, induce LET, generate *pmf* and eventually activate CO_2 fixation (Paper I and III). Under LC conditions, after ~30 s in light, the activity of Flv1/Flv3 is no longer relevant under a constant light regime, even under HL (Allahverdiyeva et al., 2013), and it is quickly diminished in order to avoid futile competition for reductants with CO_2 fixation. This fast modulation of Flv1/Flv3 activity suggests a regulation by rapid post-translational modifications likely sensing redox changes. A potential regulatory mechanism is the light-dependent Fd- thioredoxin (FTR) system as it could couple the regulation of the CBB cycle (Schürmann & Buchanan, 2008), NDH-1 (Courteille et al., 2013; Nikkanen et al., 2018) and likely Flv1/Flv3 (Guo et al., 2014). Moreover, the activity of FDPs might be modulated by reversible phosphorylation as previously proposed for *Synechocystis* Flv3 and Flv4 (Angeleri et al., 2016) inducing conformational changes in the phosphorylated protein. Indeed, a conformational switch of FDP dimers corresponding to a ‘open-active’ or a ‘closed-inactive’ form

have been recently suggested for the *Physcomitrella patens* FlvA/FlvB heterodimer in response to redox changes (Alboresi et al., 2019).

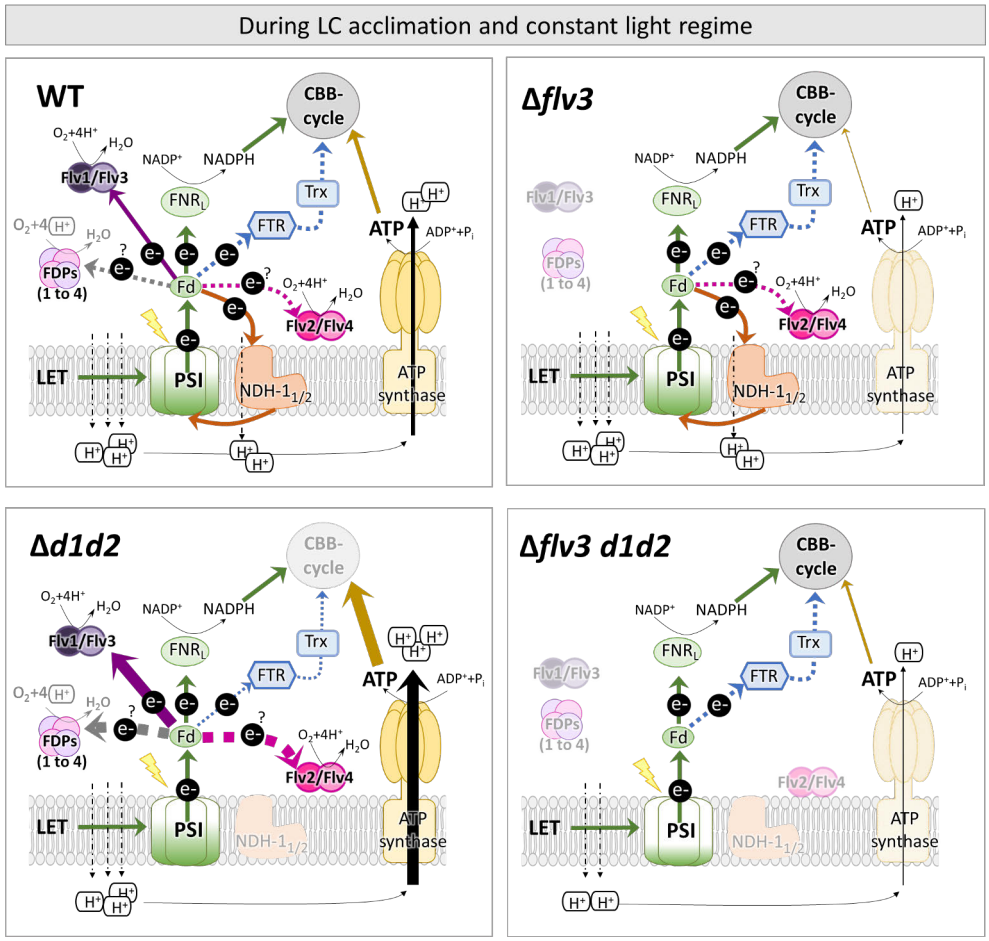

Figure 7. Schematic model of the functional redundancy between FDPs and NDH-1$_{1/2}$ in maintaining PSI oxidation in *Synechocystis* sp. PCC 6803. Efficient oxidation of PSI is depicted by the smooth gradient green color of PSI, while diminished ability to oxidize PSI is depicted by reduced green color of PSI. Delayed activation of the CBB cycle is depicted in light grey. Lower ATPase conductivity is depicted in light yellow color. Thicker arrows reflect increased flux of electrons or reductants through the corresponding pathway. Dotted arrows indicate possible/unverified electron transport pathways. Dotted black arrows indicate proton translocation across the TM. See the text for details.

(2) It is conceivable that cells employ similar post-translational modifications as those mentioned above to efficiently induce the O_2 photoreduction activity of FDPs without the need to increase the protein concentration. This could explain the FDPs

activity observed in cells grown under C_i limitation (without Na_2CO_3) or under acidic conditions (at pH 6) where the enhanced O_2 photoreduction was not concomitant with significant increase of FDPs expression (Paper I). Moreover, the strong activity of scarce Flv1(A)/Flv3(A) accumulated under HC might be partially explained by the enhanced activity *via* post-translational modification, in addition to diminished competition for electrons with the downregulated NDH-1. This modulation of the activity of FDPs adds an extra layer of complexity to their functional regulation, as protein abundance is not the only factor that determines O_2 photoreduction capacity. Nevertheless, it remains unclear which factors determine the metabolic flux distribution towards increased protein accumulation or enhanced efficiency of the expressed FDPs.

(3) A clear example of the trade-off between PSI oxidation and CO_2 fixation was exhibited in the deletion mutant of NDH-$1_{1/2}$. The boosted activity of FDPs was concomitant with a delayed activation of CO_2 fixation, likely due to a shortage of electrons for the FTR system required for activation of the CBB cycle (Paper III; Schürmann & Buchanan, 2008). The inverse was also observed in the Δ*flv3 d1d2* mutant unable to oxidize PSI *via* FDPs nor NDH-1, resulting in allocation of reductants towards CO_2 fixation (Paper III).

The Flv1/Flv3 heterodimer has been shown to have a crucial role in the generation of trans-thylakoid *pmf* during dark-to-light transitions (Paper III). This result was comparable to that of FLVA/B in *P. patens* (Gerotto et al., 2016) and *C. reinhardtii* (Chaux et al., 2017). Moreover, the bulk of *pmf* generated by Flv1/Flv3 and NDH-1, could further be requisite for CCM energization, as recently proposed in *Chlamydomonas reinhardtii* (Burlacot et al. 2021). In this work, the deletion of Flv1/Flv3 in *Synechocystis* was not correlated with a significant decrease in CCM activity (initial bump of CO_2 uptake) due to rapid compensation by downregulation of ATPase conductivity. Nevertheless, this scenario might be different in *Anabaena* which showed reduced CCM activity in the absence of Flv1A or Flv3A. However, this hypothesis requires further investigation.

Interestingly, the expression of CCM proteins showed, to some extent, coregulation with the expression of FDPs (Paper I; II; III; IV). While in S*ynechocystis*, the expression of CCM genes and the *flv4-flv2* operon have been shown to be regulated by the NdhR transcriptional regulator (Eisenhut et al., 2012), in *Anabaena*, the global transcriptional regulator PacR, the closest homolog of *Synechocystis* NdhR, has been shown to bind the promotor region of *flv1A*, *flv4* and CCM genes (Picossi et a., 2015). It is likely that the induction of CCM genes is, in addition, redox-sensitive (Burnap et al., 2014), which would explain why the Δ*flv3 d1d2* mutant failed to induce the expression of CCM during the shift to LC and HL, eventually causing lethality (Paper III).

5.4 Vegetative cell-specific Flv3A has a significant impact on the diazotrophic metabolism of the multicellular filaments of *Anabaena*

Diazotrophic filamentous heterocyst-forming cyanobacteria represent a true multicellular life form, unique in their ability to simultaneously perform two antagonistic but complementary metabolic processes: (i) O_2-producing photosynthesis in vegetative cells; and (ii) O_2-sensitive N_2 fixation in heterocysts. In order to support this division of labour, a strict control of the bioenergetics of the thylakoid membranes in both cell types is essential to provide sufficient reductants for the energy-expensive N_2 fixation reaction (Magnuson, 2019).

In Paper IV, I examined the physiological role of vegetative cell-specific Flv1A and Flv3A in the diazotrophic metabolism of *Anabaena* filaments. The strongly impaired growth of the *Anabaena* deletion mutant of Flv1A and Flv3A under FL conditions evidenced the crucial photoprotective role of the Flv1A/Flv3A heterodimer under this stress condition and suggest functional analogy with their homologs in other species (Paper IV; Allahverdiyeva et al., 2013; Gerotto et al. 2016, Jokel et al., 2018). The comprehensive phenotypic characterization of the deletion mutants of Flv1A and Flv3A under standard diazotrophic conditions suggested that:

(1) Flv3A has a more important role in light acclimation than Flv1A, regardless of nitrogen and C_i availability. Similar relevance has been previously suggested for the *Synechocystis* Flv3 under HL and HC conditions (Hackenberg et al., 2009).

(2) Flv3A is able to mediate a moderate O_2 photoreduction in the absence of Flv1A, and in coordination with Flv2 and Flv4. These results can be explained by the involvement of Flv3A in: (i) functional Flv3A/Flv2-4 oligomerization. While oligomeric arrangements between Flv2 and Flv3 were not detected in *Synechocystis* (Paper II), it is possible that functional oligomerization of FDPs in *Anabaena* has adapted differentially through evolution. Alternatively, (ii) a cooperation between the Flv3A homodimers and Flv2/Flv4 heterodimers is a plausible mechanism. Although *Synechocystis* Flv3 homodimers are not involved in O_2 photoreduction *in vivo* (Paper II), this might not be the case in diazotrophic *Anabaena*. Indeed, the O_2 photoreduction activity of putative Flv3B homodimers has been previously described in the heterocysts of diazotrophic *Anabaena* (Ermakova et al., 2014). Furthermore, Flv3A homodimers might function as a modulator of the O_2 photoreduction activity of Flv2 and Flv4 by enhancing the reversible association of Flv2/Flv4 with the TM via *pmf* generation or cation homeostasis (Zhang et al., 2012).

(3) The deletion of Flv3A is partially compensated by the strong upregulation of PTOX, which likely mediates an electron pathway other than O_2 photoreduction. Although the role of PTOX in photosynthesis is still controversial, previous studies have indicated that PTOX contributes to the oxidation of the PETC, specifically

under stress conditions, when the photosynthetic electron transport is limited (Bolte et al., 2021) and under iron limiting conditions (Bailey et al., 2008).

Nevertheless, further supporting *in vivo* experiments including different combinations of deletion mutants are required to elucidate the functional oligomeric arrangements of the vegetative cell-specific FDPs in *Anabaena*.

Strikingly, an absence of Flv3A demonstrated effects in the heterocyst metabolisms of *Anabaena*. The deletion of the vegetative cell-specific Flv3A resulted in downregulation of the heterocyst specific-protein Hup which led to enhanced nitrogenase-based H_2 photoproduction under both oxic and micro-oxic conditions (Paper IV). These results reveal a complex regulatory network between the Mehler-like reaction in the vegetative cells and the H_2 metabolism in the heterocysts of *Anabaena*. The *flv3A* and heterocyst specific *hupL* genes might both be regulated by the transcriptional regulator FurA, whose binding sites have been reported in both genes (González et al. 2014). Data from the global transcriptome analysis suggest a trade-off in iron resource allocation between photoprotection and H_2 metabolism. This is in agreement with early studies reporting the impact of PSII activity in vegetative cells on the nitrogenase activity in the heterocysts (Ketkorn et al. 2012; Chen et al., 2014).

6 Concluding remarks

The research presented in this PhD thesis expands our understanding of how photosynthesis is regulated in cyanobacterial cells in response to a dynamic environment. I focused on the functional regulation of the FDPs in cyanobacteria. Through the work undertaken in this thesis, I have demonstrated that:

- The Flv1/Flv3 heterodimer is the major contributor to the *induction* phase of O_2 photoreduction during the transition from dark-to-light or during sudden increases in light intensity. Under HC conditions, a low level of Flv1/Flv3 is sufficient to catalyse a strong and steady-state O_2 photoreduction. Meanwhile, under LC conditions, a moderate level of Flv1/Flv3 mediates a strong but transient O_2 photoreduction. I hypothesize that the activity of Flv1/Flv3 is modulated by crosstalk with the NDH-1 complex downstream of PSI. Thereby, the transient activity of Flv1/Flv3 under LC is likely due to the competition for electrons with NDH-1. Furthermore, it is possible that the fast *quenching* of Flv1/Flv3 activity under LC and enhancement of Flv1/Flv3 activity under HC is regulated by post-translational modifications, likely through sensing redox changes.
- A more exhaustive examination of the functional cooperation between FDPs and NDH-1 complexes demonstrated a partial functional redundancy between Flv1/Flv3 and NDH-$1_{1/2}$. Moreover, a dynamic coordination between both pathways was required for efficient oxidation of PSI, build-up of *pmf* and CO_2 fixation. Yet the precise regulatory mechanism enabling the dynamic coordination between FDPs and NDH-1 remains elusive. One possible mechanism hypothesized in this work involves the light-dependent Fd-thioredoxin (FTR) system, as it could couple the regulation of the CBB cycle, NDH-1 and likely, Flv1/Flv3. Although light-dependent redox modulation has been previously described in *Synechocystis* Flv1 and Flv3, the physiological relevance of these redox changes needs to be addressed in further studies.
- The Flv2/Flv4 heterodimer contributes to the Mehler-like reaction *in vivo* and catalyses a slower and limited *steady-state* reduction of O_2. Under LC (pH 6-8.2), Flv2/Flv4 functions in a coordinated and interdependent manner with

Flv1/Flv3, downstream of PSI. I propose that after the transient activity of Flv1/Flv3, Flv2/Flv4 takes over O_2 photoreduction in order to maintain LET in an oxidized state. The distinct efficiency between Flv1/Flv3 and Flv2/Flv4 might be partially regulated by their interaction with different electron donors. The *in vivo* data presented in this work strongly supports the hypothesis of Fd as the main electron donor for Flv1/Flv3. Nevertheless, further evidence of the *in vivo* protein-protein interaction of FDPs and Fd would be required to consolidate this hypothesis. Likewise, addressing the possible involvement of FNR as electron donor of FDPs, *in vitro* and/or *in vivo*, could help to understand the modulation of FDP activity.

- Under FL conditions, the essential photoprotective role of Flv1/Flv3 might become energetically disadvantageous over long-term FL exposure- if not regulated. It is conceivable that the induced Fd-dependent nitrate reductase serves as an important electron valve for WT cells under FL conditions, although the exact photoprotective mechanism remains elusive. Additionally, the Flv1/Flv1 and Flv3/Flv3 homodimers demonstrated a contribution to the photoprotection of cells under FL conditions, mediating an oxygen-independent reaction, yet unknown.
- Remarkably, the crucial photoprotective role of vegetative cell-specific Flv1A/Flv3A during sudden changes in light intensity, suggests a functional analogy with homologs in *Synechocystis*. Though, the functional regulation of *Anabaena* FDPs seem to differ. Flv3A has shown to be more important for the photoprotection of diazotrophic *Anabaena*. Moreover, *Anabaena* mutants devoid of Flv1A are likely conferred with alternative oligomeric arrangements involving the Flv3A, Flv2 and Flv4 proteins, although the specific functional oligomeric arrangements responsible for O_2 photoreduction are yet to be identified. Further experiments would likely require the study of different combinations of FDP deletion mutants and the optimization of specific antibodies against *Anabaena* FDPs. Importantly, the deletion of Flv3A resulted in increased bioproduction of H_2 due to the downregulation of the heterocyst- specific Hup enzyme. This novel regulatory network might represent an unexploited source of biotechnological potential for the improved production of H_2 in multicellular cyanobacteria. Nevertheless, much work remains to be done in understanding the mechanisms behind this regulation for future engineering strategies.

Finally, besides the knowledge on basic research provided in this thesis work, the findings presented in this research are of major relevance for paving the way towards the development of engineered cyanobacterial cells with improved production yields

of targeted solar fuels and/or bio-industrial chemicals. In particular, this work provides potential candidates and growth conditions for the strategic elimination of energetically wasteful electron sinks and possibility to redirect photosynthetic electron flux towards target pathways.

7 Acknowledgments

I want to take this opportunity to express my sincere gratitude to all of you who have supported me during this journey of completing my PhD studies.

First of all, I want to express my deepest gratitude to all the people I have encountered at the Molecular Plant Biology lab for creating such an inspiring environment for conducting high-quality research. It has been an amazing pleasure to develop my scientific career in this place, over the last 9 years! Moreover, I gratefully acknowledge the Kone Foundation, the DPMLS doctoral program, and NordAqua NCoE for their financial support.

I will be eternally grateful to Academician Eva-Mari Aro for giving me the opportunity to integrate her research group while I was still an inexperienced undergraduate student. Thanks for your feedback and follow-up on my progress during my PhD studies. I am also immensely grateful to my supervisor Prof. Yagut-Allahverdiyeva for her unconditional support, guidance, and a lot of patience during these years of research. Thanks for your honest and constructive criticism every time I needed it. I have received invaluable advice for my research thinking and a great encouragement to move forward in my career. Many thanks!

I wish to express my gratitude to Prof. Eevi Rintämaki for her support in completing my PhD studies. I also want to thank my advisory committee members Dr. Taina Tyystjärvi, Dr. Sergey Kosourov and Dr. Julia Vainonen, for their valuable comments throughout my doctoral journey. I am extremely thankful to all the co-authors of the original publications for their essential contribution to make this thesis possible. My deepest gratitude also goes to Dr. Fiona Lynch for her guidance during my Master studies and support thereafter. Many thanks for carefully checking the language and readability of this thesis. I owe a big thanks to Tuomas for his prompt help and effort in translating the Abstract of this thesis into Finnish. I am also very grateful to Prof. Amel Latifi and Prof. Josef Komenda for their effort in reviewing and improving the content of this thesis. Likewise, I am thankful to Prof. Tomas Morosinotto for accepting the invitation to be my Opponent during my doctoral disputation.

I also want to express my gratitude to all members of the PhotoMicrobe team for our weekly scientific discussions and the spirit to help each other in the lab. I also extend my gratitude to Daniel for his help in the lab and with all the PhD matters. And, I especially want to express my gratitude to Mika and Sema for their parental care during all these years. I really appreciate it!

This thesis would not have been possible without the inspiration and support of all my dear friends whom I met during my time in Turku. Special thanks to Juande and Chus, for always being there answering my infinite questions in the lab, for all the coffee breaks and advice. Muchas gracias! I especially want to thank my dear friend Luca for the amazing impact he has had on my life. Many thanks *Durazno* for showing me how to have fun while doing excellent research, for the emotional encouragement, and for all the crazy experiences we have shared in Finland, the Netherlands and Perú! I also want to thank Matina, Julia, Sara, Sindhu, Azfar, Joao, Harri, Xu, and Ville for the friendship, the funny moments inside and outside the lab, especially during our trips, dinners outings, and celebrations. I want to express my immeasurable gratitude to Natasa for her extreme care, positive energy, and support in many challenging moments. I have received just love from you and your family, and for that muchas gracias *chiquilina*! And from the bottom of my heart thanks a million to all my Peruvian friends (almost like a family) in Turku, Natalia, Jesus, Paola, Sheyla, Susan and Nelly (among others) for the infinite experiences we have shared in all these years, for your support, encouragement, and love always.

Finalmente, me van a quedar cortas las palabras para expresar mi infinito agradecimiento a mi mami Cori y mi papá Mauro, quien ahora me acompaña desde el cielo. Soy consciente del gran esfuerzo que han hecho para apoyarme en todas las decisiones que he tomado en mi vida. Mil gracias por el amor sin límites que siempre me han demostrado, a pesar de la distancia. Este logro es de Uds. también! Y a tooodo el resto de mi familia en Perú, mis hermanos Caleb, Noe y Coco, mi tía Carmen, mi tío Lino y mis primos. Gracias por estar siempre ahí pendientes de mí. Los quiero muchísimo!

Y no puedo acabar esta tesis sin mencionar a mi nueva familia Finlandesa que ha cuidado de mi durante la etapa final de mi doctorado. Un millón de gracias *Amorcito* por siempre sacarme una sonrisa aún en los momentos más complicados, por tanta paciencia y amor incondicional. A mi segunda mamá Marianne, a Roger, Rayner, y todos los hijos muchísimas gracias por su aprecio. Tack så mycket!

8 List of References

Alboresi, A., Storti, M., & Morosinotto, T. (2019). Balancing protection and efficiency in the regulation of photosynthetic electron transport across plant evolution. *New Phytologist*, *221*(1), 105–109.

Allahverdiyeva, Y., Ermakova, M., Eisenhut, M., Zhang, P., Richaud, P., Hagemann, M., … Aro, E. M. (2011). Interplay between flavodiiron proteins and photorespiration in Synechocystis sp. PCC 6803. *Journal of Biological Chemistry*, *286*(27), 24007–24014.

Allahverdiyeva, Y., Mustila, H., Ermakova, M., Bersanini, L., Richaud, P., Ajlani, G., … Aro, E. M. (2013). Flavodiiron proteins Flv1 and Flv3 enable cyanobacterial growth and photosynthesis under fluctuating light. *Proceedings of the National Academy of Sciences of the United States of America*, *110*(10), 4111–4116.

Allahverdiyeva, Y., Isojärvi, J., Zhang, P., & Aro, E. M. (2015). Cyanobacterial oxygenic photosynthesis is protected by flavodiiron proteins. *Life*, *5*(1), 716–743.

Allen, J. F. (2003). Cyclic, pseudocyclic and noncyclic photophosphorylation: New links in the chain. *Trends in Plant Science*, *8*(1), 15–19.

Almon, H., & Hme, H. B. C. (1982). Algal culture: Nostoc muscorum { Anabaena Isolation of heterocysts and preparation of sphero-, *679*, 279–286.

Angeleri, M., Muth-Pawlak, D., Aro, E. M., & Battchikova, N. (2016). Study of O-Phosphorylation Sites in Proteins Involved in Photosynthesis-Related Processes in Synechocystis sp. Strain PCC 6803: Application of the SRM Approach. *Journal of Proteome Research*, *15*(12), 4638–4652.

Appel, J., Phunpruch, S., Steinmüller, K., & Schulz, R. (2000). The bidirectional hydrogenase of Synechocystis sp. PCC 6803 works as an electron valve during photosynthesis. *Archives of Microbiology*, *173*(5–6), 333–338.

Arévalo, S., Nenninger, A., Nieves-Morión, M., Herrero, A., Mullineaux, C. W., & Flores, E. (2021). Coexistence of Communicating and Noncommunicating Cells in the Filamentous Cyanobacterium Anabaena. *MSphere*, *6*(1).

Armbruster, U., Correa Galvis, V., Kunz, H. H., & Strand, D. D. (2017). The regulation of the chloroplast proton motive force plays a key role for photosynthesis in fluctuating light. *Current Opinion in Plant Biology*, *37*, 56–62.

Arora, N., Jaiswal, D., Sengupta, S., & Wangikar, P. P. (2020). Metabolic engineering of cyanobacteria for production of platform chemicals: A synthetic biology approach. In *Handbook of Algal Science, Technology and Medicine* (pp. 127-145). Academic Press.

Artz, J. H., Tokmina-Lukaszewska, M., Mulder, D. W., Lubner, C. E., Gutekunst, K., Appel, J., … King, P. W. (2020). The structure and reactivity of the HoxEFU complex from the cyanobacterium Synechocystis sp. PCC 6803. *Journal of Biological Chemistry*, *295*(28), 9445–9454.

Asada, K. (1999). The water-water cycle in chloroplasts: Scavenging of active oxygens and dissipation of excess photons. *Annual Review of Plant Biology*, *50*, 601–639.

Bailey, S., Melis, A., Mackey, K. R. M., Cardol, P., Finazzi, G., van Dijken, G., … Grossman, A. (2008). Alternative photosynthetic electron flow to oxygen in marine Synechococcus. *Biochimica et Biophysica Acta - Bioenergetics*, *1777*(3), 269–276.

Bao, H., Melnicki, M. R., & Kerfeld, C. A. (2017). Structure and functions of Orange Carotenoid Protein homologs in cyanobacteria. *Current Opinion in Plant Biology*, *37*(April), 1–9.

Battchikova, N., Eisenhut, M., & Aro, E. M. (2011). Cyanobacterial NDH-1 complexes: Novel insights and remaining puzzles. *Biochimica et Biophysica Acta - Bioenergetics*, *1807*(8), 935–944.

Bauwe, H., Hagemann, M., & Fernie, A. R. (2010). Photorespiration: players, partners and origin. *Trends in Plant Science*, *15*(6), 330–336.

Beckmann, K., Messinger, J., Badger, M. R., Wydrzynski, T., & Hillier, W. (2009). On-line mass spectrometry: Membrane inlet sampling. *Photosynthesis Research*, *102*(2), 511–522.

Bernát, G., Appel, J., Ogawa, T., & Rögner, M. (2011). Distinct roles of multiple NDH-1 complexes in the cyanobacterial electron transport network as revealed by kinetic analysis of P700+ reduction in various ndh-deficient mutants of Synechocystis sp. strain PCC6803. *Journal of Bacteriology*, *193*(1), 292–295.

Berry, S., Schneider, D., Vermaas, W. F. J., & Rögner, M. (2002). Electron transport routes in whole cells of Synechocystis sp. Strain PCC 6803: The role of the cytochrome bd-type oxidase. *Biochemistry*, *41*(10), 3422–3429.

Bersanini, L., Battchikova, N., Jokel, M., Rehman, A., Vass, I., Allahverdiyeva, Y., & Aro, E. M. (2014). Flavodiiron protein Flv2/Flv4-related photoprotective mechanism dissipates excitation pressure of PSII in cooperation with phycobilisomes in cyanobacteria. *Plant Physiology*, *164*(2), 805–818.

Bersanini, L., Allahverdiyeva, Y., Battchikova, N., Heinz, S., Lespinasse, M., Ruohisto, E., … Aro, E. M. (2017). Dissecting the Photoprotective Mechanism Encoded by the flv4-2 Operon: a Distinct Contribution of Sll0218 in Photosystem II Stabilization. *Plant Cell and Environment*, *40*(3), 378–389.

Bolte, S., Marcon, E., Jaunario, M., Moyet, L., Paternostre, M., Kuntz, M., & Krieger-Liszkay, A. (2021). Dynamics of the localization of the plastid terminal oxidase inside the chloroplast. *Journal of Experimental Botany*, *71*(9), 2661–2669.

Borges, P. T., Romão, C. V., Saraiva, L. M., Gonçalves, V. L., Carrondo, M. A., Teixeira, M., & Frazão, C. (2019). Analysis of a new flavodiiron core structural arrangement in Flv1-ΔFlR protein from Synechocystis sp. PCC6803. *Journal of structural biology, 205*(1), 91-102.

Bothe, H., Schmitz, O., Yates, M. G., & Newton, W. E. (2010). Nitrogen Fixation and Hydrogen Metabolism in Cyanobacteria. *Microbiology and Molecular Biology Reviews*, *74*(4), 529–551.

Brändén, G., Gennis, R. B., & Brzezinski, P. (2006). Transmembrane proton translocation by cytochrome c oxidase. *Biochimica et Biophysica Acta - Bioenergetics*, *1757*(8), 1052–1063.

Brocke, H. J., Wenzhoefer, F., De Beer, D., Mueller, B., Van Duyl, F. C., & Nugues, M. M. (2015). High dissolved organic carbon release by benthic cyanobacterial mats in a Caribbean reef ecosystem. *Scientific Reports*, *5*, 1–7.

Brown, K. A., Guo, Z., Tokmina-Lukaszewska, M., Scott, L. W., Lubner, C. E., Smolinski, S., … King, P. W. (2019). The oxygen reduction reaction catalyzed by: Synechocystis sp. PCC 6803 flavodiiron proteins. *Sustainable Energy and Fuels*, *3*(11), 3191–3200.

Burgess, B. K., & Lowe, D. J. (1996). Mechanism of molybdenum nitrogenase. *Chemical Reviews*, *96*(7), 2983–3011.

Burnap, R. L., Hagemann, M., & Kaplan, A. (2015). Regulation of CO2concentrating mechanism in cyanobacteria. *Life*, *5*(1), 348–371.

Burlacot, A., Dao, O., Auroy, P., Cuiné, S., Li-Beisson, Y., & Peltier, G. (2021). Alternative electron pathways of photosynthesis drive the algal CO2 concentrating mechanism. *bioRxiv*.

Calzadilla, P. I., & Kirilovsky, D. (2020). Revisiting cyanobacterial state transitions. *Photochemical and Photobiological Sciences*, *19*(5), 585–603.

Camargo, S., Leshkowitz, D., Dassa, B., Mariscal, V., Flores, E., Stavans, J., & Arbel-Goren, R. (2021). Impaired cell-cell communication in the multicellular cyanobacterium Anabaena affects carbon uptake, photosynthesis, and the cell wall. *IScience*, *24*(1), 101977.

Cardona, T., Battchikova, N., Zhang, P., Stensjö, K., Aro, E. M., Lindblad, P., & Magnuson, A. (2009). Electron transfer protein complexes in the thylakoid membranes of heterocysts from the cyanobacterium Nostoc punctiforme. *Biochimica et*

Biophysica Acta - Bioenergetics, *1787*(4), 252–263.

Cardona, T., Murray, J. W., & Rutherford, A. W. (2015). Origin and evolution of water oxidation before the last common ancestor of the cyanobacteria. *Molecular Biology and Evolution*, *32*(5), 1310–1328.

Cassier-Chauvat, C., & Chauvat, F. (2014). Function and regulation of ferredoxins in the cyanobacterium, Synechocystis PCC6803: Recent advances. *Life*, *4*(4), 666–680.

Chandra, R., Iqbal, H. M. N., Vishal, G., Lee, H. S., & Nagra, S. (2019). Algal biorefinery: A sustainable approach to valorize algal-based biomass towards multiple product recovery. *Bioresource Technology*, *278*(November 2018), 346–359.

Chaux, F., Burlacot, A., Mekhalfi, M., Auroy, P., Blangy, S., Richaud, P., & Peltier, G. (2017). Flavodiiron proteins promote fast and transient O2 photoreduction in chlamydomonas. *Plant Physiology*, *174*(3), 1825–1836.

Checchetto, V., Teardo, E., Carraretto, L., Formentin, E., Bergantino, E., Giacometti, G. M., & Szabo, I. (2013). Regulation of photosynthesis by ion channels in cyanobacteria and higher plants. *Biophysical Chemistry*, *182*, 51–57.

Chittora, D., Meena, M., Barupal, T., & Swapnil, P. (2020). Cyanobacteria as a source of biofertilizers for sustainable agriculture. *Biochemistry and Biophysics Reports*, *22*(February), 100737.

Chukhutsina, V., Bersanini, L., Aro, E. M., & Van Amerongen, H. (2015). Cyanobacterial flv4-2 operon-encoded proteins optimize light harvesting and charge separation in photosystem II. *Molecular Plant*, *8*(5), 747–761.

Cooley, J. W., & Vermaas, W. F. J. (2001). Succinate dehydrogenase and other respiratory pathways in thylakoid membranes of Synechocystis sp. strain PCC 6803: Capacity comparisons and physiological function. *Journal of Bacteriology*, *183*(14), 4251–4258.

Cournac, L., Guedeney, G., Peltier, G., & Vignais, P. M. (2004). Sustained Photoevolution of Molecular Hydrogen in a Mutant of Synechocystis sp. Strain PCC 6803 Deficient in the Type I NADPH-Dehydrogenase Complex. *Journal of Bacteriology*, *186*(6), 1737–1746.

Cournac, L., Mus, F., Bernard, L., Guedeney, G., Vignais, P., & Peltier, G. (2002). Limiting steps of hydrogen production in Chlamydomonas reinhardtii and Synechocystis PCC 6803 as analysed by light-induced gas exchange transients. *International Journal of Hydrogen Energy*, *27*(11–12), 1229–1237.

Courteille, A., Vesa, S., Sanz-Barrio, R., Cazalé, A. C., Becuwe-Linka, N., Farran, I., … Rumeau, D. (2013). Thioredoxin m4 controls photosynthetic alternative electron pathways in Arabidopsis. *Plant Physiology*, *161*(1), 508–520.

Cramer, W. A., Hasan, S. S., & Yamashita, E. (2011). The Q cycle of cytochrome bc complexes: A structure perspective. *Biochimica et Biophysica Acta - Bioenergetics*, *1807*(7), 788–802.

Cruz, J. A., Avenson, T. J., Kanazawa, A., Takizawa, K., Edwards, G. E., & Kramer, D. M. (2005). Plasticity in light reactions of photosynthesis for energy production and photoprotection. *Journal of Experimental Botany*, *56*(411), 395–406.

DalCorso, G., Pesaresi, P., Masiero, S., Aseeva, E., Schünemann, D., Finazzi, G., … Leister, D. (2008). A Complex Containing PGRL1 and PGR5 Is Involved in the Switch between Linear and Cyclic Electron Flow in Arabidopsis. *Cell*, *132*(2), 273–285.

Dann, M., & Leister, D. (2019). Evidence that cyanobacterial Sll1217 functions analogously to PGRL1 in enhancing PGR5-dependent cyclic electron flow. *Nature Communications*, *10*(1), 1–7.

Di Matteo, A., Scandurra, F. M., Testa, F., Forte, E., Sarti, P., Brunori, M., & Giuffrè, A. (2008). The O2-scavenging flavodiiron protein in the human parasite Giardia intestinalis. *Journal of Biological Chemistry*, *283*(7), 4061–4068.

Dixon, R. O. D. (1972). Hydrogenase in legume root nodule bacteroids: Occurrence and properties. *Archiv Für Mikrobiologie*, *85*(3), 193–201.

Draber, W., & Harth, E. (1970). On a new inhibitor of photosynthetic electron-transport in isolated chloroplasts. *Zeitschrift Fur Naturforschung - Section B Journal of Chemical Sciences*, *25*(10), 1157–1159.

Drábková, M., Admiraal, W., & Maršálek, B. (2007). Combined exposure to hydrogen peroxide and light-selective effects on

cyanobacteria, green algae, and diatoms. *Environmental Science and Technology*, *41*(1), 309–314.

Durán, R. V., Hervás, M., De La Rosa, M. A., & Navarro, J. A. (2004). The Efficient Functioning of Photosynthesis and Respiration in Synechocystis sp. PCC 6803 Strictly Requires the Presence of either Cytochrome c6 or Plastocyanin. *Journal of Biological Chemistry*, *279*(8), 7229–7233.

Ehira, S., Ohmori, M., & Sato, N. (2003). Genome-wide expression analysis of the responses to nitrogen deprivation in the heterocyst-forming cyanobacterium Anabaena sp. Strain PCC 7120. *DNA Research*, *10*(3), 97–113.

Eisenhut, M., Georg, J., Klähn, S., Sakurai, I., Mustila, H., Zhang, P., … Aro, E. M. (2012). The antisense RNA As1-flv4 in the cyanobacterium Synechocystis sp. PCC 6803 prevents premature expression of the flv4-2 operon upon shift in inorganic carbon supply. *Journal of Biological Chemistry*, *287*(40), 33153–33162.

Eisenhut, M., Von Wobeser, E. A., Jonas, L., Schubert, H., Ibelings, B. W., Bauwe, H., … Hagemann, M. (2007). Long-term response toward inorganic carbon limitation in wild type and glycolate turnover mutants of the cyanobacterium Synechocystis sp. strain PCC 6803. *Plant Physiology*, *144*(4), 1946–1959.

Ekman, M., Ow, S. Y., Holmqvist, M., Zhang, X., Van Wagenen, J., Wright, P. C., & Stensjö, K. (2011). Metabolic adaptations in a H2 producing heterocyst-forming cyanobacterium: Potentials and implications for biological engineering. *Journal of Proteome Research*, *10*(4), 1772–1784.

Ermakova, M., Battchikova, N., Allahverdiyeva, Y., & Aro, E. M. (2013). Novel heterocyst-specific flavodiiron proteins in Anabaena sp. PCC 7120. *FEBS Letters*, *587*(1), 82–87.

Ermakova, M., Battchikova, N., Richaud, P., Leino, H., Kosourov, S., Isojaŕvi, J., … Aro, E. M. (2014). Heterocyst-specific flavodiiron protein Flv3B enables oxic diazotrophic growth of the filamentous cyanobacterium Anabaena sp. PCC 7120. *Proceedings of the National Academy of Sciences of the United States of America*, *111*(30), 11205–11210.

Ermakova, M., Huokko, T., Richaud, P., Bersanini, L., Howe, C. J., Lea-Smith, D. J., … Allahverdiyeva, Y. (2016). Distinguishing the roles of thylakoid respiratory terminal oxidases in the cyanobacterium Synechocystis sp. PCC 6803. *Plant Physiology*, *171*(2), 1307–1319.

Fan, D. Y., Fitzpatrick, D., Oguchi, R., Ma, W., Kou, J., & Chow, W. S. (2016). Obstacles in the quantification of the cyclic electron flux around Photosystem I in leaves of C3 plants. *Photosynthesis Research*, *129*(3), 239–251.

Fernández-Velasco, J. G., Jamshidi, A., Gong, X. S., Zhou, J., & Ueng, R. Y. (2001). Photosynthetic Electron Transfer through the Cytochrome b6f Complex Can Bypass Cytochrome f. *Journal of Biological Chemistry*, *276*(33), 30598–30607.

Fernie, A. R., & Bauwe, H. (2020). Wasteful, essential, evolutionary stepping stone? The multiple personalities of the photorespiratory pathway. *Plant Journal*, *102*(4), 666–677.

Ferreira, K. N., Iverson, T. M., Maghlaoui, K., Barber, J., & Iwata, S. (2004). Architecture of the photosynthetic oxygen-evolving center. *Science, 303*(5665), 1831-1838.

Fischer, W. W., Hemp, J., & Valentine, J. S. (2016a). How did life survive Earth's great oxygenation? *Current Opinion in Chemical Biology*, *31*, 166–178.

Fischer, W. W., Hemp, J., & Johnson, J. E. (2016b). Evolution of Oxygenic Photosynthesis. *Annual Review of Earth and Planetary Sciences*, *44*, 647–683.

Flaherty, B. L., Van Nieuwerburgh, F., Head, S. R., & Golden, J. W. (2011). Directional RNA deep sequencing sheds new light on the transcriptional response of Anabaena sp. strain PCC 7120 to combined-nitrogen deprivation. *BMC Genomics*, *12*.

Flombaum, P., Gallegos, J. L., Gordillo, R. A., Rincón, J., Zabala, L. L., Jiao, N., … Martiny, A. C. (2013). Present and future global distributions of the marine Cyanobacteria Prochlorococcus and Synechococcus. *Proceedings of the National Academy of Sciences of the United States of America*, *110*(24), 9824–9829.

Flores, E., & Herrero, A. (2010). Compartmentalized function through cell differentiation in filamentous cyanobacteria. *Nature Reviews Microbiology*, *8*(1), 39–50.

Flores, E., Herrero, A., Forchhammer, K., & Maldener, I. (2016). Septal Junctions in Filamentous Heterocyst-Forming Cyanobacteria. *Trends in Microbiology*, *24*(2), 79–82.

Flores, E., Herrero, A., Wolk, C. P., & Maldener, I. (2006). Is the periplasm continuous in filamentous multicellular cyanobacteria? *Trends in Microbiology*, *14*(10), 439–443.

Flores, E., López-lozano, A., & Herrero, A. (2015). Nitrogen Fixation in the Oxygenic (Cyanobacteria): The Fight Against Oxygen, *2*.

Flores, E., Nieves-Morión, M., & Mullineaux, C. W. (2019). Cyanobacterial septal junctions: Properties and regulation. *Life*, *9*(1), 1–14.

Flores, E., Pernil, R., Muro-Pastor, A. M., Mariscal, V., Maldener, I., Lechno-Yossef, S., … Herrero, A. (2007). Septum-localized protein required for filament integrity and diazotrophy in the heterocyst-forming cyanobacterium Anabaena sp. strain PCC 7120. *Journal of Bacteriology*, *189*(10), 3884–3890.

Folgosa, F., Martins, M. C., & Teixeira, M. (2018). Diversity and complexity of flavodiiron NO/O2 reductases. *FEMS Microbiology Letters*, *365*(3), 1–8.

Frazão, C., Silva, G., Gomes, C. M., Matias, P., Coelho, R., Sieker, L., … Le Gall, J. (2000). Structure of a dioxygen reduction enzyme from Desulfovibrio gigas. *Nature Structural Biology*, *7*(11), 1041–1045.

Friedlingstein, P., O'sullivan, M., Jones, M. W., Andrew, R. M., Hauck, J., Olsen, A., ... & Zaehle, S. (2020). Global carbon budget 2020. *Earth System Science Data*, *12*(4), 3269-3340.

Gao, F., Zhao, J., Chen, L., Battchikova, N., Ran, Z., Aro, E. M., … Ma, W. (2016). The NDH-1L-PSI supercomplex is important for efficient cyclic electron transport in cyanobacteria. *Plant Physiology*, *172*(3), 1451–1464.

Genty, B., Briantais, J. M., & Baker, N. R. (1989). The relationship between the quantum yield of photosynthetic electron transport and quenching of chlorophyll fluorescence. *Biochimica et Biophysica Acta (BBA)-General Subjects, 990*(1), 87-92.

Gerotto, C., Alboresi, A., Meneghesso, A., Jokel, M., Suorsa, M., Aro, E. M., & Morosinotto, T. (2016). Flavodiiron proteins act as safety valve for electrons in Physcomitrella patens. *Proceedings of the National Academy of Sciences of the United States of America*, *113*(43), 12322–12327.

Gonçalves, V. L., Vicente, J. B., Saraiva, L. M., & Teixeira, M. (2011). Bioenergetic Processes of Cyanobacteria. *Bioenergetic Processes of Cyanobacteria*, 631–653.

González, A., Angarica, V. E., Sancho, J., & Fillat, M. F. (2014). The FurA regulon in Anabaena sp. PCC 7120: In silico prediction and experimental validation of novel target genes. *Nucleic Acids Research*, *42*(8), 4833–4846.

Grossman, A. R., Mackey, K. R. M., & Bailey, S. (2010). A perspective on photosynthesis in the oligotrophic oceans: Hypotheses concerning alternate routes of electron flow. *Journal of Phycology*, *46*(4), 629–634.

Gunnelius, L., Hakkila, K., Kurkela, J., Wada, H., Tyystjärvi, E., & Tyystjärvi, T. (2014). The omega subunit of the RNA polymerase core directs transcription efficiency in cyanobacteria. *Nucleic Acids Research*, *42*(7), 4606–4614.

Guo, J., Nguyen, A. Y., Dai, Z., Su, D., Gaffrey, M. J., Moore, R. J., … Qian, W. J. (2014). Proteome-wide light/dark modulation of thiol oxidation in cyanobacteria revealed by quantitative site-specific redox proteomics. *Molecular and Cellular Proteomics*, *13*(12), 3270–3285.

Gutekunst, K., Chen, X., Schreiber, K., Kaspar, U., Makam, S., & Appel, J. (2014). The bidirectional NiFe-hydrogenase in synechocystis sp. PCC 6803 Is reduced by flavodoxin and ferredoxin and is essential under mixotrophic, nitrate-limiting conditions. *Journal of Biological Chemistry*, *289*(4), 1930–1937.

Hackenberg, C., Engelhardt, A., Matthijs, H. C. P., Wittink, F., Bauwe, H., Kaplan, A., & Hagemann, M. (2009). Photorespiratory 2-phosphoglycolate metabolism and photoreduction of O 2 cooperate in high-light acclimation of Synechocystis sp. strain PCC 6803. *Planta*, *230*(4), 625–637.

Hagemann, M., Song, S., & Brouwer, E. (2021). Inorganic Carbon Assimilation in Cyanobacteria: Mechanisms, Regulation, and Engineering. *Cyanobacteria Biotechnology*, 1–31.

Han, X., Sun, N., Xu, M., & Mi, H. (2017). Co-ordination of NDH and Cup proteins in CO2uptake in cyanobacterium Synechocystis sp. PCC 6803. *Journal of Experimental Botany*, *68*(14), 3869–3877.

Hanke, G. T., Satomi, Y., Shinmura, K., Takao, T., & Hase, T. (2011). A screen for potential ferredoxin electron transfer partners uncovers new, redox dependent interactions. *Biochimica et Biophysica Acta - Proteins and Proteomics*, *1814*(2), 366–374.

Happe, T., Schütz, K., & Böhme, H. (2000). Transcriptional and mutational analysis of the uptake hydrogenase of the filamentous cyanobacterium Anabaena variabilis ATCC 29413. *Journal of Bacteriology*, *182*(6), 1624–1631.

Helman, Y., Barkan, E., Eisenstadt, D., Luz, B., & Kaplan, A. (2005). Fractionation of the three stable oxygen isotopes by oxygen-producing and oxygen-consuming reactions in photosynthetic organisms. *Plant Physiology*, *138*(4), 2292–2298.

Helman, Y., Tchernov, D., Reinhold, L., Shibata, M., Ogawa, T., Schwarz, R., … Kaplan, A. (2003). Genes encoding A-type flavoproteins are essential for photoreduction of O2 in cyanobacteria. *Current Biology*, *13*(3), 230–235.

Hernández-Prieto, M. A., Schön, V., Georg, J., Barreira, L., Varela, J., Hess, W. R., & Futschik, M. E. (2012). Iron deprivation in synechocystis: Inference of pathways, non-coding RNAs, and regulatory elements from comprehensive expression profiling. *G3: Genes, Genomes, Genetics*, *2*(12), 1475–1495.

Herrero, A., & Flores, E. (2019). Genetic responses to carbon and nitrogen availability in Anabaena. *Environmental Microbiology*, *21*(1), 1–17.

Hihara, Y., Kamei, A., Kanehisa, M., Kaplan, A., & Ikeuchi, M. (2001). DNA microarray analysis of cyanobacterial gene expression during acclimation to high light. *Plant Cell*, *13*(4), 793–806.

Hitchcock, A., Hunter, C. N., & Canniffe, D. P. (2020). Progress and challenges in engineering cyanobacteria as chassis for light-driven biotechnology. *Microbial Biotechnology*, *13*(2), 363–367.

Hoffman, B. M., Lukoyanov, D., Yang, Z. Y., Dean, D. R., & Seefeldt, L. C. (2014). Mechanism of nitrogen fixation by nitrogenase: The next stage. *Chemical Reviews*, *114*(8), 4041–4062.

Hofmeyr, J. H. S., & Cornish-Bowden, A. (2000). Regulating the cellular economy of supply and demand. *FEBS Letters*, *476*(1–2), 47–51.

Houot, L., Floutier, M., Marteyn, B., Michaut, M., Picciocchi, A., Legrain, P., … Chauvat, F. (2007). Cadmium triggers an integrated reprogramming of the metabolism of Synechocystis PCC6803, under the control of the Slr1738 regulator. *BMC Genomics*, *8*, 1–16.

Huang, L., McCluskey, M. P., Ni, H., & LaRossa, R. A. (2002). Global gene expression profiles of the cyanobacterium Synechocystis sp. strain PCC 6803 in response to irradiation with UV-B and white light. *Journal of Bacteriology*, *184*(24), 6845–6858.

Ilík, P., Pavlovič, A., Kouřil, R., Alboresi, A., Morosinotto, T., Allahverdiyeva, Y., … Shikanai, T. (2017). Alternative electron transport mediated by flavodiiron proteins is operational in organisms from cyanobacteria up to gymnosperms. *New Phytologist*, *214*(3), 967–972.

Iluz, D., Alexandrovich, I., & Dubinsky, Z. (2012). The Enhancement of Photosynthesis by Fluctuating Light. *Artificial Photosynthesis*.

Johnson, X., Steinbeck, J., Dent, R. M., Takahashi, H., Richaud, P., Ozawa, S. I., … Alric, J. (2014). Proton gradient regulation 5-mediated cyclic electron flow under ATP- or redox-limited conditions: A study of ΔATPase pgr5 and ΔrbcL pgr5 mutants in the green alga Chlamydomonas reinhardtii. *Plant Physiology*, *165*(1), 438–452.

Kaneko, T., Nakamura, Y., Sasamoto, S., Watanabe, A., Kohara, M., Matsumoto, M., … Tabata, S. (2003). Structural Analysis of Four Large Plasmids Harboring in a Unicellular Cyanobacterium, Synechocystis sp. PCC 6803. *DNA Research*, *10*(5), 221–228.

Kaneko, T., Nakamura, Y., Wolk, C. P., Kuritz, T., Sasamoto, S., Watanabe, A., … Tabata, S. (2001). Complete genomic sequence of the filamentous nitrogen-fixing cyanobacterium Anabaena sp. Strain PCC 7120. *DNA Research*, *8*(5), 205–213.

Kaneko, T., Sato, S., Kotani, H., Tanaka, A., Asamizu, E., Nakamura, Y., … Tabata, S. (1996). Sequence analysis of the genome of the unicellular cyanobacterium synechocystis sp. strain PCC6803. II. Sequence determination of the entire genome and assignment of potential protein-coding regions (supplement). *DNA Research*, *3*(3), 185–209.

Kauny, J., & Sétif, P. (2014). NADPH fluorescence in the cyanobacterium Synechocystis sp. PCC 6803: A versatile probe for in vivo measurements of rates, yields and pools. *Biochimica et Biophysica Acta - Bioenergetics*, *1837*(6), 792–801.

Kerfeld, C. A., & Melnicki, M. R. (2016). Assembly, function and evolution of cyanobacterial carboxysomes. *Current Opinion in Plant Biology*, *31*, 66–75.

Khan, A. Z., Bilal, M., Mehmood, S., Sharma, A., & Iqbal, H. M. N. (2019). State-of-the-art genetic modalities to engineer cyanobacteria for sustainable biosynthesis of biofuel and fine-chemicals to meet bio–economy challenges. *Life*, *9*(3), 1–22.

Khetkorn, W., Baebprasert, W., Lindblad, P., & Incharoensakdi, A. (2012). Redirecting the electron flow towards the nitrogenase and bidirectional Hox-hydrogenase by using specific inhibitors results in enhanced H2 production in the cyanobacterium Anabaena siamensis TISTR 8012. *Bioresource Technology*, *118*, 265–271.

Kieninger, A. K., & Maldener, I. (2021). Cell–cell communication through septal junctions in filamentous cyanobacteria. *Current Opinion in Microbiology*, *61*, 35–41.

Klotz, A., Reinhold, E., Doello, S., & Forchhammer, K. (2015). Nitrogen starvation acclimation in Synechococcus elongatus: Redox-control and the role of nitrate reduction as an electron sink. *Life*, *5*(1), 888–904.

Klughammer, C., & Schreiber, U. (2016). Deconvolution of ferredoxin, plastocyanin, and P700 transmittance changes in intact leaves with a new type of kinetic LED array spectrophotometer. *Photosynthesis Research*, *128*(2), 195–214.

Kobayashi, M., Ishizuka, T., Katayama, M., Kanehisa, M., Bhattacharyya-Pakrasi, M., Pakrasi, H. B., & Ikeuchi, M. (2004). Response to oxidative stress involves a novel peroxiredoxin gene in the unicellular cyanobacterium Synechocystis sp. PCC 6803. *Plant and Cell Physiology*, *45*(3), 290–299.

Kok, B., Forbush, B., & McGloin, M. (1970). Cooperation of charges in photosynthetic O2 evolution–I. A linear four step mechanism. *Photochemistry and Photobiology, 11*(6), 457-475.

Komárek, J., Kaštovský, J., Mareš, J., & Johansen, J. R. (2014). Taxonomic classification of cyanoprokaryotes (cyanobacterial genera) 2014, using a polyphasic approach. *Preslia*, *86*(4), 295-335.

Kótai J. (1972). Instructions for preparation of modified nutrient solution Z8 for algae, publication B-11/69. Norwegian Institute for Water Research, Oslo, Norway

Kosourov, S., Böhm, M., Senger, M., Berggren, G., Stensjö, K., Mamedov, F., … Allahverdiyeva, Y. (2021). Photosynthetic hydrogen production: Novel protocols, promising engineering approaches and application of semi-synthetic hydrogenases. *Physiologia Plantarum*, (January), 1–13.

Kosourov, S., Leino, H., Murukesan, G., Lynch, F., Sivonen, K., Tsygankov, A. A., … Allahverdiyeva, Y. (2014). Hydrogen photoproduction by immobilized N2-fixing cyanobacteria: Understanding the role of the uptake hydrogenase in the long-term process. *Applied and Environmental Microbiology*, *80*(18), 5807–5817.

Kourpa, K., Manarolaki, E., Lyratzakis, A., Strataki, V., Rupprecht, F., Langer, J. D., & Tsiotis, G. (2019). Proteome Analysis of Enriched Heterocysts from Two Hydrogenase Mutants from Anabaena sp. PCC 7120. *Proteomics*, *19*(19), 1–12.

Kramer, D. M., Avenson, T. J., & Edwards, G. E. (2004). Dynamic flexibility in the light reactions of photosynthesis governed by both electron and proton transfer reactions. *Trends in Plant Science*, *9*(7), 349–357.

Kufryk, G. I., & Vermaas, W. F. J. (2006). Sll1717 affects the redox state of the plastoquinone pool by modulating quinol oxidase activity in thylakoids. *Journal of Bacteriology*, *188*(4), 1286–1294.

Kumazaki, S., Akari, M., & Hasegawa, M. (2013). Transformation of thylakoid membranes during differentiation from vegetative cell into heterocyst visualized by microscopic spectral imaging. *Plant Physiology*, *161*(3), 1321–1333.

Lang, N. J., & Fay, P. (1971). The heterocysts of blue-green algae II. Details of ultrastructure. *Proceedings of the Royal Society of London. Series B. Biological Sciences*, *178*(1051), 193–203.

Latifi, A., Ruiz, M., & Zhang, C. C. (2009). Oxidative stress in cyanobacteria. *FEMS Microbiology Reviews*, *33*(2), 258–278.

Laughlin, T. G., Bayne, A. N., Trempe, J. F., Savage, D. F., & Davies, K. M. (2019).

Structure of the complex I-like molecule NDH of oxygenic photosynthesis. *Nature*, *566*(7744), 411–414.

Laughlin, T. G., Savage, D. F., & Davies, K. M. (2020). Recent advances on the structure and function of NDH-1: The complex I of oxygenic photosynthesis. *Biochimica et Biophysica Acta - Bioenergetics*, *1861*(11), 148254.

Lea-Smith, D. J., Bombelli, P., Vasudevan, R., & Howe, C. J. (2016). Photosynthetic, respiratory and extracellular electron transport pathways in cyanobacteria. *Biochimica et Biophysica Acta - Bioenergetics*, *1857*(3), 247–255.

Lea-Smith, D. J., Ross, N., Zori, M., Bendall, D. S., Dennis, J. S., Scott, S. A., … Howe, C. J. (2013). Thylakoid terminal oxidases are essential for the cyanobacterium Synechocystis sp. PCC 6803 to survive rapidly changing light intensities. *Plant Physiology*, *162*(1), 484–495.

Lehmann, R., Machné, R., Georg, J., Benary, M., Axmann, I., & Steuer, R. (2013). How cyanobacteria pose new problems to old methods: Challenges in microarray time series analysis. *BMC Bioinformatics*, *14*(1).

Lehner, J., Berendt, S., Dörsam, B., Pérez, R., Forchhammer, K., & Maldener, I. (2013). Prokaryotic multicellularity: A nanopore array for bacterial cell communication. *FASEB Journal*, *27*(6), 2293–2300.

Lindberg, P., Devine, E., Stensjö, K., & Lindblad, P. (2012). Hupw protease specifically required for processing of the catalytic subunit of the uptake hydrogenase in the cyanobacterium Nostoc sp. Strain PCC 7120. *Applied and Environmental Microbiology*, *78*(1), 273–276.

Lindberg, P., Schütz, K., Happe, T., & Lindblad, P. (2002). A hydrogen-producing, hydrogenase-free mutant strain of Nostoc punctiforme ATCC 29133. *International Journal of Hydrogen Energy*, *27*(11–12), 1291–1296.

Lindblad, P., Fuente, D., Borbe, F., Cicchi, B., Conejero, J. A., Couto, N., … Wünschiers, R. (2019). CyanoFactory, a European consortium to develop technologies needed to advance cyanobacteria as chassis for production of chemicals and fuels. *Algal Research*, *41*(December 2018), 101510.

Liran, O., Shemesh, E., & Tchernov, D. (2018). Investigation into the CO2 concentrating step rates within the carbon concentrating mechanism of Synechocystis sp. PCC6803 at various pH and light intensities reveal novel mechanistic properties. *Algal Research*, *33*(June), 419–429.

Liu, L. N., Bryan, S. J., Huang, F., Yu, J., Nixon, P. J., Rich, P. R., & Mullineaux, C. W. (2012). Control of electron transport routes through redox-regulated redistribution of respiratory complexes. *Proceedings of the National Academy of Sciences of the United States of America*, *109*(28), 11431–11436.

Ludwig, M., Schulz-Friedrich, R., & Appel, J. (2006). Occurrence of hydrogenases in cyanobacteria and anoxygenic photosynthetic bacteria: Implications for the phylogenetic origin of cyanobacterial and algal hydrogenases. *Journal of Molecular Evolution*, *63*(6), 758–768.

Magnuson, A., & Cardona, T. (2016). Thylakoid membrane function in heterocysts. *Biochimica et Biophysica Acta - Bioenergetics*, *1857*(3), 309–319.

Magnuson, A. (2019). Heterocyst thylakoid bioenergetics. *Life, 9*(1), 13.

Mahinthichaichan, P., Morris, D. M., Wang, Y., Jensen, G. J., & Tajkhorshid, E. (2018). Selective Permeability of Carboxysome Shell Pores to Anionic Molecules. *Journal of Physical Chemistry B*, *122*(39), 9110–9118.

Malone, L. A., Proctor, M. S., Hitchcock, A., Hunter, C. N., & Johnson, M. P. (2021). Cytochrome b6f – Orchestrator of photosynthetic electron transfer. *Biochimica et Biophysica Acta - Bioenergetics*, *1862*(5), 148380.

Mangan, N. M., Flamholz, A., Hood, R. D., Milo, R., & Savage, D. F. (2016). PH determines the energetic efficiency of the cyanobacterial CO2 concentrating mechanism. *Proceedings of the National Academy of Sciences of the United States of America*, *113*(36), E5354–E5362.

Mariscal, V., Herrero, A., & Flores, E. (2007). Continuous periplasm in a filamentous, heterocyst-forming cyanobacterium. *Molecular Microbiology*, *65*(4), 1139–1145.

Mariscal, V. (2014) Cell-cell joining proteins in heterocyst-forming cyanobacteria. In E. Flores & A. Herrero (Eds.), *The Cell Biology of Cyanobacteria* (pp. 293–304). Norfolk, UK: Caister Academic Press.

Martins, M. C., Romão, C. V., Folgosa, F., Borges, P. T., Frazão, C., & Teixeira, M.

(2019). How superoxide reductases and flavodiiron proteins combat oxidative stress in anaerobes. *Free Radical Biology and Medicine*, *140*(February), 36–60.

Masukawa, H., Mochimaru, M., & Sakurai, H. (2002). Disruption of the uptake hydrogenase gene, but not of the bidirectional hydrogenase gene, leads to enhanced photobiological hydrogen production by the nitrogen-fixing cyanobacterium Anabaena sp. PCC 7120. *Applied Microbiology and Biotechnology*, *58*(5), 618–624.

Matthijs, H. C. P., Visser, P. M., Reeze, B., Meeuse, J., Slot, P. C., Wijn, G., … Huisman, J. (2012). Selective suppression of harmful cyanobacteria in an entire lake with hydrogen peroxide. *Water Research*, *46*(5), 1460–1472.

Mazard, S., Penesyan, A., Ostrowski, M., Paulsen, I. T., & Egan, S. (2016). Tiny microbes with a big impact: the role of cyanobacteria and their metabolites in shaping our future. *Marine drugs, 14*(5), 97.

McDonald, A. E., Amirsadeghi, S., & Vanlerberghe, G. C. (2003). Prokaryotic orthologues of mitochondrial alternative oxidase and plastid terminal oxidase. *Plant Molecular Biology*, *53*(6), 865–876.

Meeks, J. C., & Castenholz, R. W. (1971). Growth and photosynthesis in an extreme thermophile, Synechococcus lividus (Cyanophyta). *Archiv Für Mikrobiologie*, *78*(1), 25–41.

Mehler, A. H. (1951). Studies on reactions of illuminated chloroplasts. II. Stimulation and inhibition of the reaction with molecular oxygen. *Archives of Biochemistry and Biophysics*, *34*(2), 339–351.

Melbinger, A., & Vergassola, M. (2015). The Impact of Environmental Fluctuations on Evolutionary Fitness Functions. *Scientific Reports*, *5*, 1–11.

Merino-Puerto, V., Mariscal, V., Mullineaux, C. W., Herrero, A., & Flores, E. (2010). Fra proteins influencing filament integrity, diazotrophy and localization of septal protein SepJ in the heterocyst-forming cyanobacterium Anabaena sp. *Molecular Microbiology*, *75*(5), 1159–1170.

Merino-Puerto, V., Schwarz, H., Maldener, I., Mariscal, V., Mullineaux, C. W., Herrero, A., & Flores, E. (2011). FraC/FraD-dependent intercellular molecular exchange in the filaments of a heterocyst-forming cyanobacterium, Anabaena sp. *Molecular Microbiology*, *82*(1), 87–98.

Miller, N. T., Vaughn, M. D., & Burnap, R. L. (2021). Electron flow through NDH-1 complexes is the major driver of cyclic electron flow-dependent proton pumping in cyanobacteria. *Biochimica et Biophysica Acta - Bioenergetics*, *1862*(3), 148354.

Mills, L. A., McCormick, A. J., & Lea-Smith, D. J. (2020). Current knowledge and recent advances in understanding metabolism of the model cyanobacterium Synechocystis sp. PCC 6803. *Bioscience Reports*, *40*(4), 1–33.

Mishra, A. K., Kaushik, M. S., & Tiwari, D. N. (2018). *Nitrogenase and Hydrogenase: Enzymes for Nitrogen Fixation and Hydrogen Production in Cyanobacteria*. *Cyanobacteria: From Basic Science to Applications*. Elsevier Inc.

Mitschke, J., Vioque, A., Haas, F., Hess, W. R., & Muro-Pastor, A. M. (2011). Dynamics of transcriptional start site selection during nitrogen stress-induced cell differentiation in Anabaena sp. PCC7120. *Proceedings of the National Academy of Sciences of the United States of America*, *108*(50), 20130–20135.

Mullineaux, C. W. (2014a). Electron transport and light-harvesting switches in cyanobacteria. *Frontiers in Plant Science*, *5*(JAN), 1–6

Mullineaux, C. W. (2014b). Co-existence of photosynthetic and respiratory activities in cyanobacterial thylakoid membranes. *Biochimica et Biophysica Acta - Bioenergetics*, *1837*(4), 503–511.

Mullineaux, C. W., Mariscal, V., Nenninger, A., Khanum, H., Herrero, A., Flores, E., & Adams, D. G. (2008). Mechanism of intercellular molecular exchange in heterocyst-forming cyanobacteria. *EMBO Journal*, *27*(9), 1299–1308.

Munekage, Y., Hashimoto, M., Miyake, C., Tomizawa, K. I., Endo, T., Tasaka, M., & Shikanai, T. (2004). Cyclic electron flow around photosystem I is essential for photosynthesis. *Nature*, *429*(6991), 579–582.

Munekage, Y., Hojo, M., Meurer, J., Endo, T., Tasaka, M., & Shikanai, T. (2002). PGR5 is involved in cyclic electron flow around photosystem I and is essential for photoprotection in Arabidopsis. *Cell*, *110*(3), 361–371.

Mustila, H., Allahverdiyeva, Y., Isojärvi, J., Aro, E. M., & Eisenhut, M. (2014). The

bacterial-type [4Fe-4S] ferredoxin 7 has a regulatory function under photooxidative stress conditions in the cyanobacterium Synechocystis sp. PCC 6803. *Biochimica et Biophysica Acta - Bioenergetics*, *1837*(8), 1293–1304.

Mustila, H., Muth-Pawlak, D., Aro, E. M., & Allahverdiyeva, Y. (2021). Global proteomic response of unicellular cyanobacterium Synechocystis sp. PCC 6803 to fluctuating light upon CO2 step-down. *Physiologia Plantarum*, *173*(1), 305–320.

Nakamura, Y., Kaneko, T., Miyajima, N., & Tabata, S. (1999). Extension of CyanoBase, CyanoMutants: Repository of mutant information on synechocystis sp. strain PCC6803. *Nucleic Acids Research*, *27*(1), 66–68.

Navarro, J. A., Durán, R. V., De La Rosa, M. A., & Hervás, M. (2005). Respiratory cytochrome c oxidase can be efficiently reduced by the photosynthetic redox proteins cytochrome c6 and plastocyanin in cyanobacteria. *FEBS Letters*, *579*(17), 3565–3568.

Nguyen, J., Lara-Gutiérrez, J., & Stocker, R. (2021). Environmental fluctuations and their effects on microbial communities, populations and individuals. *FEMS Microbiology Reviews*, *45*(4), 1–16.

Nicolaisen, K., Hahn, A., & Schleiff, E. (2009). The cell wall in heterocyst formation by Anabaena sp. PCC 7120. *Journal of Basic Microbiology*, *49*(1), 5–24.

Nieves-Morión, M., Mullineaux, C. W., & Flores, E. (2017). Molecular diffusion through cyanobacterial septal junctions. *MBio*, *8*(1).

Nikkanen, L., Solymosi, D., Jokel, M., & Allahverdiyeva, Y. (2021). Regulatory electron transport pathways of photosynthesis in cyanobacteria and microalgae: Recent advances and biotechnological prospects. *Physiologia Plantarum*, *173*(2), 514–525.

Nikkanen, L., Toivola, J., Trotta, A., Diaz, M. G., Tikkanen, M., Aro, E. M., & Rintamäki, E. (2018). Regulation of cyclic electron flow by chloroplast NADPH-dependent thioredoxin system. *Plant Direct*, *2*(11).

Nyberg, M., Heidorn, T., & Lindblad, P. (2015). Hydrogen production by the engineered cyanobacterial strain Nostoc PCC 7120 δhupW examined in a flat panel photobioreactor system. *Journal of Biotechnology*, *215*, 35–43.

Ogawa, T. (1991). A gene homologous to the subunit-2 gene of NADH dehydrogenase is essential to inorganic carbon transport of Synechocystis PCC6803. *Proceedings of the National Academy of Sciences of the United States of America*, *88*(10), 4275–4279.

Ogawa, T., Harada, T., Ozaki, H., & Sonoike, K. (2013). Disruption of the ndhF1 gene affects Chl fluorescence through state transition in the cyanobacterium synechocystis sp. PCC 6803, resulting in apparent high efficiency of photosynthesis. *Plant and Cell Physiology*, *54*(7), 1164–1171.

Ogawa, T., & Mi, H. (2007). Cyanobacterial NADPH dehydrogenase complexes. *Photosynthesis Research*, *93*(1–3), 69–77.

Ohkawa, H., Dean Price, G., Badger, M. R., & Ogawa, T. (2000a). Mutation of ndh genes leads to inhibition of CO2 uptake rather than HCO3- uptake in Synechocystis sp. strain PCC 6803. *Journal of Bacteriology*, *182*(9), 2591–2596.

Ohkawa, H., Pakrasi, H. B., & Ogawa, T. (2000b). Two types of functionally distinct NAD(P)H dehydrogenases in Synechoeystis sp. strain PCC6803. *Journal of Biological Chemistry*, *275*(41), 31630–31634.

Ohta, H., Shibata, Y., Haseyama, Y., Yoshino, Y., Suzuki, T., Kagasawa, T., … Enami, I. (2005). Identification of genes expressed in response to acid stress in Synechocystis sp. PCC 6803 using DNA microarrays. *Photosynthesis Research*, *84*(1–3), 225–230.

Oliver, T., Sánchez-Baracaldo, P., Larkum, A. W., Rutherford, A. W., & Cardona, T. (2021). Time-resolved comparative molecular evolution of oxygenic photosynthesis. *Biochimica et Biophysica Acta - Bioenergetics*, *1862*(6).

Ow, S. Y., Cardona, T., Taton, A., Magnuson, A., Lindblad, P., Stensjö, K., & Wright, P. C. (2008). Quantitative shotgun proteomics of enriched heterocysts from nostoc sp. PCC 7120 using 8-plex isobaric peptide tags. *Journal of Proteome Research*, *7*(4), 1615–1628.

Ow, S. Y., Nolrel, J., Cardona, T., Taton, A., Lindblad, P., Stensjö, K., & Wright, P. C. (2009). Quantitative overview of N 2 fixation in nostoc Punctiforme ATCC 29133 through cellular enrichments and iTRAQ shotgun

proteomics. *Journal of Proteome Research*, *8*(1), 187–198.

Pan, X., Cao, D., Xie, F., Xu, F., Su, X., Mi, H., … Li, M. (2020). Structural basis for electron transport mechanism of complex I-like photosynthetic NAD(P)H dehydrogenase. *Nature Communications*, *11*(1).

Paumann, M., Bernroitner, M., Lubura, B., Peer, M., Jakopitsch, C., Furtmüller, P. G., … Obinger, C. (2004). Kinetics of electron transfer between plastocyanin and the soluble Cu A domain of cyanobacterial cytochrome c oxidase. *FEMS Microbiology Letters*, *239*(2), 301–307.

Peden, E. A., Boehm, M., Mulder, D. W., Davis, R., Old, W. M., King, P. W., … Dubini, A. (2013). Identification of global ferredoxin interaction networks in chlamydomonas reinhardtii. *Journal of Biological Chemistry*, *288*(49), 35192–35209.

Peltier, G., Aro, E. M., & Shikanai, T. (2016). NDH-1 and NDH-2 Plastoquinone Reductases in Oxygenic Photosynthesis. *Annual Review of Plant Biology*, *67*, 55–80.

Pernil, R., & Schleiff, E. (2019). Metalloproteins in the Biology of Heterocysts. *Life*, *9*(2), 32.

Pfaffl, M. W. (2001). A new mathematical model for relative quantification in real-time RT–PCR. *Nucleic Acids Research*, *29*(9), e45. Retrieved from

Picossi, S., Flores, E., & Herrero, A. (2014). ChIP analysis unravels an exceptionally wide distribution of DNA binding sites for the NtcA transcription factor in a heterocyst-forming cyanobacterium. *BMC Genomics*, *15*(1).

Picossi, S., Flores, E., & Herrero, A. (2015). The LysR-type transcription factor PacR is a global regulator of photosynthetic carbon assimilation in Anabaena. *Environmental Microbiology*, *17*(9), 3341–3351.

Pierella Karlusich, J. J., Lodeyro, A. F., & Carrillo, N. (2014). The long goodbye: The rise and fall of flavodoxin during plant evolution. *Journal of Experimental Botany*, *65*(18), 5161–5178.

Pils, D., & Schmetterer, G. (2001). Characterization of three bioenergetically active respiratory terminal oxidases in the cyanobacterium Synechocystis sp. strain PCC 6803. *FEMS Microbiology Letters*, *203*(2), 217–222.

Pisareva, T., Kwon, J., Oh, J., Kim, S., Ge, C., Wieslander, Å., ... & Norling, B. (2011). Model for membrane organization and protein sorting in the cyanobacterium Synechocystis sp. PCC 6803 inferred from proteomics and multivariate sequence analyses. *Journal of proteome research, 10*(8), 3617-3631.

Pogoryelov, D., Reichen, C., Klyszejko, A. L., Brunisholz, R., Muller, D. J., Dimroth, P., & Meier, T. (2007). The oligomeric state of c rings from cyanobacterial F-ATP synthases varies from 13 to 15. *Journal of Bacteriology*, *189*(16), 5895–5902.

Prakash, J. S. S., Krishna, P. S., Sirisha, K., Kanesaki, Y., Suzuki, I., Shivaji, S., & Murata, N. (2010). An RNA helicase, CrhR, regulates the low-temperature-inducible expression of heat-shock genes groES, groEL1 and groEL2 in Synechocystis sp. PCC 6803. *Microbiology*, *156*(2), 442–451.

Rae, B. D., Long, B. M., Badger, M. R., & Price, G. D. (2013). Functions, Compositions, and Evolution of the Two Types of Carboxysomes: Polyhedral Microcompartments That Facilitate CO 2 Fixation in Cyanobacteria and Some Proteobacteria. *Microbiology and Molecular Biology Reviews*, *77*(3), 357–379.

Rippka, R., Deruelles, J., & Waterbury, J. B. (1979). Generic assignments, strain histories and properties of pure cultures of cyanobacteria. *Journal of General Microbiology*, *111*(1), 1–61.

Rippka, R., Waterbury, J., & Cohen-Bazire, G. (1974). A cyanobacterium which lacks thylakoids. *Archives of Microbiology*, *100*(1), 419–436.

Romão, C. V., Vicente, J. B., Borges, P. T., Frazão, C., & Teixeira, M. (2016a). The dual function of flavodiiron proteins: Oxygen and/or nitric oxide reductases. *Journal of Biological Inorganic Chemistry*, *21*(1), 39–52.

Romão, C. V., Vicente, J. B., Borges, P. T., Victor, B. L., Lamosa, P., Silva, E., … Frazão, C. (2016b). Structure of Escherichia coli Flavodiiron Nitric Oxide Reductase. *Journal of Molecular Biology*, *428*(23), 4686–4707.

Roumezi, B., Avilan, L., Risoul, V., Brugna, M., Rabouille, S., & Latifi, A. (2020). Overproduction of the Flv3B flavodiiron, enhances the photobiological hydrogen production by the nitrogen-fixing cyanobacterium Nostoc PCC 7120. *Microbial Cell Factories*, *19*(1), 1–10.

Rowland, J. G., Pang, X., Suzuki, I., Murata, N., Simon, W. J., & Slabas, A. R. (2010).

Identification of components associated with thermal acclimation of photosystem II in Synechocystis sp. PCC6803. *PLoS ONE*, *5*(5).

Sánchez-Baracaldo, P. (2015). Origin of marine planktonic cyanobacteria. *Scientific Reports*, *5*, 14–17.

Sánchez-Baracaldo, P., & Cardona, T. (2020). On the origin of oxygenic photosynthesis and Cyanobacteria. *New Phytologist*, *225*(4), 1440–1446.

Sánchez-Riego, A. M., López-Maury, L., & Florencio, F. J. (2013). Glutaredoxins are essential for stress adaptation in the cyanobacterium Synechocystis sp. PCC 6803. *Frontiers in Plant Science*, *4*(NOV), 1–11.

Santamaría-Gómez, J., Mariscal, V., & Luque, I. (2018). Mechanisms for Protein Redistribution in Thylakoids of Anabaena During Cell Differentiation. *Plant and Cell Physiology*, *59*(9), 1860–1873.

Saraiva, L. M., Vicente, J. B., & Teixeira, M. (2004). The role of the flavodiiron proteins in microbial nitric oxide detoxification. *Advances in microbial physiology, 49*, 78-132.

Savir, Y., Noor, E., Milo, R., & Tlusty, T. (2010). Cross-species analysis traces adaptation of Rubisco toward optimality in a low-dimensional landscape. *Proceedings of the National Academy of Sciences of the United States of America*, *107*(8), 3475–3480.

Schirrmeister, B. E., Gugger, M., & Donoghue, P. C. J. (2015). Cyanobacteria and the Great Oxidation Event: Evidence from genes and fossils. *Palaeontology*, *58*(5), 769–785.

Schmetterer, G. (2016). (RTOs) of Cyanobacteria, 331–355.

Schreiber, U. (2017). Redox changes of ferredoxin, P700, and plastocyanin measured simultaneously in intact leaves. *Photosynthesis Research*, *134*(3), 343–360.

Schreiber, U., & Klughammer, C. (2009). New NADPH / 9-AA module for the DUAL-PAM-100 : Description , operation and examples of application . *PAM Application Notes*, *2*, 1–13.

Schubert, H., Sagert, S., & Forster, R. M. (2001). Evaluation of the different levels of variability in the underwater light field of a shallow estuary. *Helgoland Marine Research*, *55*(1), 12–22.

Schuller, J. M., Birrell, J. A., Tanaka, H., Konuma, T., Wulfhorst, H., Cox, N., … Nowaczyk, M. M. (2019). Structural adaptations of photosynthetic complex I enable ferredoxin-dependent electron transfer. *Science*, *363*(6424), 257–260.

Schuller, J. M., Saura, P., Thiemann, J., Schuller, S. K., Gamiz-Hernandez, A. P., Kurisu, G., … Kaila, V. R. I. (2020). Redox-coupled proton pumping drives carbon concentration in the photosynthetic complex I. *Nature Communications*, *11*(1).

Schürmann, P., & Buchanan, B. B. (2008). The ferredoxin/thioredoxin system of oxygenic photosynthesis. *Antioxidants and Redox Signaling*, *10*(7), 1235–1273.

Schütz, K., Happe, T., Troshina, O., Lindblad, P., Leitão, E., Oliveira, P., & Tamagnini, P. (2004). Cyanobacterial H2 production - A comparative analysis. *Planta*, *218*(3), 350–359.

Sétif, P., Boussac, A., & Krieger-Liszkay, A. (2019). Near-infrared in vitro measurements of photosystem I cofactors and electron-transfer partners with a recently developed spectrophotometer. *Photosynthesis Research*, *142*(3), 307–319.

Sétif, P., Shimakawa, G., Krieger-Liszkay, A., & Miyake, C. (2020). Identification of the electron donor to flavodiiron proteins in Synechocystis sp. PCC 6803 by in vivo spectroscopy. *Biochimica et Biophysica Acta - Bioenergetics*, *1861*(10), 148256.

Sherman, D. M., Tucker, D., & Sherman, L. A. (2000). Heterocyst development and localization of cyanophycin in N2-fixing cultures of Anabaena sp. PCC 7120 (Cyanobacteria). *Journal of Phycology*, *36*(5), 932-941.

Shevela, D., Schröder, W. P., & Messinger, J. (2018). Liquid-phase measurements of photosynthetic oxygen evolution. In S. Covshoff (Eds.), *Photosynthesis: Methods and Protocols* (pp. 197-211). Humana, New York, Press.

Shih, P. M., Wu, D., Latifi, A., Axen, S. D., Fewer, D. P., Talla, E., … Kerfeld, C. A. (2013). Improving the coverage of the cyanobacterial phylum using diversity-driven genome sequencing. *Proceedings of the National Academy of Sciences of the United States of America*, *110*(3), 1053–1058.

Shikanai, T. (2007). Cyclic electron transport around photosystem I: Genetic approaches. *Annual Review of Plant Biology*, *58*, 199–217.

Shimakawa, G., Ishizaki, K., Tsukamoto, S., Tanaka, M., Sejima, T., & Miyake, C. (2017). The liverwort, Marchantia, drives

alternative electron flow using a flavodiiron protein to protect PSI. *Plant Physiology*, *173*(3), 1636–1647.

Shimakawa, G., & Miyake, C. (2018a). Changing frequency of fluctuating light reveals the molecular mechanism for P700 oxidation in plant leaves. *Plant Direct*, *2*(7), 1–11.

Shimakawa, G., & Miyake, C. (2018b). Oxidation of P700 ensures robust photosynthesis. *Frontiers in Plant Science*, *871*(November), 1–15.

Shimakawa, G., Shaku, K., Nishi, A., Hayashi, R., Yamamoto, H., Sakamoto, K., … Miyake, C. (2015). FLAVODIIRON2 and FLAVODIIRON4 proteins mediate an oxygen-dependent alternative electron flow in synechocystis sp. pcc 6803 under CO2-limited conditions. *Plant Physiology*, *167*(2), 472–480.

Singh, A. K., Elvitigala, T., Bhattacharyya-Pakrasi, M., Aurora, R., Ghosh, B., & Pakrasi, H. B. (2008). Integration of carbon and nitrogen metabolism with energy production is crucial to light acclimation in the cyanobacterium Synechocystis. *Plant Physiology*, *148*(1), 467–478.

Singh, R., Parihar, P., Singh, M., Bajguz, A., Kumar, J., Singh, S., … Prasad, S. M. (2017). Uncovering potential applications of cyanobacteria and algal metabolites in biology, agriculture and medicine: Current status and future prospects. *Frontiers in Microbiology*, *8*(APR), 1–37.

Sitther, V., Tabatabai, B., Fathabad, S. G., Gichuki, S., Chen, H., & Arumanayagam, A. C. S. (2020). Cyanobacteria as a biofuel source: advances and applications. In P. K. Singh, A. Kumar, V. K. Singh, &A. K. Shrivastava (Eds.), *Advances in Cyanobacterial Biology* (pp. 269-289). Academic Press.

Soo, R. M., Hemp, J., & Hugenholtz, P. (2019). Evolution of photosynthesis and aerobic respiration in the cyanobacteria. *Free Radical Biology and Medicine*, *140*(March), 200–205.

Stal, L. J. (2007). Cyanobacteria. In *Algae and cyanobacteria in extreme environments* (pp. 659-680). Springer, Dordrecht.

Stirbet, A, Lazár D, Papageorgiou, C. G, Govindjee. (2019). Chlorophyll a fluorescence in cyanobacteria: relation to photosynthesis. In A.K. Mishra, D.N. Tiwari, & A.N. Rai (Eds.), *Cyanobacteria – from basic science to applications* (pp. 79–130). London: Academic Press.

Storti, M., Puggioni, M. P., Segalla, A., Morosinotto, T., & Alboresi, A. (2020a). The chloroplast NADH dehydrogenase-like complex influences the photosynthetic activity of the moss Physcomitrella patens. *Journal of Experimental Botany*, *71*(18), 5538–5548.

Storti, M., Segalla, A., Mellon, M., Alboresi, A., & Morosinotto, T. (2020b). Regulation of electron transport is essential for photosystem I stability and plant growth. *New Phytologist*, *228*(4), 1316–1326.

Strand, D. D., D'Andrea, L., & Bock, R. (2019). The plastid NAD(P)H dehydrogenase-like complex: Structure, function and evolutionary dynamics. *Biochemical Journal*, *476*(19), 2743–2756.

Strand, D. D., Fisher, N., & Kramer, D. M. (2017). The higher plant plastid NAD(P)H dehydrogenase-like complex (NDH) is a high efficiency proton pump that increases ATP production by cyclic electron flow. *Journal of Biological Chemistry*, *292*(28), 11850–11860.

Summerfield, T. C., Nagarajan, S., & Sherman, L. A. (2011). Gene expression under low-oxygen conditions in the cyanobacterium Synechocystis sp. PCC 6803 demonstrates Hik31-dependent and -independent responses. *Microbiology*, *157*(2), 301–312.

Suorsa, M., Järvi, S., Grieco, M., Nurmi, M., Pietrzykowska, M., Rantala, M., … Aro, E. M. (2012). PROTON GRADIENT REGULATION5 is essential for proper acclimation of Arabidopsis photosystem I to naturally and artificially fluctuating light conditions. *Plant Cell*, *24*(7), 2934–2948.

Theune, M. L., Hildebrandt, S., Steffen-Heins, A., Bilger, W., Gutekunst, K., & Appel, J. (2021). In-vivo quantification of electron flow through photosystem I – Cyclic electron transport makes up about 35% in a cyanobacterium. *Biochimica et Biophysica Acta - Bioenergetics*, *1862*(3), 148353.

Thomas, J. C., Ughy, B., Lagoutte, B., & Ajlani, G. (2006). A second isoform of the ferredoxin:NADP oxidoreductase generated by an in-frame initiation of translation. *Proceedings of the National Academy of Sciences of the United States of America*, *103*(48), 18368–18373.

Timm, S., & Hagemann, M. (2020). Photorespiration-how is it regulated and how does it regulate overall plant metabolism?

Journal of Experimental Botany, *71*(14), 3955–3965.

Torrado, A., Ramírez-Moncayo, C., Navarro, J. A., Mariscal, V., & Molina-Heredia, F. P. (2019). Cytochrome c6 is the main respiratory and photosynthetic soluble electron donor in heterocysts of the cyanobacterium Anabaena sp. PCC 7120. *Biochimica et Biophysica Acta - Bioenergetics*, *1860*(1), 60–68.

Tsygankov, A. A., Minakov, E. A., Zorin, N. A., Gosteva, K. S., Voronin, O. G., & Karyakin, A. A. (2007). Measuring the pH dependence of hydrogenase activities. *Biochemistry (Moscow)*, *72*(9), 968–973.

Turmo, A., Gonzalez-Esquer, C. R., & Kerfeld, C. A. (2017). Carboxysomes: metabolic modules for CO2 fixation. *FEMS Microbiology Letters*, *364*(18), 1–7.

Tyystjärvi, T., Herranen, M., & Aro, E. M. (2001). Regulation of translation elongation in cyanobacteria: Membrane targeting of the ribosome nascent-chain complexes controls the synthesis of D1 protein. *Molecular Microbiology*, *40*(2), 476–484.

Ueda, M., Kuniyoshi, T., Yamamoto, H., Sugimoto, K., Ishizaki, K., Kohchi, T., … Shikanai, T. (2012). Composition and physiological function of the chloroplast NADH dehydrogenase-like complex in Marchantia polymorpha. *Plant Journal*, *72*(4), 683–693.

Ullah, H., Nagelkerken, I., Goldenberg, S. U., & Fordham, D. A. (2018). Climate change could drive marine food web collapse through altered trophic flows and cyanobacterial proliferation. *PLoS Biology*, *16*(1), 1–21.

Umena, Y., Kawakami, K., Shen, J. R., & Kamiya, N. (2011). Crystal structure of oxygen-evolving photosystem II at a resolution of 1.9 Å. *Nature, 473*(7345), 55-60.

Valladares, A., Herrero, A., Pils, D., Schmetterer, G., & Flores, E. (2003). Cytochrome c oxidase genes required for nitrogenase activity and diazotrophic growth in Anabaena sp. PCC 7120. *Molecular Microbiology*, *47*(5), 1239–1249.

Valladares, A., Maldener, I., Muro-Pastor, A. M., Flores, E., & Herrero, A. (2007). Heterocyst development and diazotrophic metabolism in terminal respiratory oxidase mutants of the cyanobacterium Anabaena sp. strain PCC 7120. *Journal of Bacteriology*, *189*(12), 4425–4430.

Vicente, J. B., Carrondo, M. A., Teixeira, M., & Frazão, C. (2008). Structural Studies on Flavodiiron Proteins. *Methods in Enzymology*, *437*(07), 3–19.

Vicente, J. B., Gomes, C. M., Wasserfallen, A., & Teixeira, M. (2002). Module fusion in an A-type flavoprotein from the cyanobacterium Synechocystis condenses a multiple-component pathway in a single polypeptide chain. *Biochemical and Biophysical Research Communications*, *294*(1), 82–87.

Vicente, J. B., Tran, V., Pinto, L., Teixeira, M., & Singha, U. (2012). A detoxifying oxygen reductase in the anaerobic protozoan Entamoeba histolytica. *Eukaryotic Cell*, *11*(9), 1112–1118.

Viola, S., Bailleul, B., Yu, J., Nixon, P., Sellés, J., Joliot, P., & Wollman, F. A. (2019). Probing the electric field across thylakoid membranes in cyanobacteria. *Proceedings of the National Academy of Sciences of the United States of America*, *116*(43), 21900–21906.

Walsby, A. E. (2007). Cyanobacterial heterocysts: terminal pores proposed as sites of gas exchange. *Trends in Microbiology*, *15*(8), 340–349.

Walter, J., Lynch, F., Battchikova, N., Aro, E. M., & Gollan, P. J. (2016). Calcium impacts carbon and nitrogen balance in the filamentous cyanobacterium Anabaena sp. PCC 7120. *Journal of Experimental Botany*, *67*(13), 3997–4008.

Wang, H. L., Postier, B. L., & Burnap, R. L. (2004). Alterations in Global Patterns of Gene Expression in Synechocystis sp. PCC 6803 in Response to Inorganic Carbon Limitation and the Inactivation of ndhR, a LysR Family Regulator. *Journal of Biological Chemistry*, *279*(7), 5739–5751.

Wasserfallen, A., Ragettli, S., Jouanneau, Y., & Leisinger, T. (1998). A family of flavoproteins in the domains archaea and bacteria. *European Journal of Biochemistry*, *254*(2), 325–332.

Weiss, G. L., Kieninger, A. K., Maldener, I., Forchhammer, K., & Pilhofer, M. (2019). Structure and Function of a Bacterial Gap Junction Analog. *Cell*, *178*(2), 374-384.e15.

Whitehead, L., Long, B. M., Dean Price, G., & Badger, M. R. (2014). Comparing the in vivo function of α-carboxysomes and β-carboxysomes in two model cyanobacteria. *Plant Physiology*, *165*(1), 398–411.

Wilk, L., Strauss, M., Rudolf, M., Nicolaisen, K., Flores, E., Kühlbrandt, W., & Schleiff, E. (2011). Outer membrane continuity and septosome formation between vegetative cells in the filaments of Anabaena sp. PCC 7120. *Cellular Microbiology*, *13*(11), 1744–1754.

Williams, J. G. K. (1988). Construction of Specific Mutations in Photosystem II Photosynthetic Reaction Center by Genetic Engineering Methods in Synechocystis 6803. *Methods in Enzymology*, *167*(C), 766–778.

Willis, A., & Woodhouse, J. N. (2020). Defining Cyanobacterial Species: Diversity and Description Through Genomics. *Critical Reviews in Plant Sciences*, *39*(2), 101–124.

Xu, X., Elhai, J., & Wolk, C. P. (2008). Transcriptional and developmental responses by Anabaena to deprivation of fixed nitrogen. In A. Herrero & E. Flores (Eds.), *The cyanobacteria: Molecular biology, genomics and evolution* (pp. 383-422). Norfolk, UK: Caister Academic Press.

Yamori, W., Makino, A., & Shikanai, T. (2016). A physiological role of cyclic electron transport around photosystem I in sustaining photosynthesis under fluctuating light in rice. *Scientific Reports*, *6*(July 2015), 1–12.

Yamori, W., Sakata, N., Suzuki, Y., Shikanai, T., & Makino, A. (2011). Cyclic electron flow around photosystem i via chloroplast NAD(P)H dehydrogenase (NDH) complex performs a significant physiological role during photosynthesis and plant growth at low temperature in rice. *Plant Journal*, *68*(6), 966–976.

Yamori, W., & Shikanai, T. (2016). Physiological Functions of Cyclic Electron Transport Around Photosystem i in Sustaining Photosynthesis and Plant Growth. *Annual Review of Plant Biology*, *67*, 81–106.

Yamori, W., Shikanai, T., & Makino, A. (2015). Photosystem i cyclic electron flow via chloroplast NADH dehydrogenase-like complex performs a physiological role for photosynthesis at low light. *Scientific Reports*, *5*(September), 1–10.

Yan, J., Kurisu, G., & Cramer, W. A. (2006). Intraprotein transfer of the quinone analogue inhibitor 2,5-dibromo-3-methyl-6-isopropyl-p-benzoquinone in the cytochrome b6f complex. *Proceedings of the National Academy of Sciences of the United States of America*, *103*(1), 69–74.

Yeremenko, N., Jeanjean, R., Prommeenate, P., Krasikov, V., Nixon, P. J., Vermaas, W. F. J., … Matthijs, H. C. P. (2005). Open reading frame ssr2016 is required for antimycin A-sensitive photosystem I-driven cyclic electron flow in the cyanobacterium Synechocystis sp. PCC 6803. *Plant and Cell Physiology*, *46*(8), 1433–1436.

Yingping, F., Lemeille, S., Talla, E., Janicki, A., Denis, Y., Zhang, C. C., & Latifi, A. (2014). Unravelling the cross-talk between iron starvation and oxidative stress responses highlights the key role of PerR (alr0957) in peroxide signalling in the cyanobacterium NostocPCC 7120. *Environmental Microbiology Reports*, *6*(5), 468–475.

Yoshino, F., Ikeda, H., Masukawa, H., & Sakurai, H. (2007). High photobiological hydrogen production activity of a Nostoc sp. PCC 7422 uptake hydrogenase-deficient mutant with high nitrogenase activity. *Marine Biotechnology*, *9*(1), 101–112.

Zahra, Z., Choo, D. H., Lee, H., & Parveen, A. (2020). Cyanobacteria: Review of current potentials and applications. *Environments, 7*(2), 13.

Zhang, C. C., Zhou, C. Z., Burnap, R. L., & Peng, L. (2018). Carbon/Nitrogen Metabolic Balance: Lessons from Cyanobacteria. *Trends in Plant Science*, *23*(12), 1116–1130.

Zhang, C., Shuai, J., Ran, Z., Zhao, J., Wu, Z., Liao, R., … Lei, M. (2020). Structural insights into NDH-1 mediated cyclic electron transfer. *Nature Communications*, *11*(1), 1–13.

Zhang, P., Allahverdiyeva, Y., Eisenhut, M., & Aro, E. M. (2009). Flavodiiron proteins in oxygenic photosynthetic organisms: Photoprotection of photosystem II by FIv2 and FIv4 in Synechocystis sp. PCC 6803. *PLoS ONE*, *4*(4).

Zhang, P., Battchikova, N., Jansen, T., Appel, J., Ogawa, T., & Aro, E. M. (2004). Expression and functional roles of the two distinct NDH-1 complexes and the carbon acquisition complex NdhD3/NdhF3/CupA/SII1735 in Synechocystis sp PCC 6803. *Plant Cell*, *16*(12), 3326–3340.

Zhang, P., Eisenhut, M., Brandt, A. M., Carmel, D., Silén, H. M., Vass, I., … Aro, E. M. (2012). Operon flv4-flv2 provides cyanobacterial photosystem ii with flexibility

of electron transfer. *Plant Cell*, *24*(5), 1952–1971.

Zhang, X., Zhang, X., Ward, B. B., Ward, B. B., & Sigman, D. M. (2020). Global Nitrogen Cycle: Critical Enzymes, Organisms, and Processes for Nitrogen Budgets and Dynamics. *Chemical Reviews*, *120*(12), 5308–5351.

Zhao, J., Gao, F., Fan, D. Y., Chow, W. S., & Ma, W. (2018). NDH-1 is important for photosystem i function of synechocystis sp. Strain PCC 6803 under environmental stress conditions. *Frontiers in Plant Science*, *8*(January), 1–10.

Zhao, J., Rong, W., Gao, F., Ogawa, T., & Ma, W. (2015). Subunit Q is required to stabilize the large complex of NADPH dehydrogenase in synechocystis sp. Strain PCC 68031. *Plant Physiology*, *168*(2), 443–451.

TURUN
YLIOPISTO
UNIVERSITY
OF TURKU

Painosalama, Turku, Finland 2021

ISBN 978-951-29-8668-2 (PRINT)
ISBN 978-951-29-8669-9 (PDF)
ISSN 0082-7002 (Print)
ISSN 2343-3175 (Online)